AB INITIO CALCULATIONS OF PROCESSES IN LOW ENERGY ELECTRON-MOLECULE SCATTERING

Thesis by

Deborah Ann Levin

In Partial Fulfillment of the Requirements

For the Degree of

Doctor of Philosophy

California Institute of Technology

Pasadena, California

1979

(Submitted March 19 , 1979)

To my parents and my sister

ACKNOWLEDGMENTS

During the past five years as a graduate student at Caltech, I have benefitted from scientific discussions with other graduate students and members of the faculty. I have enjoyed the interdisciplinary cooperative effect found here in the form of seminars and helpful discussions about specific problems that have come up in my research. As it would be impossible to thank all these individuals, a general acknowledgment of their help is given here.

Specifically, I would like to thank my research advisor, Dr. McKoy, for his time and encouragement. Along with his many other responsibilities he has always found the time to get involved with the very mundane aspects of my research projects. I have received a lot of satisfaction in being able to solve difficult problems which, in part, is due to his constant encouragement.

Finally, my thanks to Arne Fliflet is two-fold. As a postdoctoral fellow in our research group he has introduced me to many concepts and papers that have helped bridge the gap between my formal training as a chemist and my area of research in chemical physics. Working with him as coauthor and colleague has taught me much about how one goes about tackling a research project. As my husband, I want to thank you for your patience and understanding, but mostly for your solid determination that we could make it work.

ABSTRACT

Chapter I

Calculations are reported for low energy e-N_2 scattering cross sections in the static-exchange approximation. The approach used involves solving the Lippmann-Schwinger equation for the transition operator in a sub-space of Gaussian functions. New features of the method are analytic evaluation of matrix elements of the free particle Green's function and analytic transformation to obtain single-center expansion coefficients for the scattering amplitude. Results are presented for the total elastic and rotational excitation cross sections and the momentum transfer cross section for incident electron energies of 0.5 to 10 eV. Comparison with other theoretical and experimental data is included.

The second paper of this chapter presents cross sections for e^--CO scattering in the static exchange approximation. The method of calculation is the T-matrix discrete-basis-set method as updated by Fliflet, Levin, Ma and McKoy (previous paper) along with the variational correction approach of Fliflet and McKoy. We extract the $^2\pi$ resonance parameters at equilibrium internuclear separation and compare with other theoretical and semi-empirical results. Momentum transfer cross sections are compared with the experimental data of Land and the theoretical calculation of Chandra.

Chapter II

Results are presented in this first paper for rotational and vibrational-rotational excitation of H_2 by electron impact in the static-exchange approximation. Using the T-matrix discrete-basis-set approach as described in the first paper of Chapter I we solve the fixed-nuclei scattering problem at several internuclear separations. Comparisons of our results with the experimental data of Linder and Schmidt and with other calculated results are given.

In the second paper of this chapter we obtain vibrational and vibrational-rotational excitation cross sections of N_2 by electron impact via the $^2\Pi_g$ resonance in the static-exchange approximation. To obtain highly accurate phase shifts in the Π_g channel we use the variational correction of Fliflet and McKoy applied to the discrete-basis-set method of Fliflet, Levin, Ma and McKoy. As in e-H_2 vibrational excitation, the approach involves solving the fixed-nuclei scattering problem at several internuclear separations. From these calculations one extracts the parameters necessary to calculate resonant vibrational cross sections in a compound state model. Our results are compared with the experimental data of Wong et al., and other theoretical calculations.

Finally, the last paper discusses a simple model to include polarization effects in shape resonances. The position and width of the 2eV shape resonance in e-N_2 scattering are calculated by solving the T-matrix equations with the static-exchange field of the N_2 case of the N_2^- compound state. Resonance parameters

obtained at the equilibrium separation of the molecule agree well with semi-empirical results. Most importantly, the procedure can be readily applied at several internuclear separations.

Chapter III

As was mentioned in Chapter I, an important refinement of the original T-matrix method is the analytic evaluation of Gaussian matrix elements of the free particle Green's function. Previous calculations evaluated these matrix elements by a numerical quadrature which was in practice restricted to cases of axial symmetry. In this chapter the derivation of a method for generating higher order Gaussian matrix elements is presented. Although this procedure is applicable to polyatomic systems, we list here only the types of matrix elements necessary for Σ, Π and Δ symmetries of a linear molecule.

Chapter IV

In this chapter a method for obtaining scattering wave functions at arbitrary energies is presented. Minimization of the variance integral for a trial wave function expanded in discrete basis functions only provides a criterion for choosing the expansion coefficients of the wave function. By using a separable representation of the scattering potential only one new class of matrix elements appears in the evaluation of the variance integral which is not already

required in the diagonalization of the Hamiltonian. The method is applied to some model potentials and to s-wave scattering for helium in the static-exchange approximation.

TABLE OF CONTENTS

Page

CHAPTER I

Discrete Basis Set Calculations for Elastic Scattering from Diatomic Systems

INTRODUCTION

The difficulty one encounters in electron-molecule collision processes is due to the presence of a nonspherical potential describing the interaction for an electron with a molecule. Unlike the atomic case, the application of purely numerical techniques in an ab initio manner is considerably more difficult. The importance of electron-molecule cross sections in several different areas of research encourages the development of a method which allows treating the nonspherical nature of the scattering potential in an accurate and efficient way.

This chapter describes the extension of such a method to the cases of elastic scattering from molecular N_2 and CO. The approach of Rescigno, McCurdy and McKoy[1] involves representing the scattering potential by its projection onto a set of Gaussian basis functions and solving the Lippmann-Schwinger equation for the transition operator in the discrete function subspace. The essential new features which have been incorporated in their original formulation of the T-matrix method may be summarized as follows: calculation of the Gaussian matrix elements of the free particle Green's function analytically;[2] analytic treatment of the molecular orientation by use of a single-center expansion for the scattering amplitude;[3] and, application of the Kohn variational formula[4] for the partial-wave K-matrix to correct first order errors due to the difference between the true scattering potential and that obtained by projection onto a

discrete basis set, i.e., $V-V^t$. The first two new features of the T-matrix method are discussed in detail in the papers of this chapter and Chapter III. A summary of the essential steps in the derivation of the variational correction of Fliflet and McKoy[4] is given in the second paper of this chapter. Their method was first applied to elastic e-H_2 scattering and subsequently has been used to obtain very accurate results in elastic and vibrationally inelastic e-N_2 scattering (see Chapter II). In terms of earlier attempts to include variational corrections for scattering processes,[5,6] their procedure is the first to successfully apply the Kohn formulation[7] to a non-spherical target using discrete basis functions only.

This T-matrix method is first applied to e^--N_2 scattering at low energies in the static-exchange approximation. The results are compared with other theoretical calculations and the experimental values of the total scattering and momentum transfer cross section. This work employs the first two new features of the T-matrix method that are described above, but does not include a variational correction for first order errors due to $V-V^t$.

The second paper presents momentum transfer cross sections for low energy e-CO elastic scattering in the static-exchange approximation. Again our results are compared with other theoretical calculations and experimental values for the momentum transfer cross section. Unlike its isoelectronic counterpart, namely N_2, it is necessary to include a variational correction for errors in $V-V^t$ to obtain meaningful e^--CO results.

In addition to showing that the T-matrix method is successful in predicting reasonable elastic scattering results, the calculations described in this chapter lay the ground-work for ab initio studies of vibrationally inelastic processes presented in Chapter II. Similar use of a variational correction as in CO allows one to extract resonance parameters with a high degree of accuracy. Secondly, both papers show that vigorous inclusion of static-exchange effects produces eigenphase sum and cross section energy dependence that indicate the presence of a shape resonance.

References

1. T. N. Rescigno, C. W. McCurdy, Jr. and V. McKoy, Phys. Rev. A, 11, 825 (1975).

2. D. A. Levin, A. W. Fliflet, M. Ma, and V. McKoy, J. Comp. Phys., 28, 416 (1978).

3. A. W. Fliflet, D. A. Levin, M. Ma, and V. McKoy, Phys. Rev. A, 17, 160 (1978).

4. A. W. Fliflet and V. McKoy, Phys. Rev. A, 18, 2107 (1978).

5. P. G. Burke, Potential Scattering in Atomic Physics, (Plenum Press, New York, 1971) p.75.

6. D. G. Truhlar, J. Abdallah, Jr., and R. L. Smith, Adv. Chem. Phys., 25, 211 (1974).

7. W. Kohn, Phys. Rev., 74, 1763 (1948).

SECTION A

Discrete-basis-set Calculation for $e-N_2$ Scattering Cross Sections in the Static-exchange Approximation

I. INTRODUCTION

The importance of electron-molecule collision processes in several areas of current research interest provides a strong incentive for development of accurate methods of ab initio calculation. Discrete basis set methods are of particular interest since the lack of spherical symmetry makes the application of numerical techniques considerably more difficult for molecules than for atoms. Theoretical work in electron-molecule scattering has been reviewed by Takayanagi[1] and by Golden et al.[2], and more recently by Temkin.[3] Systems larger than H_2 for which electronically elastic scattering results have been obtained include N_2, CO, and CO_2.[4-9] Discrete basis set methods have been applied to H_2, N_2, and F_2.[10-13] To date the most sophisticated calculations have employed numerical techniques. The most accurate calculation using discrete basis set methods is the R-matrix calculation of Schneider[11] for H_2. The advantages and limitations of the various approaches referenced above have yet to be thoroughly evaluated.

The subject of this paper is the discrete basis function method for non-spherical potential scattering introduced by Rescigno, McCurdy, and McKoy.[10, 14, 15] The approach involves representing the potential by its projection onto a set of Gaussian basis functions and solving the Lippman-Schwinger equation for the transition operator in the discrete function subspace. We report new features of the method and its application to electronically elastic e-N_2 scattering in the static-exchange approximation.

Solving the Lippman-Schwinger equation in a basis set requires an efficient method for computing matrix elements of the free-particle Green's function. In previous calculations this involved a numerical quadrature and was in practice restricted to cases of axial symmetry.[14] As Ostlund has shown, these matrix elements may be evaluated analytically.[16] We have extended Ostlund's results for s- and p-type Gaussians[16,17] up to Gaussians of f-type symmetry and now use these results in our computational procedure. An important feature of our prescription for the Green's function is that it is directly applicable to polyatomic systems.

In previous applications of the method, elastic cross sections were obtained from fixed-nuclei scattering amplitudes by numerically averaging over target orientation.[10] To calculate rotational excitation and momentum transfer cross sections, it is desirable to treat the target orientation dependence analytically. This is now achieved by means of a single center expansion for the scattering amplitude. We stress that the dynamical problem, represented by the Lippman-Schwinger equation, is solved as before using a multicenter basis set. The matrix elements involved in the transformation to the single-center expansion for the scattering amplitude are evaluated analytically. We also point out that, since the matrix elements used to construct the basis set representation of the potential are evaluated using techniques developed for bound state calculations,[18] all the matrix elements required in our prescription for scattering are now treated analytically using formulas completely applicable to polyatomic systems.

In this work our results do not include a variational correction for first order errors due to the truncation of the potential. Including the correction would require considerable additional computational effort and it is interesting to demonstrate that useful results can be obtained using moderately sized basis sets even when the correction is omitted. The calculation of variationally stable results will be the subject of future work. In the next section a simple method for reducing variational error at very low energies is discussed.

Results are presented for the total elastic and momentum transfer cross sections calculated in the fixed-nuclei approximation; and also for total rotational excitation cross sections calculated in the adiabatic-nuclei approximation. We compare our cross sections with the theoretical results of Burke and Sinfailam[4] and with the experimental data of Golden[19] and of Englehardt et al.[20] Our results are dominated by a resonance in the $^2\Pi_g$ channel in qualitative agreement with experiment and other calculations.

II. THEORY

In the fixed nuclei approximation the Schrödinger equation for the scattered electron is of the form (in atomic units)

$$\left(-\tfrac{1}{2}\nabla^2 + V(R, \underset{\sim}{r}) - \frac{k^2}{2}\right)\psi^+_{\underset{\sim}{k}}(R, \underset{\sim}{r}) = 0 \tag{1}$$

where $V(R, \underset{\sim}{r})$ is an optical potential for the effective interaction between the target and the scattered electron which depends parametrically on the relative coordinates of the target nuclei (denoted by R). The vector subscript $\underset{\sim}{k}$ indicates the dependence of the wavefunction on direction as well as the magnitude of the incident momentum for a non-spherical target. The scattering wavefunction vanishes at the origin and has the asymptotic form

$$\psi^+_{\underset{\sim}{k}}(\underset{\sim}{r}) \rightarrow \frac{1}{(2\pi)^{3/2}}\left[e^{i\underset{\sim}{k}\cdot\underset{\sim}{r}} + f_{\underset{\sim}{k}}(\hat{\underset{\sim}{r}})\,\frac{e^{ikr}}{r}\right] \tag{2}$$

as $r \rightarrow \infty$. This corresponds to the normalization

$$\langle \psi^+_{\underset{\sim}{k}'} | \psi^+_{\underset{\sim}{k}} \rangle = \delta(\underset{\sim}{k} - \underset{\sim}{k}') \tag{3}$$

Rather than solve Eq. (1) directly, we work with the Lippman-Schwinger equation for the transition matrix

$$T = U + U G_0^+ T, \tag{4}$$

where $U = 2V$ and G_0^+ is the free-particle Green's function for the outgoing wave boundary condition. The T matrix solution of Eq. (4) satisfies the identity:

$$\langle \underset{\sim}{k}' | T | \underset{\sim}{k} \rangle \equiv \langle \underset{\sim}{k}' | U | \psi_{\underset{\sim}{k}}^+ \rangle \tag{5}$$

where $\underset{\sim}{k}$, $\underset{\sim}{k}'$ denote plane-wave states of the form

$$\phi_{\underset{\sim}{k}}(\underset{\sim}{r}) = \frac{1}{(2\pi)^{3/2}} e^{i\underset{\sim}{k} \cdot \underset{\sim}{r}} . \tag{6}$$

In our notation the T matrix is related to the scattering matrix S according to

$$S = 1 - i\pi\delta(E - E') T, \tag{7}$$

and is related to the scattering amplitude according to

$$f_{\underset{\sim}{k}}(\hat{\underset{\sim}{r}}) = -2\pi^2 \langle \underset{\sim}{k}' | T | \underset{\sim}{k} \rangle \tag{8}$$

where $\hat{\underset{\sim}{r}} = \hat{\underset{\sim}{k}}'$.

In actual calculations it is convenient to work with the K matrix defined by the relation

$$\langle \underset{\sim}{k}' \mid K \mid \underset{\sim}{k} \rangle = -\frac{\pi}{2} \langle \underset{\sim}{k}' \mid U \mid \psi_{\underset{\sim}{k}}^{(P)} \rangle \tag{9}$$

where $\psi_{\underset{\sim}{k}}^{(P)}$ is the scattering wavefunction for the standing wave boundary condition. The on-shell K matrix satisfies the relation

$$S = \frac{1 + iK}{1 - iK} . \tag{10}$$

Defining $K' = -\frac{2}{\pi} K$, the Lippman-Schwinger equation for the K' matrix is:

$$K' = U + U G_0^P K' \tag{11}$$

where G_0^P is the free-particle Green's function for the standing wave boundary condition.

To solve Eq. (4) the potential is projected onto a subspace of square-integrable functions $\{\varphi_\alpha\}$. This forms an N × N matrix generalization of the separable potential approximation:

$$V^t(\underset{\sim}{r}, \underset{\sim}{r}') = \sum_{\alpha, \beta} \varphi_\alpha(\underset{\sim}{r}) \langle \alpha \mid V \mid \beta \rangle \varphi_\beta^*(\underset{\sim}{r}') . \tag{12}$$

Inserting the truncated potential V^t, Eq. (4) becomes a matrix equation with solution

$$T^t = \left[1 - U^t G_0^+\right]^{-1} U^t . \tag{13}$$

The momentum representation of the on-shell T matrix is obtained by the transformation:

$$\langle \underset{\sim}{k}' | T | \underset{\sim}{k} \rangle = \sum_{\alpha,\beta} \langle \underset{\sim}{k}' | \alpha \rangle \langle \alpha | T | \beta \rangle \langle \beta | \underset{\sim}{k} \rangle \quad . \tag{14}$$

The truncated potential is constructed from a basis set of Cartesian Gaussian functions of the form

$$\mu_{\ell mn}^{\alpha \underset{\sim}{A}} = N_{\ell mn} (x - A_x)^{\ell} (y - A_y)^{m} (z - A_z)^{n} \, e^{-\alpha | \underset{\sim}{r} - \underset{\sim}{A}|^2} \tag{15}$$

where $N_{\ell mn}$ is a normalization factor. The basis function centers, denoted by $\underset{\sim}{A}$ in Eq. (15), are placed at the target nuclei and at the center of mass. Cartesian Gaussian functions are widely used in molecular bound state calculations due to their convenient analytical properties.[18] The matrix solution T^t involves Gaussian matrix elements of the free-particle Green's function

$$\langle \mu_i | G_0^+ (E) | \mu_j \rangle = \lim_{\epsilon \to 0^+} \int d^3k \, \frac{\langle \mu_i | \underset{\sim}{k} \rangle \langle \underset{\sim}{k} | \mu_j \rangle}{q^2 - k^2 + i\epsilon} \tag{16}$$

where $E = \frac{q^2}{2}$. Similarly, the matrix solution K^t involves Gaussian matrix elements of the free-particle Green's function

$$\langle \mu_i | G_0^P (E) | \mu_j \rangle = P \int d^3k \, \frac{\langle \mu_i | \underset{\sim}{k} \rangle \langle \underset{\sim}{k} | \mu_j \rangle}{q^2 - k^2} \tag{17}$$

where P denotes principal value integration.

As shown by Ostlund[16] these matrix elements can be reduced analytically to an error function with complex argument for which efficient algorithims exist.[21] Based on Ostlund's techniques for evaluating scattering integrals involving Gaussian and plane-wave function, we have developed a straightforward procedure for deriving formulas for matrix elements of G_0^+ (or G_0^P) involving Gaussians of

arbitrary center and symmetry type. Formulas for s- and p-type Gaussians have also been obtained by Ostlund.[17] A description of our analytical procedure and results for Gaussians of up to f-type symmetry will be published elsewhere.[22] Formulas for s- and p-type Gaussian matrix elements of G_0 are given in Appendix I.

In order to treat the target orientation dependence of the scattering analytically, we use a single-center expansion of the scattering amplitude. For simplicity consider the case of a linear molecule. In the body-fixed frame with z-axis along the internuclear axis, the wavefunction and scattering amplitude have the expansions:[1]

$$\psi_{\underset{\sim}{k}}^{+}(\underset{\sim}{r}) = \frac{4\pi}{(2\pi)^{3/2}} \sum_{\ell\ell' m} i^{\ell'} g_{\ell\ell' m}(kr)\, Y_{\ell m}(\hat{\underset{\sim}{r}})\, Y^{*}_{\ell' m}(\hat{\underset{\sim}{k}}) \ , \tag{18}$$

$$f_{\underset{\sim}{k}}(\hat{\underset{\sim}{r}}) = 4\pi \sum_{\ell\ell' m} f_{\ell\ell' m}(k)\, Y_{\ell m}(\hat{\underset{\sim}{r}})\, Y^{*}_{\ell' m}(\hat{\underset{\sim}{k}}) \ . \tag{19}$$

The radial wavefunctions have the asymptotic form:

$$g_{\ell\ell' m}(kr) \rightarrow \frac{2i}{kr} \left[\delta_{\ell\ell'} e^{-i(kr-\ell\pi/2)} - S_{\ell\ell' m} e^{i(kr-\ell\pi/2)}\right] \tag{20}$$

as $r \rightarrow \infty$. The single center expansion coefficients for the S matrix and the scattering amplitude are related according to:

$$f_{\ell\ell' m} = \frac{i^{\ell'-\ell}}{2ik} (S_{\ell\ell' m} - \delta_{\ell\ell'}) \ . \tag{21}$$

The single-center expansion of the on-shell T matrix is of the form

$$\langle \underset{\sim}{k}' \,|T|\, \underset{\sim}{k} \rangle = \frac{1}{k} \sum_{\ell\ell' m} i^{\ell'-\ell}\, T_{\ell\ell' m}(k)\, Y_{\ell m}(\hat{\underset{\sim}{k}}')\, Y^{*}_{\ell' m}(\hat{\underset{\sim}{k}}) \quad . \tag{22}$$

Equating the right-hand sides of Eqs. (14) and (22) and using the spherical expansion of a plane wave,

$$e^{i\underset{\sim}{k}\cdot\underset{\sim}{r}} = 4\pi \sum_{\ell m} i^{\ell} j_{\ell}(kr)\, Y_{\ell m}(\hat{\underset{\sim}{r}})\, Y^{*}_{\ell m}(\hat{\underset{\sim}{k}}) , \tag{23}$$

we obtain the single center expansion for T^t:

$$T^{t}_{\ell\ell' m} = \frac{2k}{\pi} \sum_{\alpha\beta} \langle j_{\ell}\, Y_{\ell m} | \alpha \rangle \langle \alpha | T | \beta \rangle \langle \beta | j_{\ell'}\, Y_{\ell' m} \rangle \quad . \tag{24}$$

Comparing equations (7), (21), and (24), shows

$$f_{\ell\ell' m} = -i^{\ell'-\ell} \sum_{\alpha\beta} \langle j_{\ell}\, Y_{\ell m} | \alpha \rangle \langle \alpha | T | \beta \rangle \langle \beta | j_{\ell'}\, Y_{\ell' m} \rangle \tag{25}$$

Noting that the single-center expansion of the K′ matrix has the same form as Eq. (22), and recalling that $K' = -\frac{2}{\pi} K$, we have

$$K^{t}_{\ell\ell' m} = -k \sum_{\alpha\beta} \langle j_{\ell}\, Y_{\ell m} | \alpha \rangle \langle \alpha | K' | \beta \rangle \langle \beta | j_{\ell'}\, Y_{\ell' m} \rangle \tag{26}$$

The transformations (24), (25), and (26) involve the matrix element

$\langle \mu_{pqs}^{\alpha A}(\underset{\sim}{r}) \mid j_\ell(kr)\, Y_{\ell m}(\hat{\underset{\sim}{r}}) \rangle$. As pointed out by Schneider,[23] these matrix elements may be evaluated analytically. The technique for evaluating the single-center transformation matrix elements and formulas for s- and p-type Gaussians are given in Appendix II.

It is convenient to express the scattering amplitude in the laboratory frame with z′-axis in the direction of incident momentum. Using the rotational properties of spherical harmonics and introducing the rotational harmonics defined in Edmonds,[24] we find that the scattering amplitude in the laboratory frame is given by

$$f_k(R,\underset{\sim}{\beta},\hat{\underset{\sim}{r}}') = 4\pi \sum_{\ell\ell' mm'} \sqrt{\frac{2\ell'+1}{4\pi}}\, f_{\ell\ell' m}(k,R)\, D^{(\ell)}_{m'm}(\underset{\sim}{\beta}) \times$$

$$\times\, D^{(\ell')*}_{om}(\beta)\, Y_{\ell m}(\hat{\underset{\sim}{r}}') \qquad (27)$$

where R denotes the internuclear separation (for a diatomic) and $\underset{\sim}{\beta}$ denotes the target orientation in the laboratory frame (in general a function of three Euler angles). The symbol $\hat{\underset{\sim}{r}}'$ denotes the scattering angles in the laboratory frame. Temkin et al. express the laboratory frame scattering amplitude in the form[25]

$$f_k(R,\underset{\sim}{\beta},\hat{\underset{\sim}{r}}') = \sum_{\ell\ell' mm'} a_{\ell\ell' m}(k,R) D^{(\ell)}_{m'm}(\underset{\sim}{\beta})\, D^{(\ell')*}_{om}(\underset{\sim}{\beta})\, Y_{\ell m}(\hat{\underset{\sim}{r}}') \,. \quad (28)$$

Comparing Eqs. (25),(27), and (28) yields the prescription for the fixed-nuclei dynamical coefficients:

$$a_{\ell\ell' m}(k,R) = -\sqrt{4\pi(2\ell'+1)}\, i^{\ell'-\ell} \times$$

$$\times \sum_{\alpha\beta} \langle j_\ell Y_{\ell m} | \alpha \rangle \langle \alpha | T | \beta \rangle \langle \beta | j_{\ell'} Y_{\ell' m} \rangle \,. \quad (29)$$

To calculate rotational excitation cross sections we use the adibatic nuclei approximation

$$f_k(\hat{\underset{\sim}{r}}';\Gamma' \leftarrow \Gamma) = \langle \Theta_{\Gamma'}(R,\underset{\sim}{\beta}) | f_k(R,\underset{\sim}{\beta},\hat{\underset{\sim}{r}}') | \Theta_\Gamma(R,\underset{\sim}{\beta}) \rangle \quad (30)$$

where Θ_Γ, $\Theta_{\Gamma'}$ are wavefunctions for the target nuclei. This approximation, due to Chase[26] and applied to electron-molecule scattering by Chang and Temkin,[27] is valid when the speed of the projectile is fast compared to the motion of the target nuclei.

The static-exchange approximation for the scattering potential is obtained by representing the electronic part of the scattering wavefunction by an anti-symmetrized product state

$$\Psi^+_{\underset{\sim}{k}} = \frac{1}{\sqrt{(N+1)!}} A\left[\Phi(1,2,\cdots,N)\psi^+_{\underset{\sim}{k}}(N+1)\right] \quad (31)$$

where Φ is the Hartree-Fock wavefunction for the target and $\psi_{\underset{\sim}{k}}^{+}$ is the wavefunction for the projectile. Substitution of the wavefunction (31) into Schrödinger's equation leads to the non-local static-exchange potential for a closed-shell target:

$$V = \sum_i - \frac{Z_i}{|\underset{\sim}{R}_i - \underset{\sim}{r}|} + \sum_j (2J_j - K_j) \tag{32}$$

where J and K are the usual Coulomb and exchange operators. The first term on the right-hand side of Eq. (32) is summed over target nuclei, the second is summed over occupied orbitals.

At very low scattering energies variational error due to the difference $V - V^t$ may be reduced by solving Eq. (4) at eigenenergies of the separable Hamiltonian

$$H^t = \sum_{\alpha\beta}{}' |\alpha\rangle \langle\alpha| H |\beta\rangle \langle\beta| \ . \tag{33}$$

To see this, consider the positive energy eigenfunctions $\chi_k(\underset{\sim}{r})$ which satisfy

$$H^t \chi_k = \frac{k^2}{2} \chi_k \ , \tag{34}$$

and are determined by diagonalization of H^t.

We are interested in the conditions under which the solution χ_k of Eq. (34) is proportional to the scattering wavefunction

$$\psi_{\underset{\sim}{k}}^{+} = \phi_{\underset{\sim}{k}} + G_o^{+} T^{t} \phi_{\underset{\sim}{k}} \tag{35}$$

Clearly, this is not true in general because the scattering wavefunction depends on the direction of the incident particle and this boundary condition is not taken into account in the diagonalization of H^t. However, at very low energy $\psi_{\underset{\sim}{k}}^{+}$ and χ_k are dominated by the lowest contributing partial wave and, hence, have approximately the same behavior at the origin. It follows that in this energy range $\psi_{\underset{\sim}{k}}^{t}$ and χ_k are approximately proportional,

$$\psi_{\underset{\sim}{k}}^{t} (\underset{\sim}{r}) \simeq C(k)\, \chi_k (\underset{\sim}{r}) , \tag{36}$$

if we assume that the effect of truncating the kinetic energy operator in H^t is small. The Kohn prescription for the variationally stable scattering amplitude is:[28]

$$f^{s}_{\underset{\sim}{k}', \underset{\sim}{k}} = f^{t}_{\underset{\sim}{k}', \underset{\sim}{k}} - 4\pi^2 \langle \psi^{t}_{\underset{\sim}{k}'} | (H - E) | \psi^{t}_{\underset{\sim}{k}} \rangle . \tag{37}$$

If our discrete basis set is adequate to represent χ_k beyond the effective range of the potential, then approximation (36) may be used in Eq. (37). Since χ_k is determined by a variationally stable procedure, the second term on the right hand side of Eq. (37) vanishes through first order. Hence

$$f^{s}_{\underset{\sim}{k}', \underset{\sim}{k}} \simeq f^{t}_{\underset{\sim}{k}', \underset{\sim}{k}} + O^2(V - V^t) \tag{38}$$

when $E = k^2/2$ is an eigenenergy of H^t.

III. CALCULATIONS AND RESULTS

The truncated static-exchange potential V^t is calculated in two steps. The first involves an SCF calculation for the occupied orbitals of the target. A standard basis set of contracted Cartesian Gaussian functions is used. In the second step matrix elements of the static-exchange potential, defined by Eq. (32), are computed over a larger set of uncontracted functions, called the scattering basis set. The scattering basis includes the primitive (uncontracted) Gaussians used in the target SCF calculation. This insures orthogonality between the scattering subspace and the target orbital subspace. This requirement may be relaxed under certain conditions as noted below. The scattering basis also includes functions which account for components of the scattering subspace which cannot be constructed from the target SCF basis. In this calculation the target basis set is augmented by adding diffuse functions at the center or on the nuclei.

The ground state of N_2 has the electron configuration $^1\Sigma_g(1\sigma_g)^2(1\sigma_u)^2(2\sigma_g)^2(2\sigma_u)^2(3\sigma_g)^2(1\pi_u)^4$. In the SCF calculation we use a $[4s\,3p_x\,3p_y\,3p_z\,2d_{xz}\,2d_{yz}\,2d_{zz}]$ contracted basis set on each nucleus plus two diffuse p_z functions on the center. The $[4s\,3p]$ basis is constructed from a (9s 5p) set of primitives using the contraction coefficients suggested by Dunning.[29] The choice of d-type functions, which are necessary to obtain an accurate quadrupole moment, is due to Truhlar et al.[30] The quadrupole moment for this basis is -1.02 a.u.

For a homonuclear diatomic the scattering potential is block diagonal in the symmetries $^2\Sigma_g$, $^2\Sigma_u$, $^2\Pi_u$, $^2\Pi_g$, ... and, hence, the

Lippman-Schwinger equation may be solved separately for each case. In this work we consider scattering in the Σ and Π channels. Table I lists the scattering basis sets for each symmetry. Target basis functions of d-type symmetry are omitted in the scattering basis sets since these functions have little effect at the incident energies considered. The basis set calculations are carried out using standard bound state molecular integral programs.

To investigate the convergence of the scattering basis set, we varied the basis functions for each symmetry in preliminary calculations. Alternate basis sets were constructed in several ways. The use of contracted basis functions was rejected due to the lack of a criterion for choosing the contraction coefficients. One would not expect the contraction coefficients used in the SCF calculation to be appropriate, and this was verified in test calculations. Adding diffuse functions at the nuclear centers instead of at the center of mass had little effect except in certain cases when this led to linear dependence problems associated with computer round-off error. This occurred, for example, when diffuse two-center s-type functions were included in the calculation for Σ_u symmetry. Varying the number of diffuse functions added to the SCF basis, or adding tight functions, also had little effect. At the scattering energies considered in this work little effect was found for d-type functions. These functions are probably more important at higher energy. The basis sets listed in Table 1 respresent a consensus of our experience with basis sets to date. Apart from fluctuations associated with variational instability, and within the constraints discussed above, our results are insensitive to changes in the basis set. We estimate the uncertainty in our cross sections due to lack of basis set convergence at about 20%. Below 2 eV this error may be larger.

In these calculations we work with the Lippman-Schwinger equation for the T matrix, Eq. (4), which is solved for each incident electron energy and scattering symmetry. The dynamical coefficients $a_{\ell\ell'm}$ of the fixed nuclei theory are then obtained using Eq.(29). For the range of scattering energies considered here, we find that the coupled partial-wave expansion for the scattering amplitude may be truncated with negligible error after 6 partial-waves.

In the fixed-nuclei approximation, the total elastic cross section is given by[25]

$$\sigma = \sum_{\ell\ell'm} |a_{\ell\ell'm}|^2/(2\ell'+1) \ . \tag{39}$$

Our results from 0.5 to 10 eV are shown in Fig. 1, together with the experimental data of Golden[19] and the static-exchange approximation

results of Burke and Sinfailam.[4] Vibrational structure present in the data of Golden is not shown. The peak in the cross sections is due to a shape resonance in the $^2\Pi_g$ channel.

Results obtained directly from T matrix calculations for a selected grid of incident momenta are indicated by x's in Fig. 1. Failure of these points to form a smooth curve is attributed to variational error in the difference $V-V^t$. As Fig. 1 shows, this effect is quite small for incident energies above 3 eV; however, below 3 eV the effect becomes large. Our results obtained directly from T matrix calculations for energies below 3 eV are shown in Fig. 2. Note that Fig. 2 is plotted in terms of incident electron momentum. As discussed in the preceding section, we expect a reduction in variational error at the eigenenergies of H^t. Since eigenenergies are different for different symmetries, an interpolation procedure must be used. In this work we interpolate the matrix elements of the on-shell, coupled partial-wave K matrix. For energies below the $^2\Pi_g$ resonance, these matrix elements are slowly varying. Our results obtained by interpolation from T matrix calculations at eigenenergies of H^t are shown by the solid curve in Fig. 2 and by the +'s in Fig. 1. At very low energy the slope of the total elastic cross section should approach zero (for S-wave scattering in the static-exchange approximation). Instead, below $k = 0.2$ a.u. our results obtained by interpolation drop off anomolously. We attribute this behavior to the basis set approximation for the potential which becomes increasingly inadequate at very low energy. The dashed line in Fig. 2 shows the diagonal phase shift results of McCurdy et al.[12]

The momentum transfer cross section is defined by

$$\sigma_m = \int d(\cos\theta) \frac{d\sigma}{d(\cos\theta)} (1 - \cos\theta) \ . \tag{40}$$

Setting

$$\frac{d\sigma}{d(\cos\theta)} = \tfrac{1}{2} \sum_L A_L P_L (\cos\theta) \ , \tag{41}$$

we have

$$\sigma_m = A_0 - \tfrac{1}{3} A_1 \tag{42}$$

In the fixed-nuclei approximation, the expansion coefficients for the differential cross section are given by:[7]

$$A_L = \frac{1}{2L+1} \sum_{\ell\ell'\lambda\lambda' m\mu} \sqrt{(2\ell+1)(2\lambda+1)}(\ell\lambda 00 \mid L0)(\ell'\lambda' 00 \mid L0) \times$$

$$(\ell\lambda m\mu \mid Lm+\mu)(\ell'\lambda' m\mu \mid Lm+\mu) a_{\ell\ell' m} a^*_{\lambda\lambda'\mu}, \tag{43}$$

where $(\ell_1\ell_2 m_1 m_2 \mid \ell_3 m_3)$ is a Clebsch-Gordon coefficient. Our results for σ_m are shown in Fig. 3 with the results of Burke and Sinfailam[4] and the data, inferred from swarm experiments, of Englehardt et al.[20]

In the adiabatic-nuclei approximation the total rotational excitation cross section is given by:[27]

$$\sigma_{j\to j'} = \frac{k_{j'}}{k_j} \sum_{\ell\ell' m\mu} a_{\ell\ell' m}\, a^{*}_{\ell\ell'\mu}\, \frac{(-1)^{m+n}}{(2\ell'+1)} \times$$

$$\times \sum_{J} (\ell\ell' m, -m \,|J0)\,(\ell\ell'\mu, -\mu \,|J0)\,(jJ00\,|j0)^2 . \qquad (44)$$

In this work we set the ratio $k_{j'}/k_j$ equal to unity. Our results and the results of Burke and Sinfailam are shown in Fig. 4. Note that $\sigma_{0\to 4}$ is larger than $\sigma_{0\to 2}$ in the resonance region, indicating the nearly pure d-wave character of the resonance.

IV. DISCUSSION AND CONCLUSIONS

This calculation shows that useful electron-molecule scattering information can be obtained using moderately sized basis sets and working entirely within the discrete basis function subspace. Two methods of improving the accuracy of our results are currently being investigated. One approach is to improve the flexibility of the basis set by adding Gaussian functions of d-type and higher symmetry. The other approach involves the calculation of a variational correction for errors in the scattering amplitude due to the difference $V\text{-}V^t$.

A method for computing a variational correction for the K matrix is currently being applied to e-H_2 elastic scattering and will be described in a future paper. Preliminary results indicate good convergence properties for the scattering basis sets of the type used in the present calculation.

The discrepancy between our results and the diagonal phase shift results of McCurdy et al[12] below 2 eV is not understood and will be investigated further. In this energy range the approximation involved in the "low-ℓ-spoiling" method of McCurdy et al should be valid.

An important feature of our method for calculating the dynamical coefficients $a_{\ell\ell'm}$ of the fixed-nuclei theory of Temkin et al[25] is that it does not involve single-center expansions of the potential or scattering wavefunction as part of the solution of the scattering problem. Thus the usual convergence questions concerning these expansions do not arise in our method.

The dynamical coefficients $a_{\ell\ell'm}$ refer to the asymptotic part of the scattering wavefunction and converge rapidly at low incident energy since then only partial waves with low ℓ are significantly scattered by the target. In the case of e-N_2 scattering below 10 eV we find that the coefficients $a_{\ell\ell'm}$, $\ell, \ell' = 0, 1, \ldots, 5$; $m = 0, \pm 1$ are sufficient to describe the scattering amplitude. This partial wave expansion for the scattering amplitude should not be confused with the expansion for the total scattering wavefunction. At low incident energy many more partial waves contribute to the scattering wavefunction in the region of the target molecule than contribute in the asymptotic region. The high ℓ partial wave components of the scattering wavefunction are due to singularities in the potential at the target nuclei.

Morrison and Collins[31] have recently analyzed the partial wave close-coupling method for e-N_2 scattering in the static approximation. They find that convergence of the $^2\Sigma_g$ cross section requires that partial waves be included up to: $\lambda = 14$ in the multipole expansion of the electronic part of the potential, $\lambda = 28$ in the multipole expansion of the nuclear part of the potential, and $\ell = 26$ in the expansion of the

scattering wavefunction. In contrast the partial wave close-coupling calculation of Burke and Sinfailam for $e\text{-}N_2$ scattering in the static-exchange approximation includes only $\lambda = 0, 2, 4$ in the multipole expansion for the static potential and $\ell = 0, 2, 4, 6$ in the partial wave expansion for the $^2\Sigma_g$ scattering wavefunction. Morrison and Collins show that the unconverged static potential $^2\Sigma_g$ cross section lies above the converged result at low incident energy. Figure 1 of this work shows that the total scattering cross section of Burke and Sinfailam is a factor of two larger than ours at 1 eV incident energy. Thus it is probable that lack of convergence in the calculation of Burke and Sinfailam accounts for most of the discrepancy between their results and ours. Buckley and Burke[6] have recently analyzed the calculation of Burke and Sinfailam and they find that the latter's results are not converged. Unfortunately, Buckley and Burke do not present their own static-exchange results for $e\text{-}N_2$ scattering.

Our results show that the static-exchange approximation for scattering is in qualitative agreement with experimental results for the total elastic and the momentum transfer cross sections although polarization and other electron correlation effects are clearly important. The displacement of our resonance peak to about 1.5 eV above the position observed experimentally, and the rapid drop in the experimental cross section below 0.5 eV incident energy are attributed primarily to polarization of the target by the scattered electron. Methods for including polarization in our prescription for scattering are currently being investigated.

ACKNOWLEDGMENTS

We thank Dr. T. N. Rescigno for many helpful discussions during the course of this work. We also thank Dr. N. S. Ostlund for helpful correspondence and for sending us his results for p-type Gaussian matrix elements of the free-particle Green's function prior to publication. One of us (A. W. F.) thanks Dr. A. Temkin for an enlightening discussion regarding the single center expansion for the scattering amplitude. We thank Professor W. A. Goddard III for making his molecular bound state computer codes available and B. Olafson for help with these programs.

APPENDIX I: GAUSSIAN MATRIX ELEMENTS OF FREE-PARTICLE GREEN'S FUNCTION

The Fourier transform of a normalized Cartesian Gaussian is given by

$$\langle \mu^{\alpha \underset{\sim}{A}}_{\ell mn} | \underset{\sim}{k} \rangle = \frac{(\frac{2\pi}{\alpha})^{3/4} \, i^{\ell+m+n}}{\sqrt{(2\ell-1)!!(2m-1)!!(2n-1)!!}} H_\ell(\frac{k_x}{2\sqrt{\alpha}}) \times$$

$$\times H_m(\frac{k_y}{2\sqrt{\alpha}}) H_n(\frac{k_z}{2\sqrt{\alpha}}) e^{i\underset{\sim}{k}\cdot\underset{\sim}{A} - k^2/4\alpha} \qquad \text{(A1)}$$

where $H_\ell(x)$ is a Hermite polynomial. Substituting (A1) into the Fourier integral representation for Gaussian matrix elements of the free-particle Green's function Eq. (16),

$$\langle \mu^{\alpha \underset{\sim}{A}}_{\ell mn} | G_0^+(E) | \mu^{\beta \underset{\sim}{B}}_{\ell' m' n'} \rangle = -\frac{\sqrt{2}}{\sqrt{\pi}\,(\alpha\beta)^{3/4}} \times$$

$$\times [(2\ell-1)!!(2\ell'-1)!!(2m-1)!!(2m'-1)!!(2n-1)!!(2n'-1)!!]^{-1/2} \times$$

$$\times \; i^{\ell-\ell'+m-m'+n-n'} \times \int d^3k \, \frac{e^{-ak^2+i\underset{\sim}{k}\cdot\underset{\sim}{R}}}{k^2-q^2-i\epsilon} \times$$

$$\times \; H_\ell(\frac{k_x}{2\sqrt{\alpha}}) H_{\ell'}(\frac{k_x}{2\sqrt{\beta}}) H_m(\frac{k_y}{2\sqrt{\alpha}}) H_{m'}(\frac{k_y}{2\sqrt{\beta}}) H_n(\frac{k_z}{2\sqrt{\alpha}}) H_{n'}(\frac{k_z}{2\sqrt{\beta}}) \qquad \text{(A2)}$$

where ϵ is a positive infinitesimal, $E = q^2/2$, and

$$a = \frac{\alpha + \beta}{4\alpha\beta} \quad . \tag{A3}$$

Substituting the spherical expansion for a plane wave, Eq. (22), for $e^{i\underset{\sim}{k}\cdot\underset{\sim}{R}}$ in Eq. (A1), and carrying out the angular integrations, the following formulas for Σ and Π symmetries and s- and p-type functions are obtained:

$$\langle \mu_{000}^{\alpha\underset{\sim}{A}} \mid G_0^+ \mid \mu_{000}^{\beta\underset{\sim}{B}} \rangle = A I_0^2 \tag{A4.1}$$

$$\langle \mu_{001}^{\alpha\underset{\sim}{A}} \mid G_0^+ \mid \mu_{000}^{\beta\underset{\sim}{B}} \rangle = \frac{A}{\sqrt{\alpha}} P_1(\hat{\underset{\sim}{R}}) I_1^3 \tag{A4.2}$$

$$\langle \mu_{001}^{\alpha\underset{\sim}{A}} \mid G_0^+ \mid \mu_{001}^{\beta\underset{\sim}{B}} \rangle = \frac{A}{\sqrt{\alpha\beta}} \left[-\tfrac{2}{3} P_2(\hat{\underset{\sim}{R}}) I_2^4 + \tfrac{1}{3} I_0^4 \right] \tag{A4.3}$$

$$\langle \mu_{100}^{\alpha\underset{\sim}{A}} \mid G_0^+ \mid \mu_{100}^{\beta\underset{\sim}{B}} \rangle = \frac{A}{\sqrt{\alpha\beta}} \left[-\sqrt{\frac{2\pi}{15}} Q_{22}(\hat{\underset{\sim}{R}}) I_2^4 + \tfrac{1}{3} P_2(\hat{\underset{\sim}{R}}) \times \right.$$

$$\left. \times \; I_2^4 + \tfrac{1}{3} I_0^4 \right] \quad . \tag{A4.4}$$

In Eqs. (A4.1) to (A4.4), the integrations over k are denoted by

$$I_L^n = \int_0^\infty \frac{dk\, k^n e^{-ak^2}}{k^2 - q^2 - i\epsilon} j_L(kR) \tag{A5}$$

where $j_L(kR)$ is a spherical Bessel junction. The constant

$$A = \sqrt{\frac{2}{\pi}}\,(\alpha\beta)^{-3/4}\,, \tag{A6}$$

$P_L(\hat{\underset{\sim}{R}})$ is a Legendre polynomial, and

$$Q_{LM} = Y_{LM}(\hat{\underset{\sim}{R}}) + Y_{L-M}(\hat{\underset{\sim}{R}})\ . \tag{A7}$$

As shown in reference 15, the principal value part of this integral may be reduced to an error function with complex argument. Explicit expressions for the real (principal value) part of the integrals appearing in Eq. (A4) are:

$$\mathrm{Re}\,I_0^2 = \frac{\pi}{2R}\,e^{-aq^2}\,\mathrm{Re}\left[e^{iqR}\,\mathrm{erf}\left(\frac{R}{2\sqrt{a}} + i\sqrt{aq}\right)\right] \tag{A8.1}$$

$$\mathrm{Re}\,I_0^4 = q^2\,\mathrm{Re}\,I_0^2 + \frac{\sqrt{\pi}}{4}\,a^{-3/2}\,e^{-R^2/4a} \tag{A8.2}$$

$$\mathrm{Re}\,I_1^3 = \frac{\pi}{2}\,e^{-aq^2}\,\mathrm{Re}\left[\left(\frac{1}{R^2} - \frac{iq}{R}\right)e^{iqR}\,\mathrm{erf}\left(\frac{R}{2\sqrt{a}} + i\sqrt{aq}\right) - \right.$$

$$\left. - \frac{\sqrt{\pi}}{2}\,e^{-R^2/4a}\,\frac{a^{-1/2}}{R}\right] \tag{A8.3}$$

$$\mathrm{Re}\,I_2^4 = \frac{3}{R}\,\mathrm{Re}\,I_1^3 - \mathrm{Re}\,I_0^4 \tag{A8.4}$$

The imaginary parts are given by

$$\mathrm{Im}\, I_L^n = -\frac{\pi}{2}\, q^{n-1}\, e^{-aq^2}\, j_L(qR)\,. \tag{A9}$$

APPENDIX II: BESSEL GAUSSIAN OVERLAP INTEGRALS

To derive analytic formulas for the transformation matrix elements $\langle \mu^{\alpha \underset{\sim}{A}}_{\ell mn}(\underset{\sim}{r}) | j_\ell(kr) Y_{\ell m}(\hat{\underset{\sim}{r}}) \rangle$, we insert the spherical expansion for a plane wave, Eq. (22), on both sides of Eq. (A1), the Fourier transform of a Gaussian, and equate coefficients of $Y^*_{LM}(\hat{\underset{\sim}{k}})$. For an s-type Gaussian we have immediately:

$$\langle \mu^{\alpha \underset{\sim}{A}}_{000} | j_L Y_{LM} \rangle = (\frac{2\pi}{\alpha})^{3/4} e^{-k^2/4\alpha} j_L(kA) Y_{LM}(\hat{\underset{\sim}{A}}) . \qquad (A10)$$

Derivation of formulas for Gaussian of higher symmetry is straightforward. For p-type Gaussians we obtain:

$$\langle \mu^{\alpha \underset{\sim}{A}}_{001} | j_L Y_{LM} \rangle = (\frac{2\pi}{\alpha})^{3/4} \frac{k}{\sqrt{\alpha}} e^{-k^2/4\alpha} \left[\sqrt{\frac{(L-M)(L+M)}{(2L+1)(2L-1)}} j_{L-1}(kA) Y_{L-1,M}(kA) - \right.$$

$$\left. - \sqrt{\frac{(L+M+1)(L-M+1)}{(2L+1)(2L+3)}} j_{L+1}(kA) Y_{L+1,M}(\hat{\underset{\sim}{A}}) \right] \qquad (A11.1)$$

$$\langle \mu^{\alpha \underset{\sim}{A}}_{100} | j_L Y_{LM} \rangle = (\frac{2\pi}{\alpha})^{3/4} \frac{k}{2\sqrt{\alpha}} e^{-k^2/4\alpha} \times$$

$$\times \left\{ \sqrt{\frac{(L-M)(L-M-1)}{(2L+1)(2L-1)}} j_{L-1}(kA) Y_{L-1,M+1}(\hat{\underset{\sim}{A}}) + \right.$$

$$+ \sqrt{\frac{(L+M+2)(L+M+1)}{(2L+1)(2L+3)}}\, j_{L+1}(kA)\, Y_{L+1,M+1}(\hat{\underset{\sim}{A}}) \quad -$$

$$- \sqrt{\frac{(L+M)(L+M-1)}{(2L+1)(2L-1)}}\, j_{L-1}(kA)\, Y_{L-1,M-1}(\hat{\underset{\sim}{A}}) \quad -$$

$$- \sqrt{\frac{(L-M+2)(L-M+1)}{(2L+1)(2L+3)}}\, j_{L+1}(kA)\, Y_{L+1,M-1}(\hat{\underset{\sim}{A}}) \Bigg\} \qquad \text{(A11.2)}$$

$$\langle \mu_{010}^{\alpha \underset{\sim}{A}} | j_L Y_{LM} \rangle = i\left(\frac{2\pi}{\alpha}\right)^{3/4} \frac{k}{2\sqrt{\alpha}}\, e^{-k^2/4\alpha} \quad \times$$

$$\times \Bigg\{ \sqrt{\frac{(L-M)(L-M-1)}{(2L+1)(2L-1)}}\, j_{L-1}(kA)\, Y_{L-1,M+1}(\hat{\underset{\sim}{A}}) \quad +$$

$$+ \sqrt{\frac{(L+M+2)(L+M+1)}{(2L+1)(2L+3)}}\, j_{L+1}(kA)\, Y_{L+1,M+1}(\hat{\underset{\sim}{A}}) \quad +$$

$$+ \sqrt{\frac{(L+M)(L+M-1)}{(2L+1)(2L-1)}}\, j_{L-1}(kA)\, Y_{L-1,M-1}(\hat{\underset{\sim}{A}}) \quad +$$

$$+ \sqrt{\frac{(L-M+2)(L-M+1)}{(2L+1)(2L+3)}}\, j_{L+1}(kA)\, Y_{L+1,M-1}(\hat{\underset{\sim}{A}}) \Bigg\} \qquad \text{(A11.3)}$$

Footnotes and References

*Supported by a grant from the National Science Foundation.

†National Science Foundation/Undergraduate Research Participant, Summer Program 1976.

‡Contribution No. 5489

[1] K. Takayanagi, Progress Theor. Phys. (Kyoto) Suppl. 40, 216 (1967).

[2] D. E. Golden, N. F. Lane, A. Temkin, and E. Gerjuoy, Rev. Mod. Phys. 43, 642 (1971).

[3] A. Temkin, Comm. Atomic and Molecular Phys. 5, 129 (1976).

[4] P. G. Burke and A. L. Sinfailam, J. Phys. B 3, 641 (1970).

[5] N. Chandra and A. Temkin, Phys. Rev. A 13, 188 (1976).

[6] B. D. Buckley and P. G. Burke, Scattering of low energy electrons by diatomic molecules (preprint).

[7] N. Chandra, Phys. Rev. A 12, 2342 (1975).

[8] M. A. Morrison, L. A. Collins, and N. F. Lane, Chem. Phys. Lett. 42, 356 (1976).

[9] D. G. Truhlar, M. A. Brandt, A. Chutjian, S. K. Srivastava, and S. Trajmar, J. Chem. Phys. 65, 2962 (1976).

[10] T. N. Rescigno, C. W. McCurdy, Jr., and V. McKoy, Phys. Rev. A 11, 825 (1975).

[11] B. I. Schneider, Phys. Rev. A 11, 1957 (1975).

[12] C. W. McCurdy, Jr., T. N. Rescigno, and V. McKoy, J. Phys. B 9, 691 (1976).

[13] B. I. Schneider and P. J. Hay, Phys. Rev. A 13, 2049 (1976).

[14] T. N. Rescigno, C. W. McCurdy, Jr., and V. McKoy, Chem. Phys. Lett. 27, 401 (1974).

[15] T. N. Rescigno, C. W. McCurdy, Jr., and V. McKoy, Phys. Rev. A 10, 2240 (1974).

[16] N. S. Ostlund, Chem. Phys. Lett. 34, 419 (1975).

[17] N. S. Ostlund, private communication.

[18] I. Shavitt, Methods of Theoretical Physics (Academic, New York, 1963), Vol. II.

[19] D. E. Golden, Phys. Rev. Lett. 17, 847 (1966).

[20] A. M. Englehardt, A. V. Phelps, C. G. Risk, Phys. Rev. 135, A1566 (1964).

[21] W. Gautschi, SIAM J. Num. Anal. 7, 187 (1970).

[22] D. A. Levin, A. W. Fliflet, M. Ma, and V. McKoy, J. Comp. Phys., (to be published).

[23] B. I. Schneider, Chem. Phys. Lett. 25, 140 (1974).

[24] A. R. Edmonds, Angular Momentum in Quantum Mechanics (Princeton University Press, Princeton, 1960).

[25] A. Temkin, K. V. Vasavada, E. S. Chang, and A. Silver, Phys. Rev. 186, 57 (1969).

[26] D. M. Chase, Phys. Rev. 104, 838 (1956).

[27] E. S. Chang and A. Temkin, Phys. Rev. Lett. 23, 399 (1969).

[28] N. F. Mott and H. S. W. Massey, The Theory of Atomic Collisions (Oxford, London, 1965) p. 133.

[29] T. H. Dunning, J. Chem. Phys. 53, 2823 (1970).

[30] D. G. Truhlar, F. A. Van-Catledge, and J. H. Dunning, J. Chem. Phys 57, 4788 (1972).

[31] M. A. Morrison and L. A. Collins, J. Phys. B, accepted for publication.

TABLE I. Scattering basis sets

$^2\Sigma_g$			$^2\Sigma_u$		
$\underset{\sim}{A}^1$=(0,0,±1.034)	(0,0,±1.034)	(0,0,0)	$\underset{\sim}{A}$=(0,0,±1.034)	(0,0,±1.034)	(0,0,0)
$(\ell, m, n)^2$=(0,0,0)	(0,0,1)	(0,0,0)	(ℓ, m, n)=(0,0,0)	(0,0,1)	(0,0,1)
5909.44	26.786	0.128	5909.44	26.786	0.1
887.451	5.9564	0.0768	887.451	5.9564	0.06
204.749	1.7074	0.0461	204.749	1.7074	0.036
59.837	0.5314	0.0276	59.837	0.5314	0.0216
19.9981	0.1654	0.0166	19.9981	0.1654	0.0130
2.686		0.00995	2.686		0.0078
7.1927		0.00597	7.1927		0.003
0.7		0.003	0.7		0.0015
0.213		0.0015	0.213		
		0.006			

$^2\Pi_u$		$^2\Pi_g$	
$\underset{\sim}{A}$=(0,0,±1.034)	(0,0,0)	$\underset{\sim}{A}$=(0,0,±1.034)	
(ℓ, m, n)=(1,00)	(1,0,0)	(ℓ, m, n)=(1,0,0)	
26.786	0.0992	26.786	0.0357
5.9564	0.0595	5.9564	0.0214
1.7074	0.0357	1.7074	0.0129
0.5314	0.0214	0.5314	0.00772
0.276	0.0129	0.276	0.00463
0.1654	0.00772	0.1654	0.00278
	0.004	0.0992	0.00167
	0.002	0.0595	0.001
	0.0007		

[1] $\underset{\sim}{A}$ denotes the coordinates of the center of the basis function $\mu^{\alpha \underset{\sim}{A}}_{\ell mn}(\underset{\sim}{r})$.

[2] (ℓ, m, n) denotes the symmetry type of $\mu^{\alpha \underset{\sim}{A}}_{\ell mn}(\underset{\sim}{r})$.

FIG. 1. Total scattering cross section. Broken solid line: this work. The crosses indicate results obtained directly from T matrix calculations. The plusses indicate results obtained from T matrix calculations at eigenenergies and interpolation of K matrix. Circles: experimental data of Golden,[19] observed vibrational substructure is not shown. Dashed line: static-exchange results of Burke and Sinfailam.[4]

FIG. 2. Total cross section below $^2\Pi_g$ resonance. Crosses are defined as in Fig. 1. Solid line: results obtained by interpolation from T matrix calculation at eigenenergies. Dashed line: diagonal phase shift results of McCurdy et al.[12]

FIG. 3. Momentum transfer cross section. Broken solid line: this work. Crosses and plusses are defined as in Fig. 1. Circles: experimental data of Englehardt et al.[20] Dashed line: static exchange results of Burke and Sinfailam.

FIG. 4. Rotational excitation cross sections. Solid lines: this work. Dashed lines: results of Burke and Sinfailam.

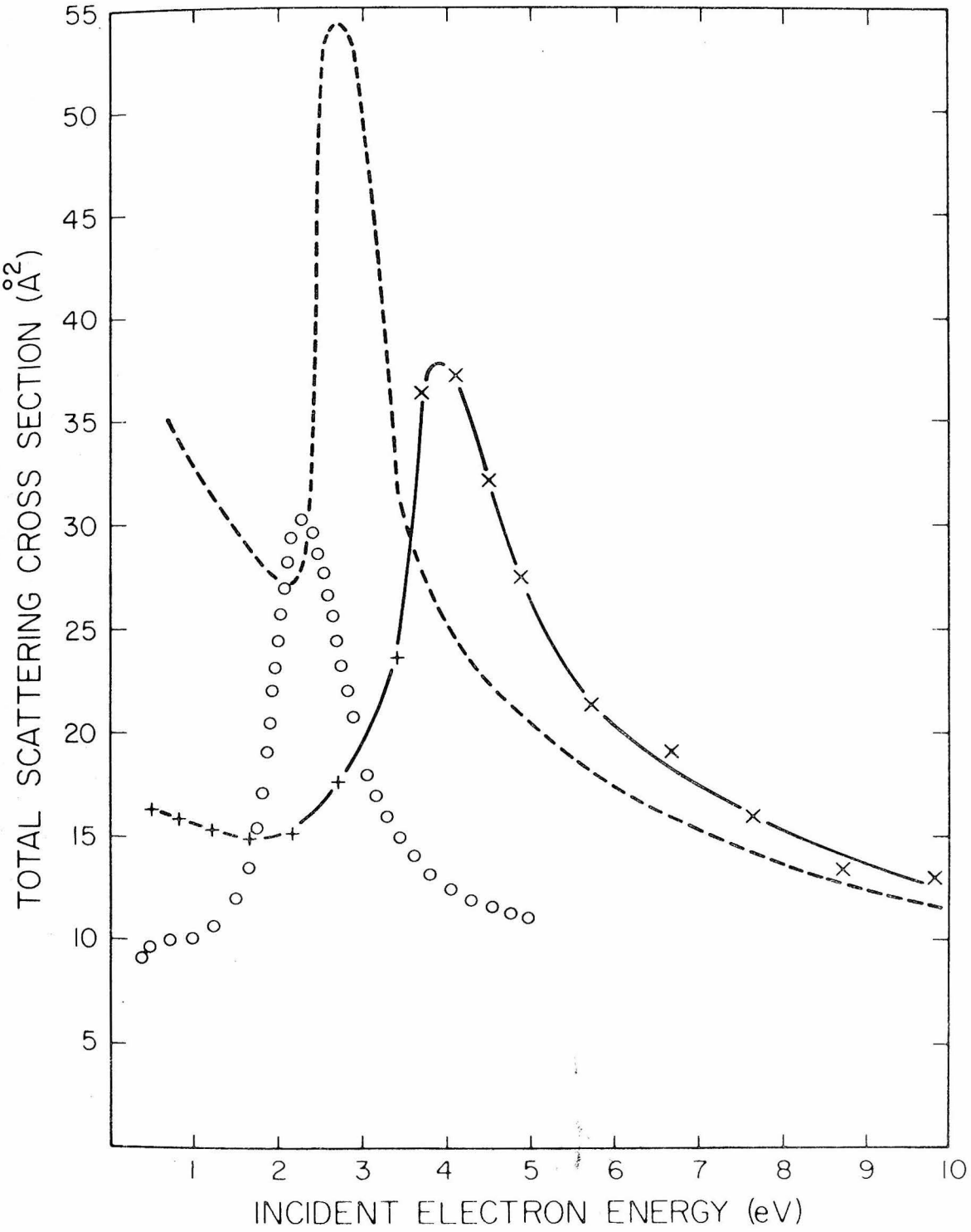
TOTAL SCATTERING CROSS SECTION (Å²)
INCIDENT ELECTRON ENERGY (eV)
55
50
45
40
35
30
25
20
15
10
5
1
2
3
4
5
6
7
8
9
10

Figure 1

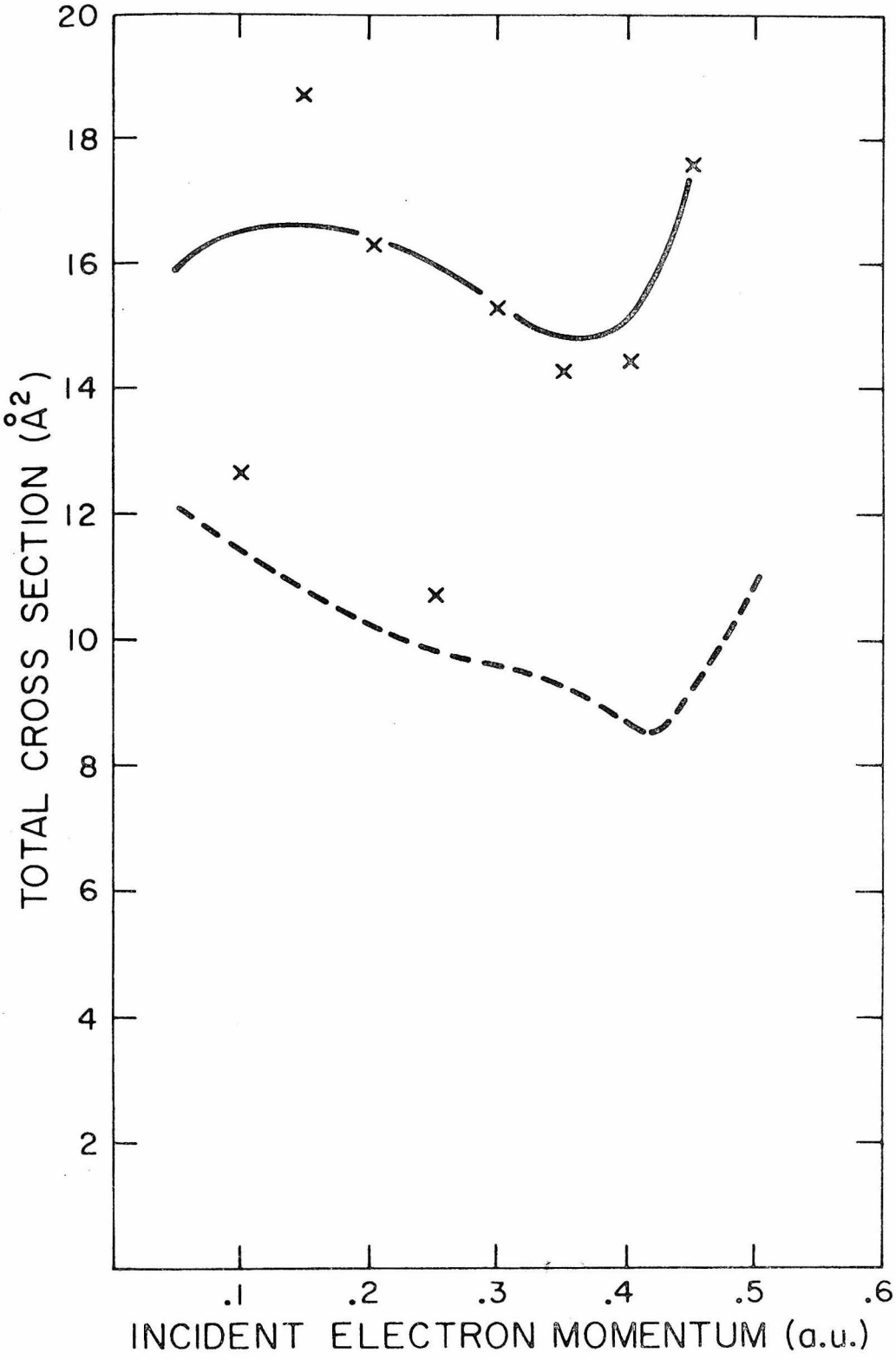
20
18
16
14
12
10
8
6
4
2
TOTAL CROSS SECTION (Å²)
.1
.2
.3
.4
.5
.6
INCIDENT ELECTRON MOMENTUM (a.u.)

Figure 2

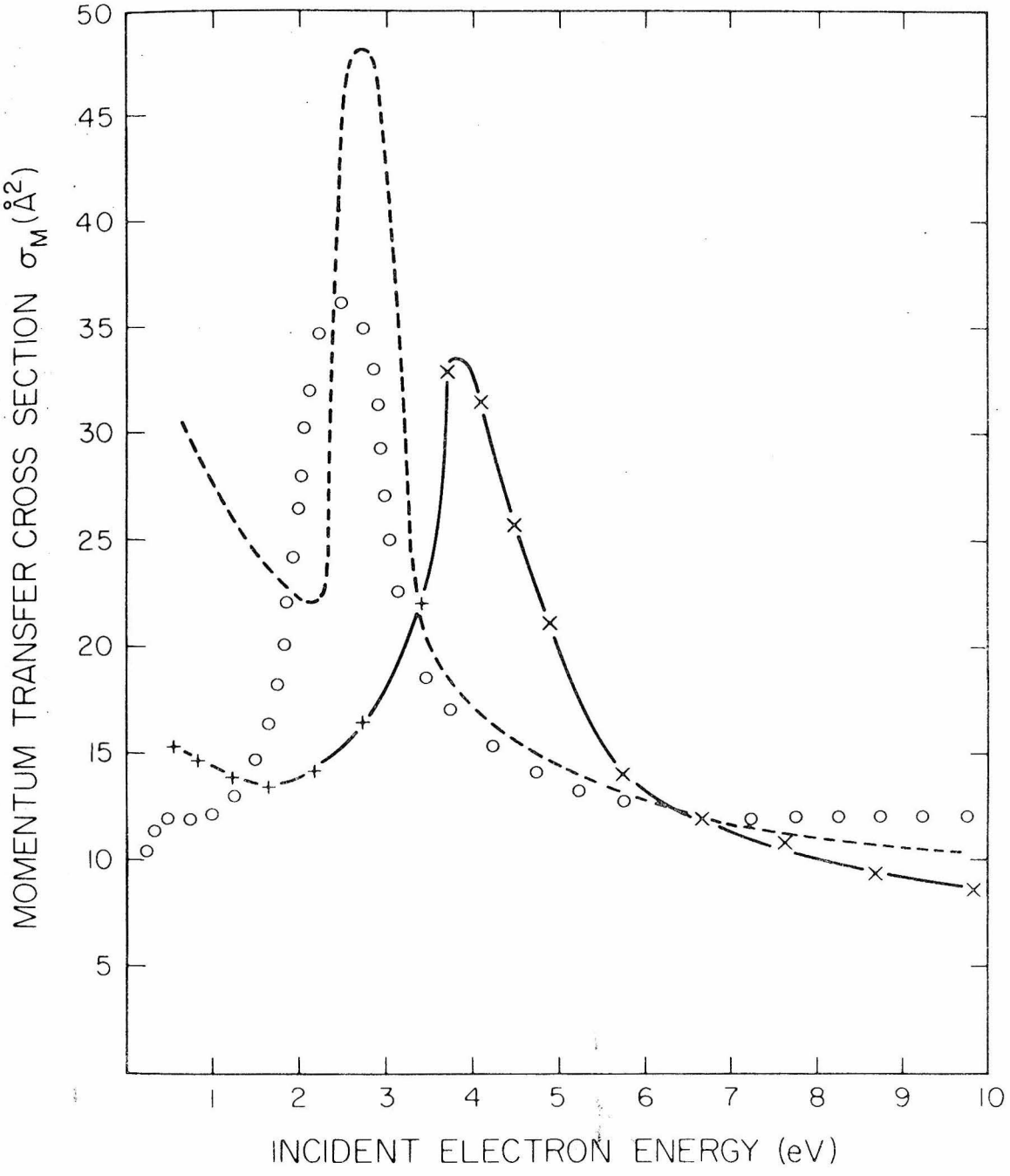
MOMENTUM TRANSFER CROSS SECTION $\sigma_M(Å^2)$
50
45
40
35
30
25
20
15
10
5
1
2
3
4
5
6
7
8
9
10
INCIDENT ELECTRON ENERGY (eV)

Figure 3

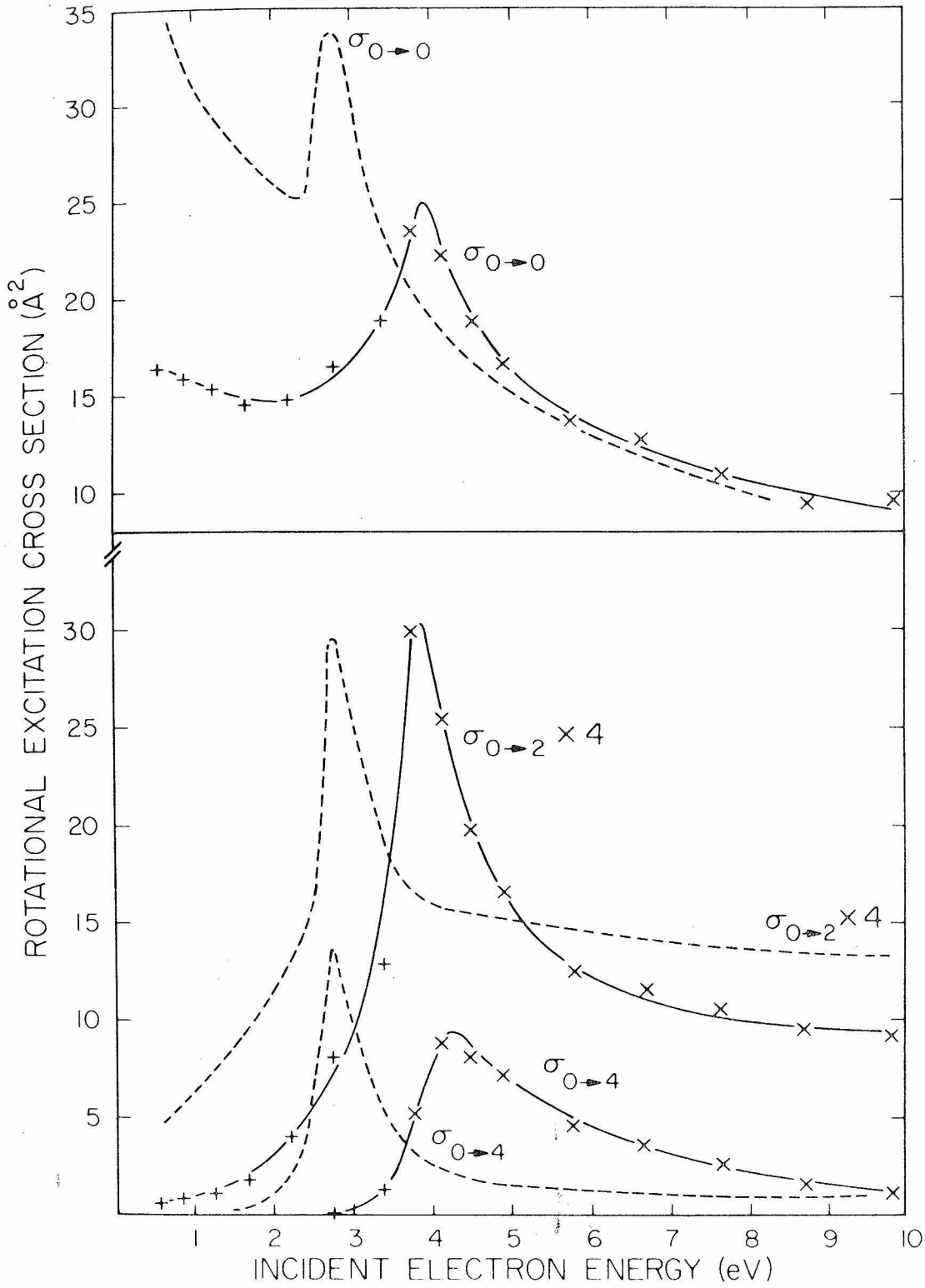
ROTATIONAL EXCITATION CROSS SECTION (Å²)
INCIDENT ELECTRON ENERGY (eV)
σ0→0
σ0→0
σ0→2 × 4
σ0→2 × 4
σ0→4
σ0→4

Figure 4

SECTION B

Low Energy e^--CO Scattering in the Static-exchange Approximation

I. INTRODUCTION

Ab initio calculations are an important source of dynamical information for low-energy electron-molecule collision processes. The complexity of these calculations has limited applications for the most part to simple homonuclear diatomics such as H_2,[1,2] N_2,[3,4] and F_2.[5] Elastic scattering by N_2 has received particular attention because the $^2\Pi_g$ shape resonance is characteristic of low-energy electron scattering by molecules.[6] Several calculations have shown that the static-exchange approximation for the electron-molecule interaction potential accounts for most of the dynamical features of e^- - N_2 scattering even though polarization effects are not included.[3,4,7] Advantages of the static-exchange approximation are that it involves no adjustable parameters and it treats the exchange interaction correctly.

An important test of a theoretical model is the ability to correctly reproduce dynamical trends when applied to different systems. In this regard it is of interest to apply the static-exchange approximation to low-energy e^- - CO scattering, especially in light of the considerable theoretical attention given to the isoelectronic e^- - N_2 system. The absence of inversion symmetry in CO introduces important new dynamical features due to the strong coupling between odd and even partial waves and the presence of a permanent dipole moment. However, one expects a strong family resemblance between the cross sections and resonance parameters of these two isoelectronic systems. In the case of N_2 and CO this has been verified experimentally as discussed

in a review by Schulz.[6]

More recently, experimental data for the momentum transfer cross section of CO have been obtained by Land,[8] and semi-empirical results for the resonance parameters of the $^2\Pi$ resonance in CO have been obtained by Zubek and Szmytkowski.[9] Theoretical results for e^-- CO scattering have been obtained by Chandra[10] from a numerical close-coupling calculation which used a pseudopotential plus a semi-empirical polarization potential.

This paper reports a theoretical study of low-energy e^-- CO scattering in the static exchange approximation. The theoretical approach is the T-matrix discrete-basis-set method for electron-molecule scattering introduced by Rescigno, McCurdy, and McKoy,[11] and developed by McKoy and coworkers.[4,12] This approach has been successfully applied to electron scattering by H_2[11-13] and N_2[4,7] in the static-exchange approximation. The method makes use of a separable form of the potential

$$V^t = \sum_{\alpha\beta} | \alpha \rangle \langle \alpha | V | \beta \rangle \langle \beta | \qquad (1)$$

where $\{| \alpha \rangle\}$ is a finite set of Gaussian functions. The scattering amplitude or the K-matrix for the truncated potential V^t contains errors due to the difference $V - V^t$. These errors are corrected to first order by application of the variational formula for the partial-wave K-matrix[12]

$$K^{s}_{\ell\ell' m} = K^{t}_{\ell\ell' m} + 2k \langle \psi_{k\ell m} | (V - V^{t}) | \psi^{t}_{k\ell' m} \rangle , \qquad (2)$$

where $\psi^{t}_{k\ell m}$ is a scattering wave function for the potential V^{t}.

This study considers the energy region in which the scattering is dominated by short-range interactions. Thus, only low partial-wave elements of the K-matrix are important and the effect of the long-range dipole moment is small. Eigenphases and eigenphase sums are presented for the $^{2}\Sigma$ and $^{2}\Pi$ scattering symmetries. The width and position of the $^{2}\Pi$ shape resonance is obtained from the eigenphase sum. The momentum transfer cross section is calculated in the fixed-nuclei approximation.

II. THEORY

In the fixed-nuclei approximation the Schrödinger equation for an elastically scattered electron is of the form:

$$[-\nabla^{2} + U(R, \vec{r}) - k^{2}] \psi_{\vec{k}}(R, \vec{r}) = 0 \qquad (3)$$

where $U = 2V$ and R is the internuclear separation for a diatomic. Except as noted, atomic units are assumed throughout. The incident-direction dependence of the scattering wave function may be expanded in the partial-wave series

$$\psi_{k}(\vec{r}) = \sqrt{\frac{2}{\pi}} \sum_{\ell m} i^{\ell} \psi_{k\ell m}(\vec{r}) \, Y^{*}_{\ell m}(\hat{k}) \qquad (4)$$

In the case of a linear target with internuclear axis along the z-axis, $\psi_{k\ell m}$ may in turn be expanded in the partial-wave series

$$\psi_{k\ell m}(\vec{r}) = \sum_{\ell'} g_{\ell\ell' m}(k, r)\, Y_{\ell' m}(\hat{r}) \tag{5}$$

Equation (5) defines a set of radial continuum functions with the aymptotic form for standing boundary conditions:

$$g_{\ell\ell' m}(k, r) \rightarrow j_{\ell'}(kr)\, \delta_{\ell\ell'} - K_{\ell\ell' m}\, y_{\ell'}(kr) \tag{6}$$

as $r \rightarrow \infty$, where $j_\ell(kr)$, $y_\ell(kr)$ are regular and irregular spherical Bessel functions.

The scaled K-matrix

$$K' = -\frac{2}{\pi} K \tag{7}$$

satisfies the Lippmann-Schwinger equation

$$K' = U + U G_0^P K' \tag{8}$$

where G_0^P is the principal-value part of the free-particle Green's function. Inserting the separable potential $U^t = 2V^t$ into Eq. (8) leads to the finite matrix equation

$$\langle \alpha | K' | \beta \rangle = \langle \alpha | U | \beta \rangle + \sum_{\alpha\delta} \langle \alpha | U | \alpha \rangle \langle \alpha | G_0^P | \delta \rangle \langle \delta | K' | \beta \rangle \tag{9}$$

which has the solution

$$K'^{t} = (1 - U^{t} G_{o}^{P})^{-1} U^{t} \tag{10}$$

The on-shell partial-wave K-matrix is obtained by the transformation

$$K^{t}_{\ell\ell' m} = -k \sum_{\alpha\beta} \langle j_{\ell}\, Y_{\ell m} \,|\, \alpha \rangle \langle \alpha \,|K'|\, \beta \rangle \langle \beta \,|\, j_{\ell'}\, Y_{\ell' m} \rangle \tag{11}$$

The solution K'^{t} corresponds to the wave function

$$\psi^{t}_{k\ell m} = \phi_{k\ell m} + G_{o}^{P} K'^{t} \phi_{k\ell m} \tag{12}$$

Introducing the single-center expansion

$$\psi^{t}_{k\ell m}(\vec{r}) = \sum_{\ell'} g^{t}_{\ell\ell' m}(k, r)\, Y_{\ell' m}(\hat{r}) \tag{13}$$

leads to the asymptotic form

$$\psi^{t}_{k\ell m} \rightarrow \sum_{\ell'} [\, j_{\ell'} \delta_{\ell\ell'} - y_{\ell'}\, K^{t}_{\ell'\ell m}\,]\, Y_{\ell' m} \tag{14}$$

as $r \rightarrow \infty$. Thus $\psi^{t}_{k\ell m}$ satisfies the appropriate boundary conditions for use in the Kohn variational formula[14] [Eq. (2)]. The distorted-wave approximation form of Eq. (2) follows from the fact that the free-particle Green's function is not approximated in Eq. (12).[12]

The scattering amplitude in the laboratory-frame (with z′- axis in the direction of the incident electron) has the single-center expansion (for a diatomic target)[15]

$$f_k(\hat{R}', \hat{r}') = \sum_{\ell\ell' mm'} a_{\ell\ell' m}(k, R)\, D^{(\ell)}_{m'm}(\hat{R}')\, D^{(\ell')*}_{om}(\hat{R}') \times Y_{\ell m'}(\hat{r}') \qquad (15)$$

where $\hat{R}'$ denotes the target orientation angles and $\hat{r}'$ denotes the scattering angles in the laboratory frame. The dynamical coefficients introduced by Temkin et al[15] are given by[4]

$$a_{\ell\ell' m}(k, R) = i^{\ell' - \ell} \sqrt{4\pi(2\ell' + 1)} \sum_{\ell''} (1 - iK)^{-1}_{\ell\ell'' m} K_{\ell''\ell' m} \qquad (16)$$

The single-center expansions are defined with respect to the center-of-mass of the target.

In the fixed-nuclei approximation the total elastic cross section is given by[15]

$$\sigma_T = \sum_{\ell\ell' m} | a_{\ell\ell' m} |^2 / (2\ell' + 1)\,. \qquad (17)$$

The momentum-transfer cross section is defined as

$$\sigma_m = \int d(\cos\theta) \frac{d\sigma}{d(\cos\theta)} (1 - \cos\theta)$$

where $\frac{d\sigma}{d(\cos\theta)}$ is the differential cross section per unit polar angle averaged with respect to target orientation. The momentum-transfer cross section may be expressed as[4,16]

$$\sigma_m = 4\pi \left(A_0 - \frac{1}{3} A_1 \right) \tag{18a}$$

where

$$A_L = \frac{1}{4\pi(2L+1)} \sum_{\substack{\ell\ell' \lambda\lambda' \\ m\mu}} [(2\ell+1)(2\lambda+1)]^{1/2} (\ell\lambda 00 | L0)(\ell'\lambda' 00 | L0)$$

$$\times (\ell\lambda m\mu | Lm+\mu)(\ell'\lambda' m\mu | Lm+\mu)\, a_{\ell\ell' m}\, a^*_{\lambda\lambda'\mu} \,. \tag{18b}$$

Garrett[17] and Takayanagi[18] have shown that due to the presence of a permanent dipole moment, which gives rise to a long-range r^{-2} potential, the total fixed-nuclei cross section diverges for heteronuclear molecules. The time-averaged field of a rotating dipole is zero, hence, one obtains finite total cross sections by taking account of the rotational motion of the target. As shown by Garrett[17] the divergence of Eq. (17) for polar molecules is due to the divergence of the forward scattering cross section. The momentum-transfer cross section, however, has a weighting factor of $(1 - \cos\theta)$ which removes contributions from forward scattering. Chandra[16] has proved that σ_m is finite for polar molecules in the fixed-nuclei approximation.

The width and position of a shape resonance in nonspherical potential scattering can be extracted from the eigenphase sum by applying the formula[19]

$$\Delta(k) = f(k) + \tan^{-1}\left[\frac{\Gamma/2}{E_r - k^2/2}\right] \tag{19a}$$

where Γ and E_r are the resonance width and position and Δ is the eigenphase sum. The function $f(k)$ represents the nonresonant scattering and may be expanded in powers of k^2:

$$f(k) = a_0 + a_2 \frac{k^2}{2} + a_4 \frac{k^4}{4} + \ldots\ldots . \tag{19b}$$

The static-exchange potential for a closed-shell diatomic molecule is of the form

$$V = -\frac{Z_A}{|\vec{r} - \vec{A}|} - \frac{Z_B}{|\vec{r} - \vec{B}|} + \sum_{\sigma=1}^{N} (2J_\sigma - K_\sigma) \tag{20}$$

where the Coulomb operator

$$J_\sigma(\vec{r}) = \int d^3r' \frac{\phi_\sigma^*(\vec{r}')\phi_\sigma(\vec{r}')}{|\vec{r} - \vec{r}'|} \tag{21}$$

and K_σ is the corresponding exchange operator. The nuclear charges

are denoted by Z_A and Z_B, the nuclei are located at $\vec{A}$ and $\vec{B}$, and N is the number of occupied orbitals ϕ_σ. The variational formula [Eq. (2)] involves the matrix elements $\langle \psi^t_{k\ell m} | U | \psi^t_{k\ell' m} \rangle$ and $\langle \psi^t_{k\ell m} | U^t | \psi^t_{k\ell' m} \rangle$. The latter is given by:

$$\langle \psi^t_{k\ell m} | U^t | \psi^t_{k\ell' m} \rangle = \langle j_\ell Y_{\ell m} | (K'^t G_o^P + 1) U^t (1 + G_o^P K'^t) | j_{\ell'} Y_{\ell' m} \rangle \tag{22}$$

and involves only components of $K' G_o^P$, and U within the discrete-basis-set subspace. The matrix element

$$\langle \psi^t_{k\ell m} | U | \psi^t_{k\ell' m} \rangle = \sum_{pq} \langle g^t_{\ell mp} Y_{pm} | (U^{(s)} - U^{(ex)}) | g^t_{\ell' qm} Y_{qm} \rangle \tag{23}$$

is evaluated using single-center expansions of the Coulomb interaction and each occupied orbital:

$$\phi_\sigma(\vec{r}) = \sum_s \phi_{sm_\sigma}(r) Y_{sm_\sigma}(\hat{r}) . \tag{24}$$

Expressions for $\langle g^t_{\ell pm} | U^{(i)} | g^t_{\ell' qm} \rangle$, $U^{(i)} = U^{(s)}, U^{(ex)}$ are given in Ref. 20. The direct matrix element involves a multipole expansion of the static potential:

$$U^{(s)}(\vec{r}) = 2 \sum_\lambda V_\lambda(r) P_\lambda(\hat{r}) , \tag{25}$$

where P_λ is a Legendre polynomial. A prescription for obtaining a numerical representation of the continuum orbital $g^t_{\ell\ell'm}$ is given in Ref. 12.

III. CALCULATIONS AND RESULTS

The electronic configuration of the ground state of CO is $X\,^1\Sigma^+\ 1\sigma^2\,2\sigma^2\,3\sigma^2\,4\sigma^2\,5\sigma^2\,1\pi^4$. To construct the static-exchange potential we preformed an SCF calculation for the ground state at an internuclear separation of 2.132 a.u. The SCF basis set consisted of a (9s, 5p, d) set of primitive Gaussians on each nucleus contracted to [4s, 3p, d]. The exponents and contraction coefficients of this basis, which are due to Dunning,[21] are given in Table I. A. The dipole moment of the CO ground state in this basis is 0.106 a.u.

The truncated scattering potential U^t is constructed separately for the Σ and Π scattering symmetries.[4] The scattering basis set includes the uncontracted Gaussians used to represent occupied orbitals of the same symmetry as well as more diffuse Gaussians. The scattering basis sets used in this calculation are listed in Table I. B.

Our prescription for the matrix element $\langle \psi^t_{k\ell m} \mid U \mid \psi^t_{k\ell' m} \rangle$ involves single-center expansions of the occupied orbitals [Eq.(24)], the static potential [Eq.(25)], and the scattering functions [Eq.(13)]. To converge the static potential matrix element we included $s, 0, \ldots, 30$ in the expansion of each occupied orbital; $\lambda = 0, \ldots, 30$ in the expansion of the electronic part of the static potential, and

$\lambda = 0, \ldots, 60$ in the nuclear part; and $\ell' = 0, \ldots, 30$ in the expansion of the scattering wave function. Evaluation of the exchange potential matrix elements involves a five-fold sum over the expansion indices of the occupied orbitals, the Coulomb interaction, and the continuum functions. This summation over partial-wave indices was truncated by means of a cutoff on the magnitude of individual terms in the expansion. This cutoff was typically on the order of 10^{-5} or 10^{-6}. The one- and two-electron radial integrals that occur in the expansions for $\langle \psi^t_{k\ell m} \mid U \mid \psi_{k\ell' m} \rangle$ are evaluated by Simpson's rule quadrature. A variable mesh was used for these quadratures with the step size increased for larger distances from the origin. The two sets of radial increments used in this calculation are presented in Table II. We used the finer mesh (grid B in Table II) to improve the numerical accuracy of the exchange radial integrals for Π symmetry scattering in the energy region of the shape resonance. All other radial integrals were evaluated using grid A in Table II. The numerical accuracy of the variational correction matrix elements is most critical in the region of a resonance because the $\langle \psi^t \mid U \mid \psi^t \rangle$ and $\langle \psi^t \mid U^t \mid \psi^t \rangle$ tend to be large and significant figures are lost in the difference. We estimate the uncertainty in the corrected K-matrix elements $K^s_{\ell\ell' m}$ not associated with basis set errors at about 15%. This uncertainty is due to truncation of partial wave expansions and round-off error in the radial quadratures occurring in the evaluation of $\langle \psi^t_{k\ell m} \mid U \mid \psi^t_{k\ell' m} \rangle$.

Figure 1 shows eigenphases and eigenphase sums for s- , p- , and d-wave scattering in the $^2\Sigma$ channel. Contributions from higher

partial-waves are small at the energies studied and have been neglected. Eigenphases obtained from matrix elements of the corrected K-matrix, $K^{s}_{\ell\ell' m}$, and from uncorrected K-matrix elements, $K^{t}_{\ell\ell' m}$, are shown. The eigenphases are labelled by the partial-wave with largest mixing coefficient. Table III gives the eigenphases and mixing coefficients obtained from corrected $^2\Sigma$ symmetry K-matrix elements at several energies. In Figure 1 the eigenphase sum and the "sσ" and "pσ" eigenphases extrapolate toward π radians at low energy, while the "dσ" eigenphase extrapolates toward zero. This behavior is consistent with Levinson's theorem[22] and with the behavior of the Σ-symmetry eigenphases in N_2.[3] Comparison of corrected and uncorrected results shows that the variational correction tends to dampen oscillations in the uncorrected eigenphases due to basis set truncation. It is interesting to note that the individual uncorrected eigenphases oscillate out of phase with each other as a function of energy. The uncertainty in our results due to basis set truncation is related to the difference between the corrected and uncorrected results. Rough estimates of this uncertainty are: 10% for the corrected sσ eigenphase, 20% for the pσ eigenphase, and a factor of two for the dσ eigenphase.

Results for $^2\Pi$ channel eigenphases obtained from p-, d-, and f-wave K-matrix elements are shown in Fig. 2. The difference between corrected and uncorrected results is smaller than in the $^2\Sigma$ channel. This is probably a consequence of the fact that discrete-basis-set methods are particularly appropriate for scattering via a resonance state. The assignment of eigenphases in the

vicinity of a resonance is governed by the avoided-crossing rule for eigenphases.[23] Table IV lists the eigenphases shown in Fig. 2 together with their p- and d-wave mixing coefficients. The contribution from f-wave scattering is small and has been neglected. The mixing coefficients are defined by the relation

$$\psi_k(\eta_i^1) \cong |C_p^i| \psi_{kp1} \pm |C_d^i| \psi_{kd1} \quad . \tag{26}$$

In the resonance region we assign the $|C_p| - |C_d|$ combination to the resonant eigenphase and the combination $|C_p| + |C_d|$ to the slowly varying eigenphase. Outside the resonance region the eigenphases are labelled by the partial-wave with largest mixing coefficient. In analogy with N_2 we label the resonant eigenphase "$\eta_{d\pi}$" and the nonresonant eigenphase "$\eta_{p\pi}$". Our results indicate that only one eigenphase shows resonance behavior even though p-d coupling is very strong in the resonance region.

Our results for the position and width of the $^2\Pi$ shape resonance are given in Table V. We give results extracted from the eigenphase sums of both uncorrected and corrected eigenphases through Eqs. (19a) and (19b). Our best result for the width of $\Gamma = 1.65 \pm 0.15$ eV is about twice the semi-empirical result of Zubek and Symytkowski[9] which is also given in Table V. Our best result for the position of 3.4 ± 0.1 eV is 1.5 eV higher than the semi-empirical result.[9] Results for the position and width of the $^2\Pi_g$ resonance of N_2 in static-exchange approximation[7] are given in Table V together with the semi-empirical results of

Birtwistle and Herzenberg.[24] These results indicate that in N_2 the static-exchange approximation overestimates the width by about a factor of two and puts the position about 1.5 eV above the best fit to experiment.[24] Thus the difference between static-exchange results and semi-empirical results fit to experiment is about the same in CO and N_2. We attribute this difference to the attractive polarization potential which generally lowers the position of a resonance and decreases its width.

Table V includes theoretical results for the CO shape resonance obtained by Chandra[1] and for the N_2 shape resonance obtained by Chandra and Temkin.[25] Both these calculations use the numerical close-coupling approach and the pseudopotential method in which exchange is approximately accounted for by imposing orthogonality conditions.[26] These calculations also include a semi-empirical polarization potential which is "tuned" to give the resonance position correctly. The trends shown by these results are in complete disagreement with those obtained from the static-exchange approximation and from semi-empirical calculations: Chandra's width[10] for the CO resonance is smaller than Chandra and Temkin's[25] result for N_2 and the resonance position for CO is higher for CO than for N_2. In addition, Chandra's width for CO is a factor of three smaller than the semi-empirical result of Zubek and Szmytkowski.[9]

Figure 3 shows our static-exchange result for the total momentum-transfer cross section of CO. This cross section was obtained by including s- through f-wave scattering and is insensitive to contributions

from higher partial-waves. Figure 3 also shows the experimental results of Land[8] and the pseudopotential plus semi-empirical polarization results of Chandra.[10] In agreement with the resonance parameters given above, the resonance structure of σ_m in the static-exchange approximation is broader than experimentally observed and is shifted to higher energy. The experimental resonance peak is about 50% higher than the static-exchange result. The static-exchange and experimental cross section are in good agreement above the resonance region. Our results for the momentum transfer cross section are given in Table VI.

IV. DISCUSSION AND CONCLUSIONS

Our results show that the static-exchange approximation gives the correct trends in the resonance parameters of the isoelectronic systems N_2 and CO: The resonance in CO occurs at lower energy than in N_2 and has a larger width. Physically, these changes are expected because, unlike N_2, the CO resonance contains p-wave as well as d-wave character. Thus the potential barrier, which is responsible for the shape resonance in both systems, is weaker in CO than in N_2. We find that the effects of polarization are similar in CO and N_2. The attractive polarization potential tends to lower the resonance energy and reduce the resonance width. We are studying a simple method of including polarization effects in our approach.[27] The failure of the pseudopotential plus semi-empirical polarization potential to give the trends discussed above confirms the importance of including exchange

correctly. It is also possible that the semi-empirical polarization potential is unreliable for resonance scattering processes.

The behavior of the individual CO eigenphases is qualitatively similar to the behavior of the corresponding N_2 eigenphases even though the coupling between partial-waves is much stronger in CO. The $^2\Pi$ channel eigenphase sum clearly shows a resonance but it passes through considerably less than π radians in the resonance region. This is due to significant contributions from nonresonant scattering. Chang[28] has shown that a model based on a single resonant eigenphase accounts for scattering via the $^2\Pi$ resonance in CO. Our results verify this model, at least for the static-exchange approximation. The inclusion of polarization effects is unlikely to change this conclusion.

A discrete-basis-set expansion of the potential [Eq. (1)] is not expected to accurately account for the long-range component of the potential due a permanent dipole moment. In this calculation the effect of the CO dipole moment is included to first order by the variational correction [Eq. (22)]. This approach would not be appropriate at very low scattering energies ($\ll 1$ eV), but it should be adequate for the scattering processes considered in this work. The scattering of low partial-waves is dominated by short-range interactions, particularly when a resonance is involved. Moreover, the dipole moment of CO is relatively small.

Several discrete-basis-set methods for single-channel scattering from spherically symmetric potentials use the fact that basis set errors are minimized at eigenenergies of the basis set representation

of the Hamiltonian.[29] As discussed in previous work,[4] improved uncorrected results can be obtained at eigenenergies for nonspherical potential scattering if the coupling is weak. Not surprisingly, this effect breaks down completely in CO due to the strong coupling: when the uncorrected "s" eigenphase is most accurate, the "p" eigenphase is least accurate, and conversely.

ACKNOWLEDGMENTS

This research was supported by grant No. CHE76-05157 from the National Science Foundation and by an Institutional Grant from the U. S. Department of Energy , No. EY-76-G-03-1305. We would like to thank Dr. Land for the use of experimental results prior to publication.

References

[1] J. C. Tully and R. S. Berry, J. Chem. Phys. 51, 2056 (1969).

[2] A. Klonover and U. Kaldor, "Ab initio electron-molecule scattering theory including polarization: Vibrational-rotational excitation of H_2"; accepted for publication, Phys. Rev. A.

[3] M. A. Morrison and B. I. Schneider, Phys. Rev. A 16, 1003 (1977).

[4] A. W. Fliflet, D. A. Levin, M. Ma, and V. McKoy, Phys. Rev. A 17, 160 (1978).

[5] B. I. Schneider and P. J. Hay, Phys. Rev. A 13, 2049 (1976).

[6] G. J. Schulz, Rev. Mod. Phys. 45, 378 (1973).

[7] D. A. Levin and V. McKoy, "Low Energy Vibrational and Vibrational-Rotational Cross Sections for N_2 by Electron Impact," to be published.

[8] J. E. Land, "Electron Momentum-Transfer Cross Section for Carbon Monoxide," to be published.

[9] M. Zubek and C. Szmytkowski, J. Phys. B: Atom. Molec. Phys. 10, L27 (1977).

[10] N. Chandra, Phys. Rev. A 16, 80 (1977).

[11] T. N. Rescigno, C. W. McCurdy, Jr., and V. McKoy, Phys. Rev. A 11, 825 (1975).

[12] A. W. Fliflet and V. McKoy, Phys. Rev. A 18, 2107 (1978).

[13]D. A. Levin, A. W. Fliflet, and V. McKoy, "Low Energy Rotational and Vibrational-Rotational Excitation Cross Sections for H_2 by Electron Impact," accepted for publication, Phys. Rev. A.

[14]W. Kohn, Phys. Rev. 74, 1763 (1948).

[15]A. Temkin, K. V. Vasavada, E. S. Chang, and A. Silver, Phys. Rev. 186, 57 (1969).

[16]N. Chandra, Phys. Rev. A 12, 2342 (1975).

[17]W. R. Garrett, Mol. Phys. 24, 465 (1972).

[18]K. Takayanagi, Comments At. Mol. Phys. 3, 95 (1972).

[19]P. G. Burke and A. L. Sinfailam, J. Phys. B 3, 641 (1970).

[20]A. W. Fliflet and V. McKoy, Phys. Rev. A 18, 1048 (1978).

[21]T. H. Dunning, Jr., J. Chem. Phys. 53, 2823 (1970).

[22]R. G. Newton, Scattering Theory of Waves and Particles, (McGraw-Hill, New York, 1966), p. 471.

[23]J. Macek, Phys. Rev. A 2, 1101 (1970).

[24]D. T. Birtwistle and A. Herzenberg, J. Phys. B 4, 53 (1971).

[25]N. Chandra and A. Temkin, Phys. Rev. A 13, 188 (1976).

[26]P. G. Burke and N. Chandra, J. Phys. B: Atom. Molec. Phys. 5, 1696 (1972).

[27] D. A. Levin and V. McKoy, "A Simple Model for the Inclusion of Polarization Effects in Shape Resonances," in preparation.

[28] E. S. Chang, Phys. Rev. A 16, 1850 (1977).

[29] P. G. Burke, Potential Scattering in Atomic Physics, (Plenum Press, New York, 1971), p. 75.

TABLE I. A. Target Basis Set[a]

$\vec{A}$ = (0., 0., -1.218), C atomic center

(p, q, r)	α_i	C_i
(0, 0, 0)	4232.61	0.002029
"	634.882	0.015535
"	146.097	0.0754110
"	42.4974	0.257121
"	14.1892	0.596555
"	1.9666	0.242517
"	5.1477	1.0
"	0.4962	"
"	0.1533	"
(1, 0, 0)	18.1557	0.039196
"	3.98640	0.244144
"	1.142900	0.8167750
"	0.3954	1.0
"	0.1146	"
(0, 1, 0)	same α_i's and C_i's as (1, 0, 0)	
(0, 0, 1)	same α_i's and C_i's as (1, 0, 0)	
(0, 0, 2)	0.75	1.0
(1, 0, 1)	"	"
(0, 1, 1)	"	"

(continued)

TABLE I. A. (continuation)

$\vec{A}$ = (0., 0., 0.9140), O atomic center		
(p, q, r)	α_i	C_i
(0, 0, 0)	7816.54	0.002031
"	1175.82	0.015436
"	272.188	0.0737710
"	81.1696	0.247606
"	27.1896	0.611832
"	3.4136	0.2412050
"	9.5322	1.0
"	0.9398	"
"	0.2846	"
(1, 0, 0)	35.1832	0.040023
"	7.904	0.253849
"	2.3051	0.806842
"	0.7171	1.0
"	0.2137	"
(0, 1, 0)	same α_i's and C_i's as (1, 0, 0)	
(0, 0, 1)	same α_i's and C_i's as (1, 0, 0)	
(0, 0, 2)	0.85	1.0
(1, 0, 1)	"	"
(0, 1, 1)	"	"

[a]The Cartesian Gaussian function is of the form $\mu_{pqr}^{\alpha_i \vec{A}} \equiv N_{pqr}(x - A_x)^p (y - A_y)^q (z - A_z)^r e^{-\alpha_i | \vec{r} - \vec{A} |^2}$ where N_{pqr} is a normalization factor. C_i denotes the contraction coefficient of the ith basis function.

TABLE I. B. Scattering basis set exponents. [a, b]

A = (0. 0, 0. 0, -1. 218)	(0. 0, 0. 0, 0. 9140)	(0. 0, 0. 0, 0. 0)
	$^2\Sigma$	
	(p, q, r) = (0, 0, 0)	
4232. 610	7816. 54	0. 1
634. 882	1175. 82	0. 05
146. 097	273. 188	0. 025
42. 4974	81. 1696	0. 0125
14. 1892	27. 1896	0. 005
1. 9666	3. 4136	
5. 14770	9. 5322	
0. 49620	0. 93980	
0. 15330	0. 284600	
	(p, q, r) = (0, 0, 1)	
18. 1557	35. 1832	0. 07
3. 9864	7. 904	0. 0375
1. 1429	2. 3051	0. 01875
0. 3954	0. 7171	0. 0075
0. 1146	0. 2137	
	$^2\Pi$	
	(p, q, r) = (1, 0, 0)	
18. 1557	35. 1832	0. 08
3. 9864	7. 904	0. 048
1. 1429	2. 3051	0. 0290
0. 650	0. 7171	0. 0173
0. 3594	0. 4	0. 01
0. 20	0. 2137	0. 006
0. 1146	0. 1	0. 002
	(p, q, r) = (1, 0, 1)	
0. 75	0. 85	0. 75
0. 3	0. 40	0. 03
0. 10	0. 15	0. 01

[a] See Table I. A. for explanation of symbols.

[b] The contraction coefficients are unity for each basis function.

TABLE II. Step sizes for numerical integrations

Grid A					
i^{th} interval[a]	1	2	3	4	5
h_i[b]	0.03807	0.0764	0.15228	0.30456	0.6091
n_i[c]	48	96	192	216	600

Grid B						
i^{th} interval	1	2	3	4	5	6
h_i	0.019035	0.03807	0.07614	0.15228	0.30456	0.6091
n_i	96	192	288	384	480	600

[a] The quadrature mesh is broken up into different step sizes.

[b] h_i is the incremental step size for the i^{th} interval and has units of a. u. /point.

[c] n_i is the number of points for the i^{th} interval.

TABLE III. Assignment of variationally corrected $^2\Sigma$ channel eigenphases (units of radians).

eV	$\eta_{s\sigma}$	C_s	C_p	C_d	$\eta_{p\sigma}$	C_s	C_p	C_d	$\eta_{d\sigma}$	C_s	C_p	C_d
1. 2244	2. 348	0. 9939	-0. 6013	0. 0928	2. 897	0. 0517	0. 9945	0. 0905	-0. 0559	-0. 0976	-0. 0852	0. 9915
2. 1768	2. 158	0. 9778	-0. 1505	0. 1453	2. 801	0. 1225	0. 9751	0. 1850	-0. 1047	-0. 169	-0. 163	0. 9719
3. 40125	1. 962	0. 9576	-0. 20199	0. 2052	2. 700	0. 1925	0. 9791	0. 0656	-0. 1057	-0. 214	-0. 0233	0. 9765
4. 8978	1. 872	0. 9117	-0. 29007	0. 2907	2. 549	0. 2706	0. 9568	0. 1061	-0. 0662	-0. 3089	-0. 0180	0. 9509
6. 666	1. 694	0. 8797	-0. 3393	0. 333	2. 349	0. 3323	0. 9397	0. 07968	-0. 0617	-0. 340	-0. 0406	0. 9395

TABLE IV. Assignment of variationally corrected Π channel eigenphases. [a]

eV	"$\eta_{p\pi}$"	C_p	C_d	"$\eta_{d\pi}$"	C_p	C_d
1.2244	3.079	0.553	0.752	0.0696	0.789	-0.612
2.1768	3.0179	0.642	0.749	0.220	0.755	-0.655
2.755	2.991	0.723	0.681	0.462	0.683	-0.729
3.069	2.967	0.701	0.711	0.724	0.711	-0.703
3.4013	2.784	0.759	0.643	1.078	0.644	-0.764
4.1155	2.909	0.751	0.654	1.781	0.646	-0.756
4.4982	2.908	0.768	0.638	0.90	0.634	-0.769
4.8978	2.901	0.763	0.642	2.017	0.637	-0.767
5.748	2.870	0.783	0.555	2.108	0.592	-0.803
6.666	2.840	0.755	0.654	2.194	0.648	-0.755

[a]Given in units of radians.

TABLE V. Comparison of CO and N_2 resonance parameters.

CO $^2\Pi$ Resonance Parameters in eV		
	E_r (eV)	Γ (eV)
Uncorrected T-matrix	3.3 ± 0.2	2.0 ± 0.2
Corrected T-matrix	3.4 ± 0.1	1.65 ± 0.15
Zubek, et al.[9]	1.52 ± 0.02	0.80 ± 0.03
Chandra[10]	1.740	0.242

N_2 $^2\Pi_g$ Resonance Parameters in eV		
	E_r (eV)	Γ(eV) width
Corrected T-matrix[7]	3.83 ± 0.12	1.19 ± 0.04
Birtwistle and Herzenberg[24]	1.925 ± 0.015	0.57 ± 0.02
Chandra and Temkin[25]	1.197	0.4

TABLE VI. Momentum transfer cross section ($Å^2$).

Electron energy (eV)	σ_m
1.224	19.95
2.177	18.59
2.755	21.71
3.069	25.10
3.402	28.46
4.116	22.23
4.498	18.95
4.898	16.41
6.666	12.171

Figure Captions

Fig. 1 Calculated eigenphases and the eigenphase sum for the $^2\Sigma$ channel. The circles represent the corrected and the squares represent the uncorrected results.

Fig. 2 Calculated eigenphases and the eigenphase sum for the $^2\Pi$ channel. The circles and squares follow the convention set in Fig. 1. See the text for the explanation of the assignment of individual eigenphases.

Fig. 3 Comparison of calculated momentum transfer cross section (open circles) with the frame-transformation calculation of Chandra[10] (open triangles and the experimental results of Land[8] (open squares).

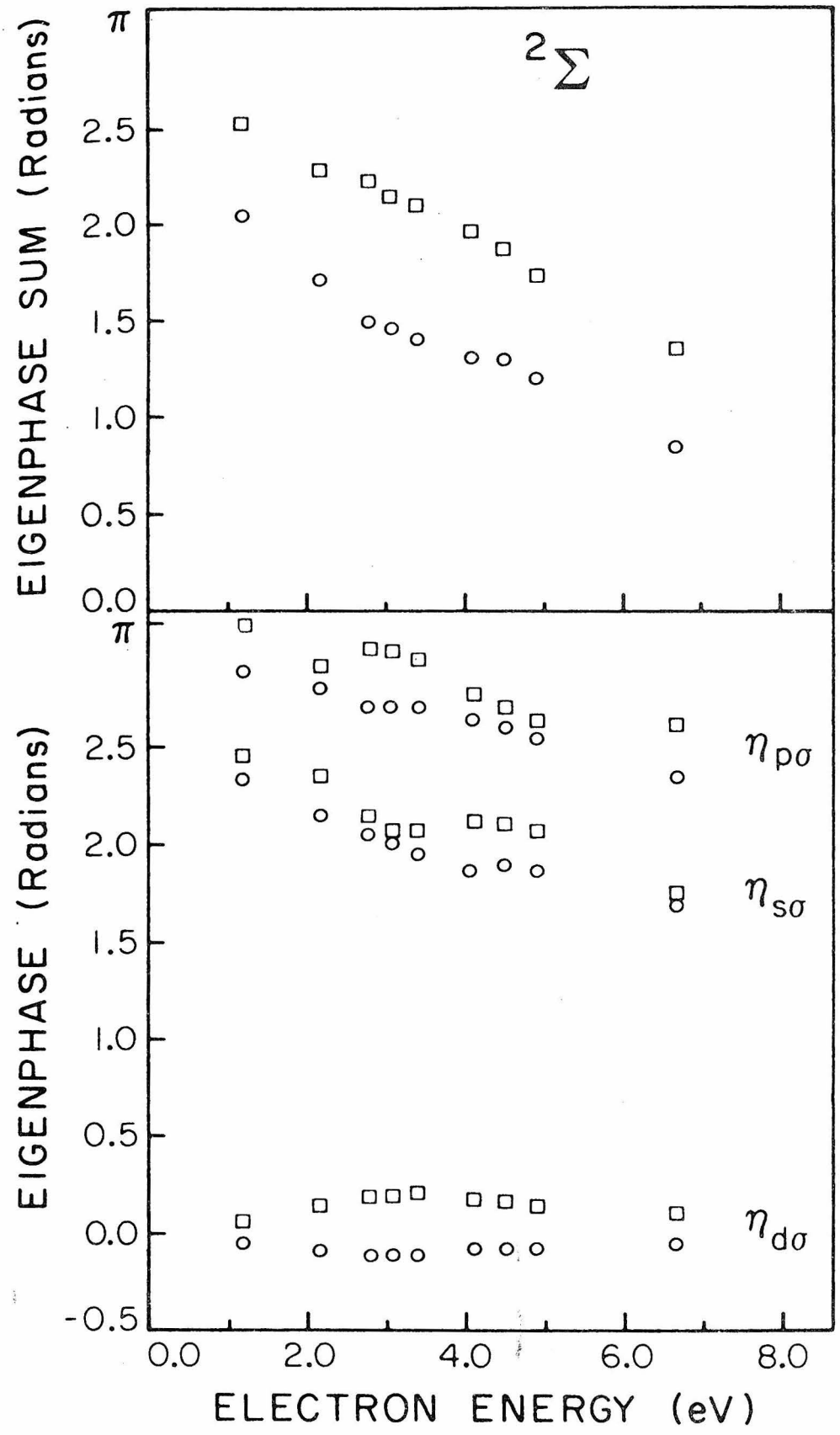
$^2\Sigma$
EIGENPHASE SUM (Radians)
EIGENPHASE (Radians)
$\eta_{p\sigma}$
$\eta_{s\sigma}$
$\eta_{d\sigma}$
ELECTRON ENERGY (eV)
π
2.5
2.0
1.5
1.0
0.5
0.0
-0.5
0.0
2.0
4.0
6.0
8.0

Figure 1

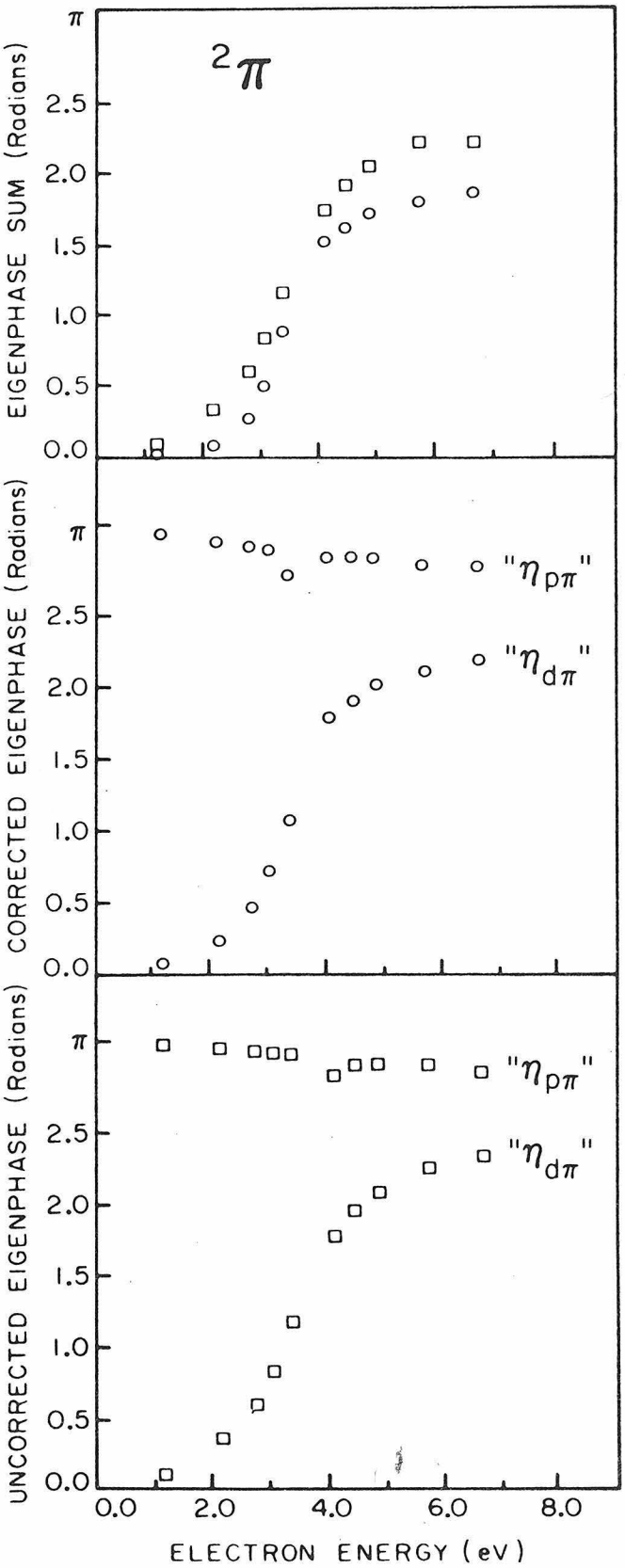
$^2\pi$
EIGENPHASE SUM (Radians)
CORRECTED EIGENPHASE (Radians)
UNCORRECTED EIGENPHASE (Radians)
"$\eta_{p\pi}$"
"$\eta_{d\pi}$"
"$\eta_{p\pi}$"
"$\eta_{d\pi}$"
π
2.5
2.0
1.5
1.0
0.5
0.0
0.0
2.0
4.0
6.0
8.0
ELECTRON ENERGY (eV)

Figure 2

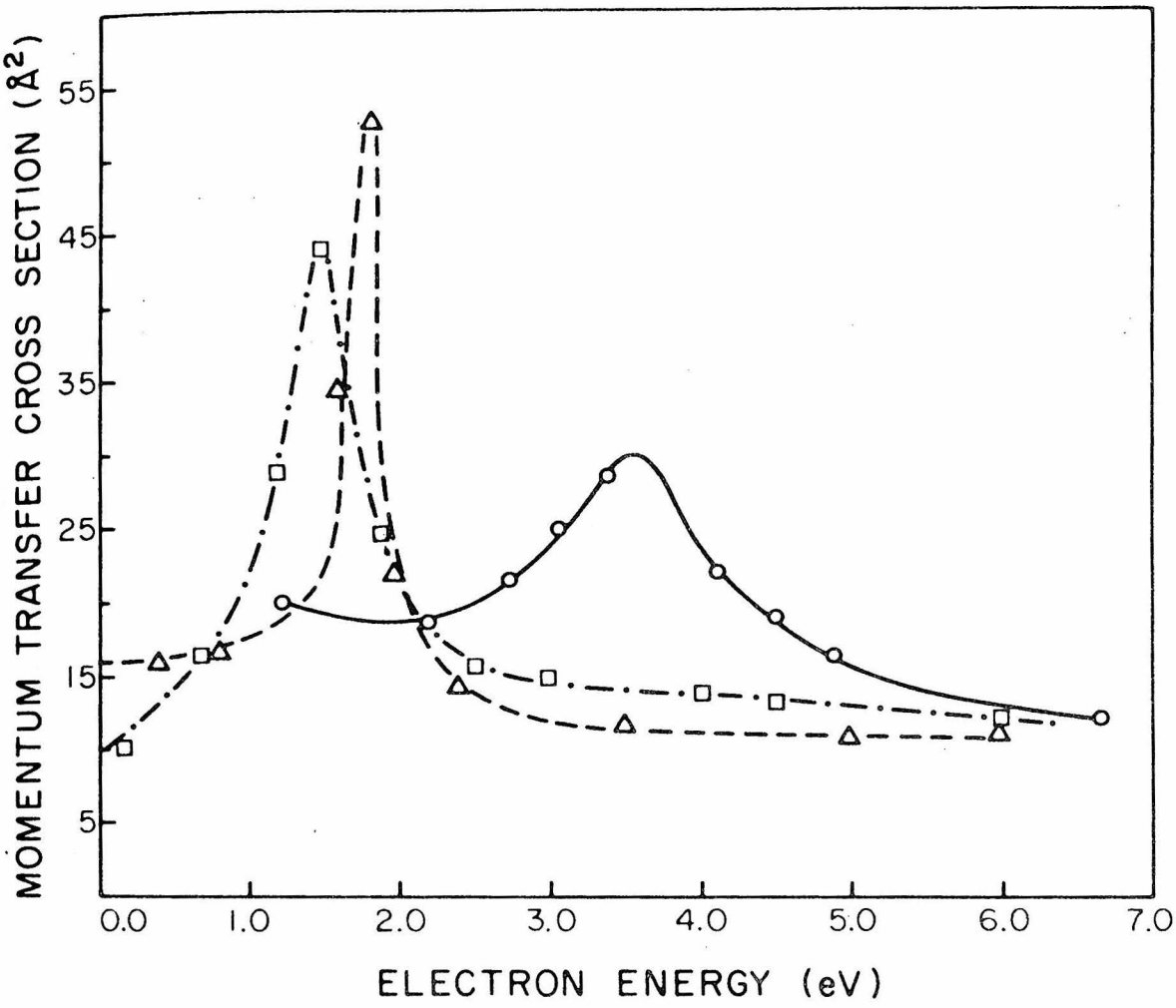
MOMENTUM TRANSFER CROSS SECTION (Å²)
55
45
35
25
15
5
0.0
1.0
2.0
3.0
4.0
5.0
6.0
7.0
ELECTRON ENERGY (eV)

Figure 3

CHAPTER II

Calculation of Low Energy Rotational and Rotational-Vibrational Excitation Cross Sections for Diatomic Systems by Electron Impact

INTRODUCTION

The purpose of this introduction is to place the work presented in these papers in the context of previous work on vibrational and vibrational-rotational excitation processes and to explain the relationships among the three calculations presented in this chapter.

Resonances, the formation of temporary negative ions, are of much interest in collisions of low energy electrons with molecules. Compared to direct scattering processes (when a metastable state is not formed) resonance scattering leads to a large enhancement in the cross section. The specific type of resonance, or compound state, which will be discussed here is a shape resonance. These are associated with the ground electronic state, occur at low energies (0-4 eV) and exhibit lifetimes in the range of 10^{-15} to 10^{-10} seconds.[1]

Previous theoretical studies have shown that a resonance mechanism does well in accounting for observed vibrational excitation.[1] Hence one finds it convenient to analyze the type of vibrational excitation spectra for a given molecule in terms of its resonance lifetime and position. Whether vibrational substructure is observed at all depends on the ratio of the resonance width to the vibrational frequency. For a short lifetime, as in H_2, the energy dependence of the cross section shows a broad peak; for a long lifetime, as in O_2, the compound state can vibrate thus giving a energy dependence to the cross section of a series of spikes located at the vibrational levels of the compound state. Intermediate between these

two cases is a lifetime of the compound state that is on the order of the vibrational time thus giving a cross section behavior of several broadened spikes. This is the situation in the N_2 $^2\Pi_g$ resonance.[1]

In this chapter calculations for H_2 and N_2 are presented. Due to the difference in the resonance lifetime the nature of the vibrational excitation calculation will be different for these two systems. The underlying similarity between the calculations is, however, that one invokes the Born-Oppenheimer approximation to factor the electronic and vibrational motion. This approach is unanimously agreed to be correct for e^--H_2 scattering; however, until recently there has been much confusion on this point for the e^--N_2 system. The work of Chandra and Temkin[2] on this system asserts that in order to obtain structure in the vibrational excitation cross section one must close couple the vibrational and electronic degrees of freedom of the total scattering wave function: i.e.,

$$\Psi(\vec{r}_i, \vec{R}) = \Phi(\vec{r}_i, \vec{R}) \sum_v F_v(\vec{r}) \chi_v(\vec{R}) \qquad (1)$$

where $\vec{r}_i$ are the N+1 electron coordinates, $\vec{R}$ is the internuclear separation, $\vec{r}$ is the scattered electron coordinate, $\chi_v(\vec{R})$ are the vibrational wave functions of the ground electronic state, and Φ is the wave function of the target. As Schneider[3] has explained, the source of this confusion lies in the misunderstanding of the difference between the Born-Oppenheimer and the adiabatic-nuclei approximation.[4]

The latter is given as

$$f_{v'\Gamma', v\Gamma}(\hat{r}) = \langle \psi_{v'\Gamma'}(\vec{R}) | f(\hat{r}, \vec{R}) | \psi_{v,\Gamma}(\vec{R}) \rangle_{\vec{R}} + \Sigma \qquad (2)$$

where f is the scattering amplitude and $\psi_{v'\Gamma'}$ are the target rotational-vibrational wavefunctions. The error term, Σ, is only small when the lifetime of the compound state is small compared to the vibrational period of the neutral molecule. Hence Eq. (2) is valid for calculating vibrational excitation in H_2.[5] For e-N_2 scattering one can still use Eq (1) to separate the calculation in terms of the electronic and vibrational solutions. This simplification is incorporated into our procedure in that we extract the parameters needed in a compound state model[6] from T-matrix calculations performed at a few internuclear separations. Use of the compound state model[6] to calculate vibrational excitation cross sections replaces Eq. (2). Our calculations are the first to calculate in an ab initio manner the resonance width and position as a function of internuclear separation and to use these parameters in a compound state model. Moreover, we have extended the compound state model formalism to obtain absolute and simultaneous vibrational-rotational cross sections. The use of a close-coupled discrete basis set T-matrix formalism has been proposed by Kaldor;[7] however, the chief disadvantage with the close coupling formalism is that the expansion used in Eq. (1) converges very slowly.

The calculations presented here for H_2 and N_2 have used the static-exchange approximation for the scattering potential. The

results show that in both systems that the static-exchange potential is stable enough to support a resonance and will qualitatively reproduce the magnitude and vibrational substructure of the excitation cross section. This is contrary to the general consensus in the literature that polarization effects must be included to see any resonance behavior.[8] These calculations are the first ab initio calculations to incorporate exchange effects exactly. Previous calculations have used model potentials to simulate the non-local behavior of the exchange interaction;[2] however, recent work on other molecular systems indicates that these approximate methods can be unreliable.[9]

Inclusion of polarization effects will bring the position of the resonance into better agreement with experiment. For H_2, N_2 and CO we find that the static-exchange approximation gives a resonance position which is about 1.5 eV too high. Also, we expect that the width would decrease by about a factor of two which would bring it into closer agreement with semi-empirical results.[10] To obtain these effects, a method for inclusion of polarization effects is proposed. In contrast with previous methods which stressed the long range behavior of the polarization potential,[2] it is shown here that for resonances one needs to emphasize its short range behavior.

References

1. G. J. Schulz, Rev. Mod. Phys., 45, 378 (1973).
2. N. Chandra and A. Temkin, Phys. Rev. A, 13, 188 (1976).
3. B. I. Schneider, Phys. Rev. A, 14, 1923 (1976).
4. D. M. Chase, Phys. Rev., 104, 838 (1956).
5. F. H. M. Faisal and A. Temkin, Phys. Rev. Lett., 28, 203 (1972).
6. W. Domrke and L. S. Cedubaum, Phys. Rev. A., 16, 1465 (1977).
7. U. Kaldor, Chem. Phys. Lett., 58, 509 (1978).
8. R. J. W. Henry and E. S. Chang, Phys. Rev. A, 5, 276 (1972).
9. B. I. Schneider, private communication.
10. D. T. Birtwistle and A. Herzenberg, J. Phys. B, 4, 53 (1971).

SECTION A

Low Energy Rotational and Vibrational-Rotational Excitation Cross Sections for H_2 by Electron Impact

I. INTRODUCTION

Recent[1,2,3] applications of discrete basis set methods for non-spherical potential scattering have established their importance in ab initio calculations of electron-molecule processes. Discrete basis set techniques have an advantage in that they are particularly well suited for representing the bound state nature of resonances. Compound states,[4] or resonances, decay by the emission of the temporarily trapped incident electron into final states which are energetically accessible. In molecules there are various decay channels possible, among them are vibrational and rotational excitation.

The subject of this paper is the discrete basis function method, introduced by Rescigno, McCurdy, and McKoy,[1] applied to vibrational, rotational, and vibrational-rotational excitation of H_2 by low-energy electrons. Our approach involves solving the Lippmann-Schwinger equation for the transition operator in a Gaussian basis representation at different internuclear spacings, R, positioned about the equilibrium point. We present the first ab initio static-exchange discrete basis set calculation for vibrational excitation in H_2 and compare these results with other theoretical results and experimental measurements.

Until now there has been some doubt as to whether one could reproduce the low-energy vibrational excitation cross section of molecules by including just the static-exchange interaction. Henry and Chang[5] (HC) include a static field, effective polarization and exchange effects; however, they neglect the R dependence of their exchange term.

Furthermore, to include the effects of polarization they use a cut-off parameter, whose functional form is related to an undetermined parameter. This adjustable parameter is chosen to give the best fit to the experimental results of Linder.[6] Our results show that by treating the static-exchange potential correctly one can account for the qualitative features of the vibrational excitation cross section.

Results are presented for the pure rotational excitation and simultaneous rotational-vibrational excitation cross sections in the adiabatic-nuclei approximation. In Sec. III we compare with theoretical results of Temkin and Chang,[7] Henry and Chang,[5] Henry and Lane,[8] and experimental measurements of Linder and Schmidt.[6] Variationally corrected results[9] are presented for differential cross sections for rotational excitation.

II. THEORY

In a previous paper,[3] hereafter referred to as I, we presented a method for calculating rotational excitation and momentum transfer cross sections analytically from the matrix solution of the Lippman-Schwinger equation. We will review the highlights of the theory and extend it to include simultaneous vibrational-rotational effects.

Our starting point is the Lippmann-Schwinger equation for the transition matrix

$$T = U + U G_0^+ T \qquad (1)$$

where $U = 2V$ and G_0^+ is the free-particle Green's function with the outgoing wave boundary condition.[10] To solve Eq. (1) we approximate the fixed-nuclei scattering potential by its projection onto a subspace of discrete basis functions:

$$V^t(\underset{\sim}{r}, \underset{\sim}{r}') = \sum_{\alpha,\beta=1}^{N} |\alpha\rangle \langle \alpha | V | \beta \rangle \langle \beta| \tag{2}$$

Inserting Eq. (2) into Eq. (1) we obtain an $N \times N$ matrix form of the Lippmann-Schwinger equation with solution:

$$T^t = [1 - U^t G_0^+]^{-1} U^t. \tag{3}$$

The momentum representation of the on-shell T matrix is constructed by the transformation

$$\langle \underset{\sim}{k}' | T | \underset{\sim}{k} \rangle = \sum_{\alpha\beta} \langle k' | \alpha \rangle \langle \alpha | T | \beta \rangle \langle \beta | \underset{\sim}{k} \rangle \tag{4}$$

where $\underset{\sim}{k}$ and $\underset{\sim}{k}'$ denote plane wave states of the form

$$\varphi_{\underset{\sim}{k}}(\underset{\sim}{r}) = \frac{1}{(2\pi)^{3/2}} e^{i\underset{\sim}{k} \cdot \underset{\sim}{r}} \tag{5a}$$

and α denotes a Cartesian Gaussian of the form

$$\mu_{\ell mn}^{\alpha, \underset{\sim}{A}}(\underset{\sim}{r}) = N_{\ell mn} (x-A_x)^{\ell} (y-A_y)^{m} (z-A_z)^{n} e^{-\alpha |\underset{\sim}{r}-\underset{\sim}{A}|^2} \tag{5b}$$

The on-shell T matrix is related to the scattering amplitude by

$$f_{\underset{\sim}{k}}(\hat{\underset{\sim}{r}}) = -2\pi^2 \langle \underset{\sim}{k}' \mid T \mid \underset{\sim}{k} \rangle \tag{6}$$

where $\hat{\underset{\sim}{r}} = \hat{\underset{\sim}{k}}'$.

Equations (4) and (6) for the on-shell T matrix and the scattering amplitude couple the dynamical and geometric factors of the scattering problem. Using a single center expansion for the scattering amplitude

$$f_{\underset{\sim}{k}}(\hat{\underset{\sim}{r}}) = 4\pi \sum_{\ell\ell' m} f_{\ell\ell' m}(k)\, Y_{\ell m}(\hat{\underset{\sim}{r}})\, Y^*_{\ell' m}(\hat{\underset{\sim}{k}}) \tag{7}$$

we can treat the target orientation dependence analytically. We need to relate the partial wave matrix elements of the scattering amplitude, $f_{\ell\ell' m}$, to the basis set representation of the T matrix, $T_{\alpha\beta}$. This allows us to solve the dynamical problem in the body fixed frame and then transform to the laboratory frame using the rotational properties of spherical harmonics. The single center expansion of the on-shell T matrix is of the form

$$\langle \underset{\sim}{k}' \mid T \mid \underset{\sim}{k} \rangle = \frac{1}{k} \sum_{\ell\ell' m} i^{\ell' - \ell}\, T_{\ell\ell' m}\, Y_{\ell m}(\hat{k}')\, Y^*_{\ell' m}(\hat{\underset{\sim}{k}}) \,. \tag{8}$$

Equating the right hand sides of Eqs. (4) and (8) and using the spherical expansion of a plane wave

$$e^{i\underset{\sim}{k}\cdot\underset{\sim}{r}} = 4\pi \sum_{\ell m} i^{\ell} j_{\ell}(kr)\, Y_{\ell m}(\hat{\underset{\sim}{r}})\, Y^{*}_{\ell m}(\hat{\underset{\sim}{k}}) \tag{9}$$

we obtain the body frame single center expansion coefficients for T^t:

$$T^{t}_{\ell\ell' m} = \frac{2k}{\pi} \sum_{\alpha\beta} \langle j_{\ell}\, Y_{\ell m} \,|\, \alpha \rangle \langle \alpha \,|\, T \,|\, \beta \rangle \langle \beta \,|\, j_{\ell'}\, Y_{\ell' m} \rangle . \tag{10}$$

By substituting Eq. (10) into Eq. (8) and equating coefficients of spherical harmonics in Eqs. (7) and (6) we get

$$f_{\ell\ell' m}(k) = -i^{\ell'-\ell} \sum_{\alpha\beta} \langle j_{\ell}\, Y_{\ell m} \,|\, \alpha \rangle \langle \alpha \,|\, T \,|\, \beta \rangle \langle \beta \,|\, j_{\ell'} Y_{\ell' m} \rangle . \tag{11}$$

In I we discuss the analytic evaluation of the matrix element $\langle j_{\ell}(kr)\, Y_{\ell m}(\hat{\underset{\sim}{r}}) \,|\, \alpha(\underset{\sim}{r}) \rangle$. The laboratory frame scattering amplitude is related to $f_{\ell\ell' m}(k)$ according to

$$f_k(\underset{\sim}{R}, \underset{\sim}{r}') = 4\pi \sum_{\ell\ell' m m'} \sqrt{\frac{2\ell'+1}{4\pi}}\, f_{\ell\ell' m}(k)\, D^{(\ell)}_{m' m}(\hat{\underset{\sim}{R}}) \times$$

$$D_{0\, m}^{(\ell')^{*}}(\hat{\underset{\sim}{R}})\, Y_{\ell m'}(\hat{\underset{\sim}{r}}') \tag{12}$$

where $\underset{\sim}{R}$ denotes the internuclear separation of the homonuclear diatomic and its orientation in the laboratory frame. Using the expressions given by Temkin *et al*[11] for the scattering amplitude we obtain a prescription for their fixed-nuclei dynamical coefficients:

$$a_{\ell\ell'm}(kR) = -\sqrt{4\pi(2\ell'+1)}\, i^{\ell'-\ell} \sum_{\alpha\beta} \langle j_\ell Y_{\ell m} | \alpha \rangle \langle \alpha | T | \beta \rangle \times$$

$$\langle \beta | j_{\ell'} Y_{\ell' m} \rangle \qquad (13)$$

In terms of the dynamical coefficients, the laboratory frame scattering amplitude is given by

$$f_k(\underset{\sim}{R}, \hat{\underset{\sim}{r}}') = \sum_{\ell\ell' mm'} a_{\ell\ell' m}(kR)\, D^{(\ell)}_{m'm}(\hat{R})\, D^{(\ell')*}_{0m}(\hat{R})\, Y_{\ell m'}(\hat{r}'). \qquad (14)$$

To calculate rotational, vibrational, or rotational-vibrational excitation cross sections we use the adiabatic nuclei approximation[12]

$$f_{\Gamma\Gamma'}(\hat{\underset{\sim}{r}}') = \langle \psi_{\Gamma'}(\underset{\sim}{R}) | f_k(\underset{\sim}{R}, \hat{\underset{\sim}{r}}') | \psi_\Gamma(R) \rangle + \epsilon \qquad (15)$$

where ψ_Γ, $\psi_{\Gamma'}$ are target wavefunctions with initial (final) vibrational-rotational quantum states $\Gamma(\Gamma')$. The error term, ϵ, is small for rotational excitation when the speed of the incident electron is large compared to the motion of the target nuclei. For vibrational excitation the error is small when the delay time for scattering is $\ll \hbar / \Delta E_{v'v}$. We will see that the Σ_u resonance in H_2 is broad enough to satisfy the above conditions. To incorporate vibrational excitation into our formalism we perform the analytic angular integrations and then numerically integrate over R. Thus for vibrational-rotational excitation the dynamical coefficients become:

$$a_{\ell\ell' m}(v', v) = \int_0^\infty \chi_{v'}(R)\, a_{\ell\ell' m}(R)\, \chi_v(R)\, R^2\, dR \qquad (16)$$

where χ_v and $\chi_{v'}$ are the initial and final vibrational wavefunctions for the target molecule.

In the adiabatic-nuclei approximation the total electronically elastic cross section is given by

$$\sigma_{v'v} = \frac{k_{v'}}{k_v} \sum_{\ell\ell' m} \frac{\left| a_{\ell\ell' m}(v, v') \right|^2}{(2\ell' + 1)} \tag{17}$$

Also, the differential-rotational and differential-rotational-vibrational cross sections are respectively

$$\frac{d\sigma_{j' \leftarrow j}}{d(\cos\theta)} = \frac{k_{j'}}{k_j} \sum_L A_L(j', j)\, P_L(\cos\theta)\,, \tag{18a}$$

$$\frac{d\sigma_{j'v' \leftarrow jv}}{d(\cos\theta)} = \frac{k_{j'v'}}{k_{j'v}} \sum_L A_L(j'\,v';\, j,\, v)\, P_L(\cos\theta)\,, \tag{18b}$$

where the fixed-nuclei expansion coefficients are given by:

$$A_L(j', j) = \frac{1}{2} \sum_{\substack{\ell\ell' m \\ \lambda\lambda'\eta}} a_{\ell\ell' m}(R)\, a^*_{\lambda\lambda'\eta}(R)\, (-1)^{m+\eta+J+\ell'+\lambda'} \times$$

$$\sqrt{(2\ell+1)(2\lambda+1)}\, (\ell\ell' m - m \,|\, J\,0)\, (\lambda\lambda'\,\eta - \eta \,|\, J\,0) \times$$

$$(\ell\lambda\,00 \,|\, L\,0)(\ell'\lambda'\,00 \,|\, L0)(j\,J\,00 \,|\, j'0)^2 \begin{Bmatrix} \ell & \lambda & L \\ \ell' & \lambda' & J \end{Bmatrix}. \tag{19}$$

The $A_L(j'v';jv)$ coefficients are calculated by replacing the fixed-nuclei dynamic coefficients $a_{\ell\ell'm}(R)$ by $a_{\ell\ell'm}(v', v)$. For the $0 \rightarrow 1$ vibrational excitation the only significant term in the sum is $\ell, \ell', \lambda, \lambda' = 1$; $m, \eta = 0$. Then

$$A_L(j', v' = 1; j, v = 0) \cong |a_{110}(1,0)|^2 (-1)^J (1100|J0)^2 \times$$

$$(1100|L0)^2 (jJ00|j'0)^2 \begin{Bmatrix} 1 & 1 & L \\ 1 & 1 & J \end{Bmatrix} \tag{20}$$

As we discuss in the next section, Eq. (20) is a good approximation in H_2 because only the p_σ phase shift varies significantly with internuclear separation. The total rotational excitation cross section is given by:

$$\sigma_{j' \leftarrow j} = \frac{k_{j'}}{k_j} \sum_{\ell\ell'm\mu} \frac{(-1)^{m+\mu}}{(2\ell'+1)} a_{\ell\ell'm}(R)\, a^*_{\ell\ell'\mu}(R)$$

$$\times \sum_J (\ell\ell' m - m \,|\, J0)(\ell\ell'\mu - \mu \,|\, J0)(jJ00|j'0)^2 \tag{21}$$

Analogously with Eq. (20) we get

$$\sigma_{j'1 \leftarrow j0} = \frac{k_{j'1}}{k_{j0}} \frac{|a_{110}|^2}{3} \sum_J (1100|J0)^2 (jJ00|j'0)^2 \tag{22}$$

Recently, we presented a method for including a variational correction[9] in the discrete basis set results. This is necessary because in certain cases the accuracy of our results may be limited by the lack of variational stability with respect to errors due to the approximation of the scattering potential by an N× N matrix, i.e., the difference $U - U^t$. The approach follows Kohn's[13] prescription for the variationally corrected scattering amplitude in three dimensions. Assuming axial symmetry for the target molecule one obtains an equation for the variationally stable partial-wave K matrix:

$$K^s_{\ell\ell'm} = K^t_{\ell\ell'm} + \langle \psi^t_{out} | (U - U^t) | \psi^t_{in} \rangle_{\ell\ell'm} \quad . \tag{23}$$

The trial wavefunctions ψ^t_{in}, ψ^t_{out} and the approximate K matrix element $K^t_{\ell\ell'm}$ are constructed from the discrete basis set solution of the Lippmann-Schwinger equation

$$K = U + U G_0{}^P K \tag{24}$$

where $G_0{}^P$ is the principal value part of the free particle Green's function. Application of the method to e^- - H_2 scattering in the static-exchange approximation showed that higher partial-wave K matrix elements and nondiagonal matrix elements were most improved by the variational correction. This suggests that the variational correction will be important in differential rotational excitation cross sections where off-diagonal terms become important. For a process which is dominated by a single partial-wave we expect the uncorrected results of Eq. (3) to be valid.

III. CALCULATIONS AND RESULTS

The procedure used in calculating the truncated static-exchange (SE) potential V^t has been described in I. For the SCF calculation of the target σ_g occupied orbital we used a $(10s5p_z)$ set of primitive Gaussians contracted to $[7s5p_z]$ on each nucleus. The exponents and contraction coefficients for these bases are those of Huzinaga[14] and are given in Table I. To construct a basis set which defines the matrix elements of the static-exchange potential we augment the target basis set with diffuse Gaussian functions that span the asymptotic region. For a homonuclear diatomic molecule the scattering potential is block diagonal in the symmetries $^2\Sigma_g$, $^2\Sigma_u$, $^2\Pi_g$, $^2\Pi_u$, ..., thus allowing us to solve the Lippmann-Schwinger equation separately for each symmetry. In Table II we list the scattering basis sets used for each symmetry.

For vibrational excitation we need to calculate $V^t_{SE}(R)$ and $E_{HF}(R)$, the H_2 ground state potential curve. The Hartree-Fock approximation to the energy of the ground state of H_2 is valid for small displacements about the internuclear equilibrium position (R_e). To obtain $E_{HF}(R)$ we repeat the SCF calculation of the target occupied orbital for R = 1.0, 1.7, and 2.0 a.u. (see Table III). Using a cubic spline fit to these values we get a vibrational frequency, ω_e = .0218 a.u. and R_e = 1.41 a.u. McLean[15] has extracted spectroscopic constants from HF potential curves and reports an ω_e = .0208 a.u. for R_e = 1.4 a.u.

Since we are interested in low lying vibrational states we use harmonic oscillator functions (defined by our spectroscopic parameters),

as our vibrational wavefunctions. We find that the sum in Eq. (17) can be truncated after 4 partial waves.

For the $0 \rightarrow 1$ vibrational excitation we expect the sum in Eq. (17) to be dominated by the partial waves that vary most with internuclear separation, about R_e. The excitation cross section can be approximated by:

$$\sigma_{01} \alpha \sum_{\ell\ell' m} \delta_{\ell\ell'} \frac{\langle 0|(R-R_e)|1\rangle^2}{2\ell'+1} \left[\frac{1}{4} \left(\frac{\partial}{\partial R} \sin \frac{\delta_{\ell m}}{2} \right)^2_{R_e} + \left(\frac{\partial}{\partial R} \sin^2 \delta_{\ell m} \right)^2_{R_e} \right] \tag{25a}$$

$$= \frac{1}{2\alpha^2} \sum_{\ell m} \frac{1}{2\ell+1} \left[\frac{1}{4} \left(\frac{\partial}{\partial R} \sin \frac{\delta_{\ell m}}{2} \right)^2_{R_e} + \left(\frac{\partial}{\partial R} \sin^2 \delta_{\ell m} \right)^2_{R_e} \right] \tag{25b}$$

where $\alpha = \sqrt{\mu\omega}$ and μ is the reduced mass. Temkin and Faisal[16] applied a similar analysis to prove the validity of adiabatic nuclei theory for e-H_2 scattering. In Fig. 1 we plot the s_σ, p_σ, and p_π phase shifts derived from the T^t matrix, Eq. (3), and those of HC, as a function of internuclear separation. Since the dependence of the phase shift upon internuclear separation will also vary with energy, a more meaningful comparison is possible if we choose energies that are the same

relative distance from the location of the near-resonance peak. For this reason the T-matrix results are given at 5.32 eV, whereas the results of Henry and Chang are extrapolated from their paper at 4.5 eV. From Fig. 1 and Eq. (24b) we see that one need only consider the $\ell = 1$, $m = 0$ contribution. This resonance wave is well represented by a discrete basis set so that the variational correction is small. All T-matrix $0 \rightarrow 1$ vibrational excitation cross sections are calculated in the above approximation. The R dependence of HC's p_σ phase shift differs significantly from ours. Their larger slope at R_e is partly due to the effect of polarization which increases with increase in internuclear separation.[17] However, their treatment of both polarization and exchange is approximate.

In Fig. 2 we present our $0 \rightarrow 1$ vibrational cross section as well as the frame transformation calculation of HC and the experimental data of Linder and Schmidt.[6] Our smaller cross sections are consistent with our analysis of the p_σ phaseshift. Our cross section peaks at a higher energy than experiment because we have neglected polarization. Using Eq. (23) we calculate simultaneous rotational-vibrational ($0 \rightarrow 1$) cross sections and in Fig. 3 compare with Henry and Chang and the experimental results of Linder and Schmidt.[6] In Figs. 4 and 5 we present differential rotational-vibrational ($0 \rightarrow 1$) cross sections at one set of energies in the resonance region (T-matrix results at 5.32 eV and HC at 1.5 eV) and the second set at lower energies (T-matrix at 2.32 eV, HC at 1.5 eV). The magnitude of our cross sections are consistent with our total vibrational results. The static-exchange results exhibit the correct qualitative behavior.

Differential cross sections for rotational excitation contain information about higher partial-wave K matrix elements since pure s-wave scattering does not contribute. Unlike cross sections for vibrational excitation of H_2, which are dominated by p-wave scattering, pure rotational excitation cross sections include significant contributions from off-diagonal K matrix elements. The variationally corrected Σ and π symmetry fixed-nuclei K matrix elements used to calculate the rotational excitation cross sections at 3.40 eV and 6.67 eV incident energy presented here are given in reference 9. Similar calculations were carried out at 4.42 eV incident energy. In addition we have included diagonal d_Δ phase shifts in the Born approximation.

Differential cross sections for $j = 1 \rightarrow j = 3$ rotational excitation are shown in Fig. 6 for 3.40, 4.42, and 6.67 eV incident energy. The solid lines denote our results. The circles indicate the experimental data of Linder and Schmidt[6] at approximately the same incident energies: 3.5 eV, 4.5 eV, and 6.0 eV. The dashed line shows theoretical results of Henry and Lane[8] at 4.42 eV collision energy. Their calculation includes exchange and approximate polarization. The theoretical and experimental results shown in Fig. 6 are in good qualitative agreement except in the region of 6.0 eV collision energy where the experimental result is significantly larger at small scattering angles. This is the region of the Σ_u symmetry resonance enhancement. As in the case of vibrational excitation, we attribute the discrepancy between theory and experiment in this energy region to polarization effects. This has recently been verified by Kaldor and Klonover[18] using the T-matrix method. They account for polarization

effects by including second order contributions to the optical potential. Their static-exchange results for $j = 1 \rightarrow j = 3$ rotational excitation, which are not variationally corrected, are in good agreement with ours, and their results including including polarization are in much better agreement with experiment.

To show the effect of off-diagonal K matrix elements, Fig. 7 compares our diagonal K matrix approximation result (dashed line) with our complete K matrix result (solid line) at 4.42 eV collision energy. Fig. 7 also shows the semi-empirical adiabatic-nuclei results of Chang and Temkin[7] (dotted line) normalized to our results. Their results were obtained by assuming the diagonal phase shift approximation and it is interesting to note the excellent qualitative agreement between their results and our diagonal phase shift approximation results.

IV. DISCUSSION AND CONCLUSIONS

Our results indicate that the static-exchange model is a useful quantitative first step in the calculation of vibrational and rotational cross sections. There are limitations in the predictions of this model. For example, the maximum in the vibrational excitation cross sections occurs 1.5 eV higher than is experimentally observed. However, there are no significant qualitative changes in these inelastic cross sections in going from the static-exchange potential to the static-exchange plus polarization potentials. This is confirmed by the recent results of Klonover and Kaldor[19] who introduced polarization effects into the present L-2 T-matrix approach. This consideration is not often fully appreciated when semi-empirical polarization potentials are introduced into calculations.

The results for the e-H_2 system have encouraged us to study the more difficult problem of resonant vibrational excitation of N_2.

Preliminary results again indicate that considerable structure in these vibrational excitation cross sections already occur in the static-exchange approximation. Methods for including polarization at different internuclear spacings are currently being investigated with results on both questions forthcoming.

Rotational excitation cross sections contain information about the anisotropic components of the molecular target potential. Our results show that the sd off-diagonal K matrix element contributes significantly to pure rotational excitation of H_2. Since this effect should increase for scattering by other molecules, experimental results for rotational excitation of other molecules would be of considerable interest.

ACKNOWLEDGMENT

This research was supported by grant number CHE76-05157 from the National Science Foundation and by an Institutional Grant from the Department of Energy EX-76-G03-1305.

*Supported by a grant from the National Science Foundation.

†Contribution No. 5722.

[1]T.N. Rescigno, C.W. McCurdy, Jr., and V. McKoy, Phys. Rev. A 11, 825 (1975).

[2]B. I. Schneider, Phys. Rev. A. 11, 1957 (1975).

[3]A.W. Fliflet, D. A. Levin, M. Ma, and V. McKoy, Phys. Rev. A 17, 160 (1978).

[4]G.J. Schulz, Rev. Mod. Phys. 45, 378 (1973).

[5]R.J.W. Henry and E.S. Chang, Phys. Rev. A. 5, 276 (1972).

[6]F. Linder and H. Schmidt, Z. Naturforsch 26a, 1603 (1971).

[7]E.S. Chang and A. Temkin, Phys. Rev. Lett. 23, 399 (1969).

[8]R.J.W. Henry and N.F. Lane, Phys. Rev. 183, 221 (1969).

[9]A. W. Fliflet and V. McKoy, "Variationally corrected discrete basis set calculation for electron-molecule scattering in the static-exchange approximation," Phys. Rev. A, accepted for publication.

[10]D. A. Levin, A.W. Fliflet, M. Ma, and V. McKoy, "Gaussian Matrix Elements of the Free Particle Green's Function," J. Comp. Phys., accepted for publication.

[11]A. Temkin, K. V. Vasavada, E. S. Chang, and A. Silver, Phys. Rev. 186, 57 (1969).

[12]D. M. Chase, Phys. Rev. 104, 838 (1956).

[13]W. Kohn, Phys. Rev. 74, 1763 (1948).

[14]S. Huzinaga, J. Chem. Phys. 42, 1293 (1965).

[15]A. P. McLean, J. Chem. Phys. 40, 243 (1964).

[16]F. H. M. Faisal and A. Temkin, Phys. Rev. Lett. 28, 203 (1972).

[17]W. Kolos and L. Wolniewicz, J. Chem. Phys. 46, 1426 (1967).

[18]U. Kaldor and A. Konover, J. Phys. B 11, 1623 (1978).

[19]A. Klonover and U. Kaldor, "Ab initio Electron-Molecule Scattering Theory Including Polarization: Vibrational-Rotational Excitation of H_2." preprint August (1978).

TABLE I. Valence Σ basis set.

	Type	Center	Exponent	Contraction Coefficient
1.	(000)	(0, 0, ± 0.7003)*	1685.517	0.0042273
2.	"	"	249.9384	0.035026
3.	"	"	55.65834	0.1920389
4.	"	"	15.2743	0.8333764
5.	"	"	4.8628	
6.	"	"	1.7316	
7.	"	"	0.66805	
8.	"	"	0.27437	
9.	"	"	0.11698	
10.	"	"	0.041133	
11.	(001)	"	4.8	
12.	"	"	2.53	
13.	"	"	1.33	
14.	"	"	0.701	
15.	"	"	0.369	

*For the three additional internuclear spacings the centers are for R = 1.0, 1.7, and 2.0 au.: (0, 0, ± .5), (0, 0 ± 0.85), and (0, 0, ± 1.0) respectively. The exponents are the same for all four internuclear spacings.

TABLE II. Scattering basis sets

$^2\Sigma_g^+$ [c]			$^2\Sigma_u^+$ [d]		
$\underset{\sim}{A}$[a] = (0, 0, ± 0.7003) (ℓ, m, n)[b] = (0, 0, 0)	(0, 0, ±0.7003) (0, 0, 1)	(0, 0, 0) (0, 0, 0)	$\underset{\sim}{A}$ = (0, 0, ± 0.7003) (ℓ, m, n) = (0, 0, 0)	(0, 0, ± 0.7003) (0, 0, 1)	(0, 0, 0) (0, 0, 1)
1685.517	4.8	0.025	1685.517	4.8	0.1
249.9584	2.53	0.15	249.9584	2.53	0.05
55.65834	1.33	0.009	55.65834	1.33	0.025
15.2743	0.701	0.0054	15.2743	0.701	0.0125
4.8628	0.369	0.00324	4.8628	0.369	0.00625
1.7316		0.001944	1.7316		0.003125
0.66805		0.001166	0.66805		
0.27437		0.0006	0.27437		
0.11698			0.11698		
0.041133			0.041133		

$^2\Pi_u$ [e]		$^2\Pi_g$ [f]	
$\underset{\sim}{A}$ = (0, 0, ± 0.7003) (ℓ, m, n) = (1, 0, 0)	(0, 0, 0) (1, 0, 0)	$\underset{\sim}{A}$ = (0, 0, ± 0, 7003) (ℓ, m, n) = (1, 0, 0)	
17.3	0.221	17.3	0.132
9.12	0.132	9.12	0.0792
4.8	0.0792	4.8	0.0474
2.53	0.0474	2.53	0.0284
1.33	0.0284	1.33	0.017
0.701	0.017	0.701	0.01
0.369	0.01	0.369	0.006
	0.006	0.221	0.003
	0.003		0.0015
	0.0015		

[a] $\underset{\sim}{A}$ denotes the coordinates of the center of the basis function $\mu_{\ell mn}^{\alpha \underset{\sim}{A}}(\underset{\sim}{r})$.

[b] (ℓ, m, n) denotes the symmetry type of $\mu_{\ell mn}^{\alpha \underset{\sim}{A}}(\underset{\sim}{r})$.

[c] See the footnote for Table I. The Σ_g^+ contribution to the total cross section was computed for additional internuclear spacings equal to 1.0 and 2.0 a.u.

[d] See the footnote at the bottom of Table I. The Σ_u^+ contribution to the total cross section was computed for additional internuclear spacings equal to 1.0, 1.7, and 2.0 a.u.

[e] See the footnote for Table I. The Π_u contribution to the total cross section was computed for additional internuclear spacings equal to 1.0 and 2.0 a.u.

TABLE III. Ground state potential curve of H_2.

R(a.u.)	$E_{HF}(R)$ (a.u.)
1.0	-1.0850906
1.4006	-1.1335439
1.7	-1.1192306
2.0	-1.0914487

Figure Captions

Fig. 1 Comparison of static-exchange and uncoupled adiabatic approximation of Henry and Chang's phase shifts for different internuclear spacings. The T-matrix results (solid line) are given for 5.32 eV whereas the results of Henry and Chang (broken line) are given for 4.5 eV. See text for explanation.

Fig. 2 Vibrational Excitation Cross Section.
— T-matrix results
---- Henry and Chang (adjustable parameter)
□ Linder and Schmidt (experimental)

Fig. 3 Rotational-vibrational ($0 \rightarrow 1$) cross section.
Curves defined as in Fig. 2.

Fig. 4 Differential vibrational ($0 \rightarrow 1$) -rotational cross section (non-resonant energy region). Curves defined as in Fig.2. T-matrix calculation given at 2.32 eV HC and experiment are multiplied by .5 for $\Delta j = 0$ and given at 1.5 eV.

Fig. 5 Differential-vibrational ($0 \rightarrow 1$)-rotational cross section section (resonant energy region). Curves defined as in Fig. 2. T-matrix calculation given at 5.32 eV HC and experiment are given at 4.5 eV and multiplied by .5 for $\Delta j = 0$.

(Figues Captions-con'd)

Fig. 6 Differential cross sections for rotational excitation ($j=1 \rightarrow j=3$) at collision energies indicated.

Fig. 7 Differential cross section for rotational excitation ($j=1 \rightarrow j=3$) at 4.42 eV collision energy. Solid line: full K matrix SE result; dashed line: diagonal phase shift approximation SE result; dotted line: semi-empirical diagonal phaseshift approximation result from Ref. 7 normalized to present theory.

Fig. I

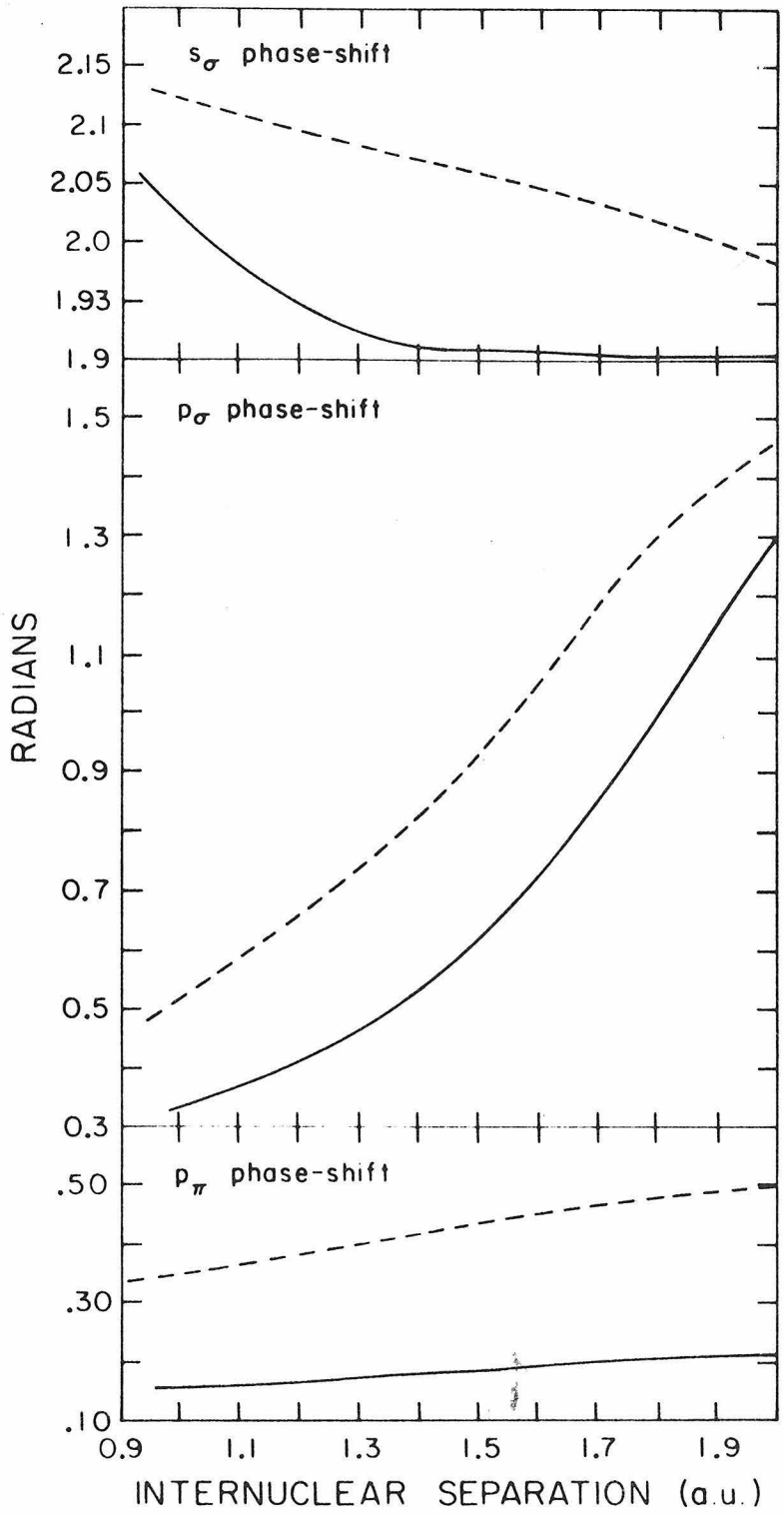

Figure 1

Fig. I

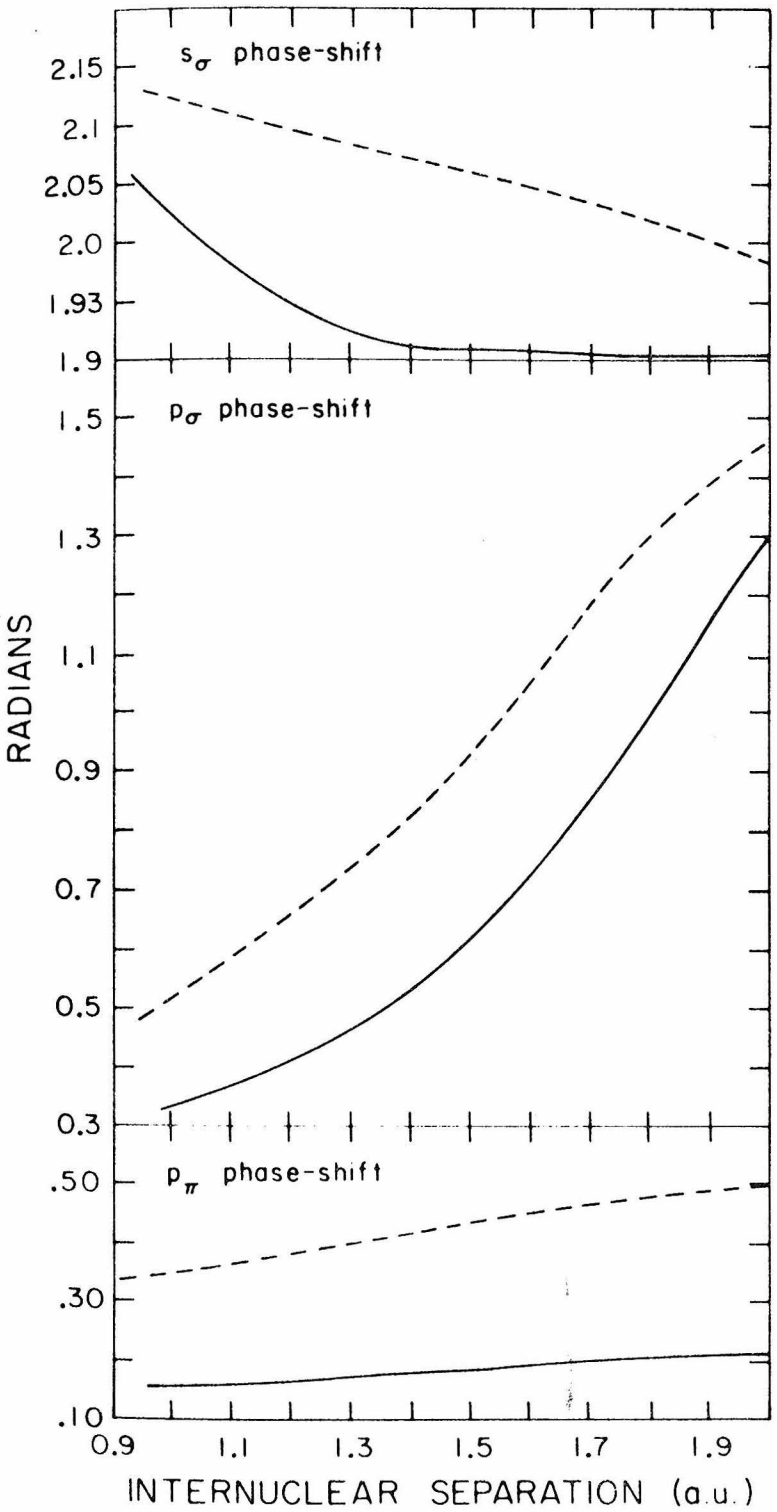

Figure 1

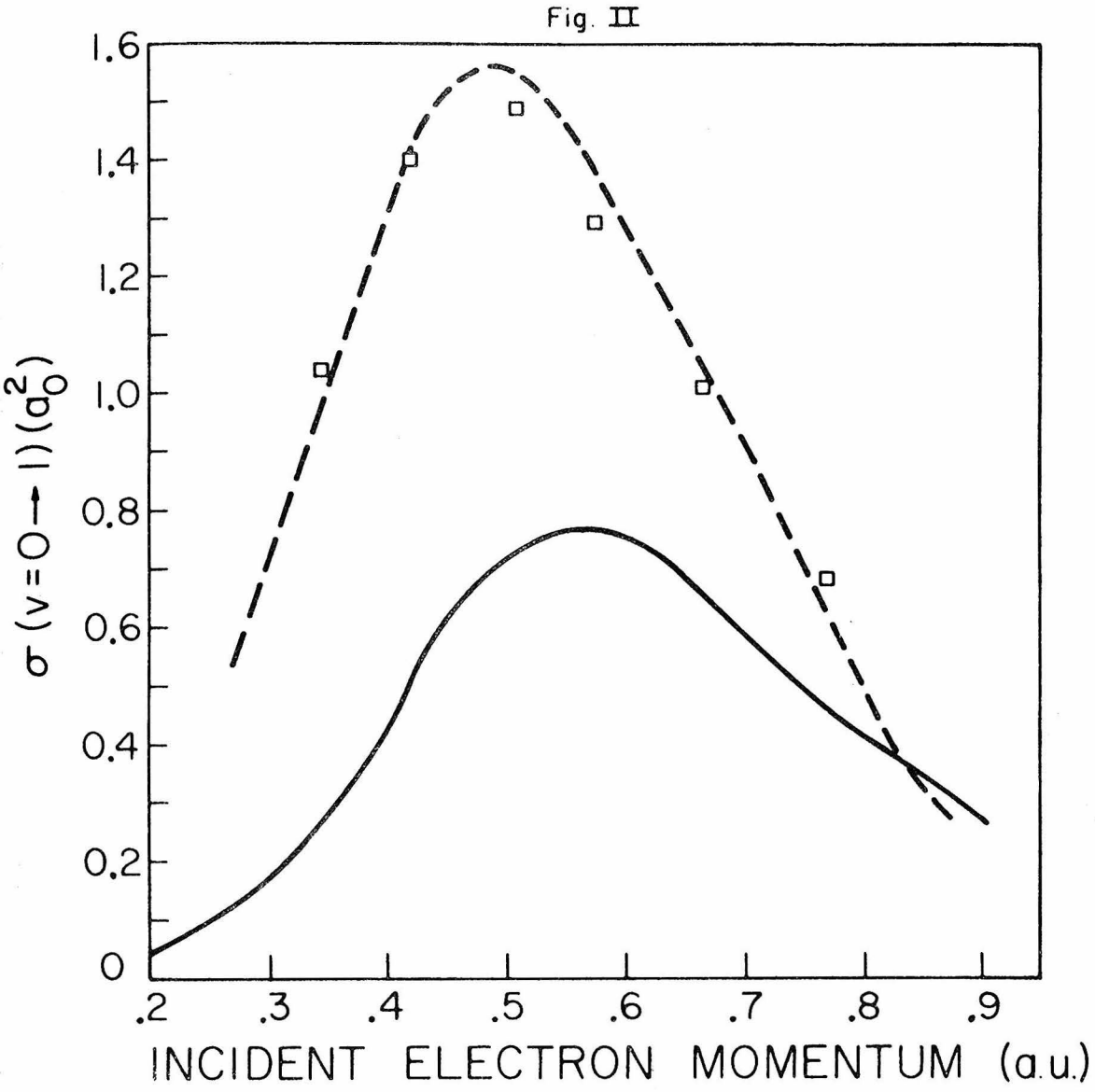
Fig. II
1.6
1.4
1.2
1.0
0.8
0.6
0.4
0.2
0
σ (v=0→1) (a₀²)
.2
.3
.4
.5
.6
.7
.8
.9
INCIDENT ELECTRON MOMENTUM (a.u.)

Figure 2

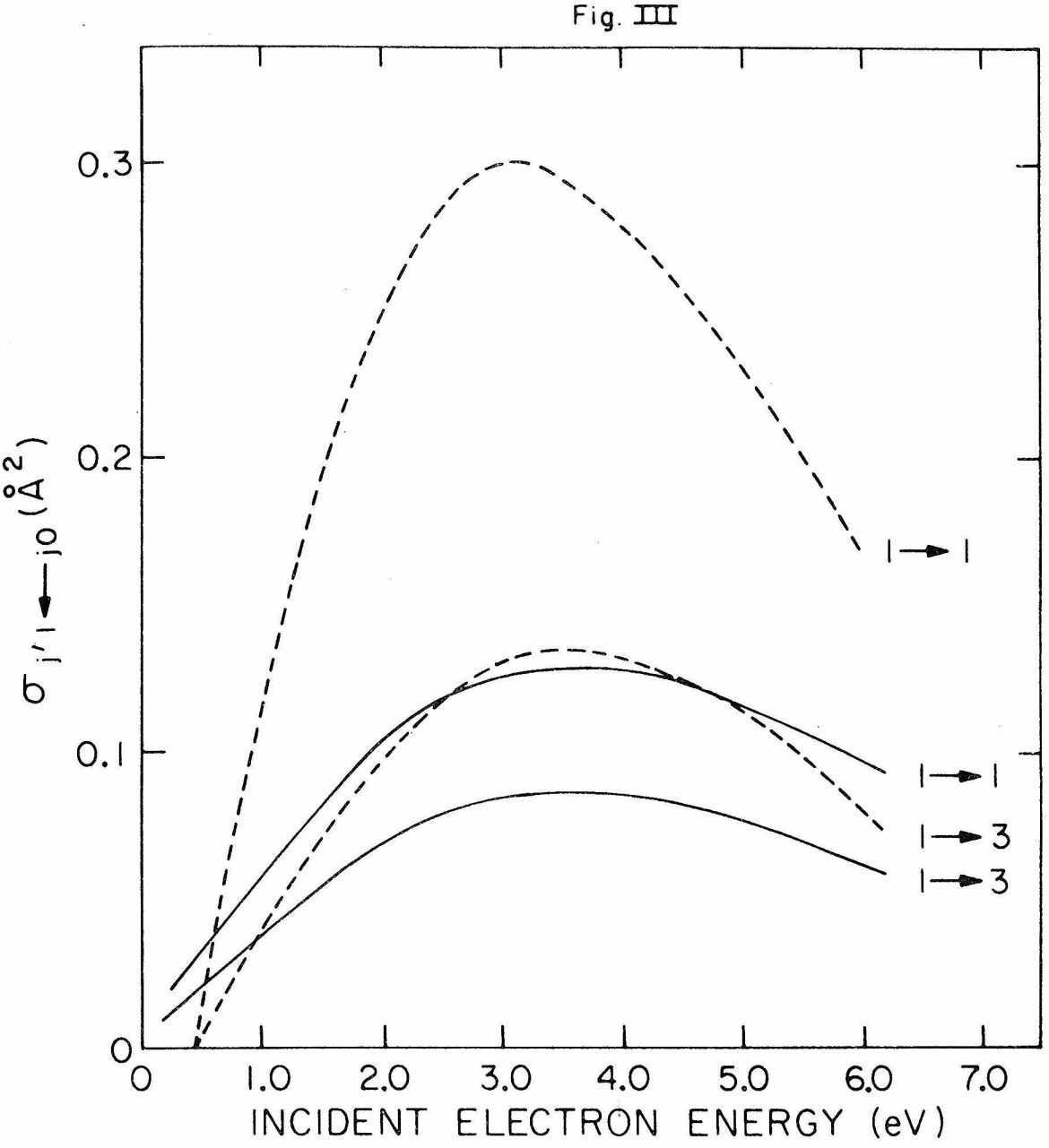
Fig. III
0.3
0.2
0.1
0
$\sigma_{j'1 \leftarrow j0}$ (Å^2)
1→1
1→1
1→3
1→3
0
1.0
2.0
3.0
4.0
5.0
6.0
7.0
INCIDENT ELECTRON ENERGY (eV)

Figure 3

Fig. IV

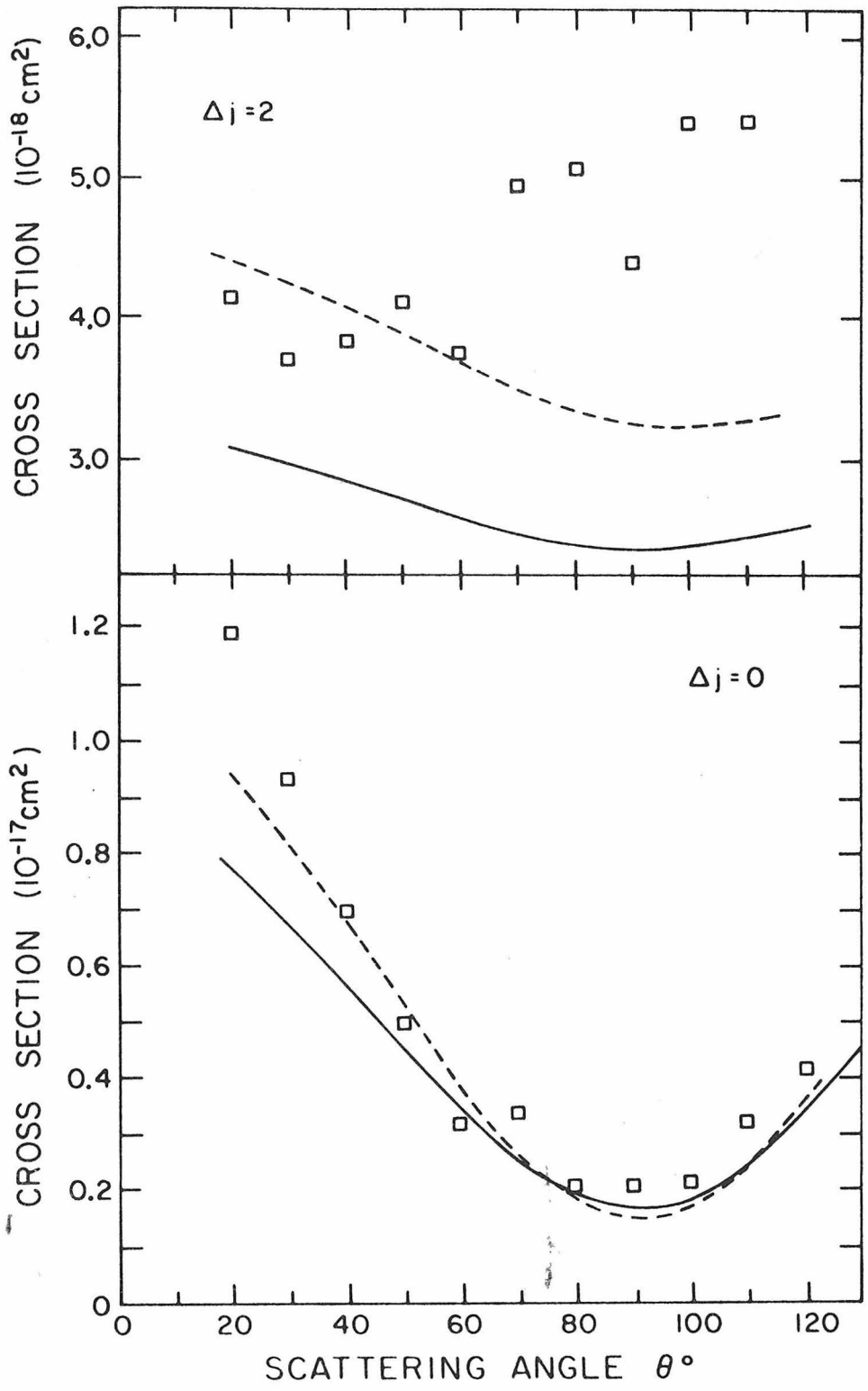

Figure 4

Fig. V

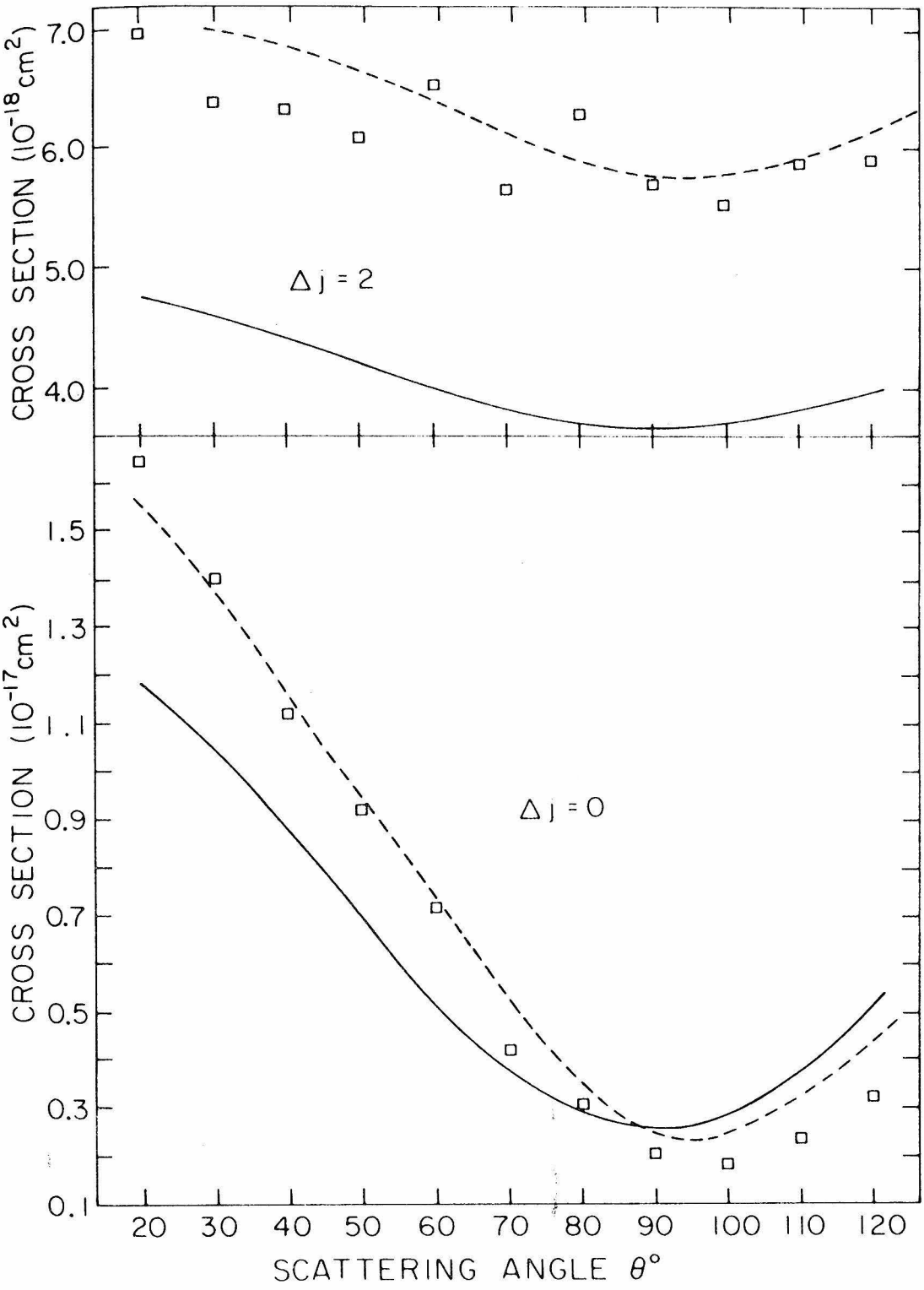

Figure 5

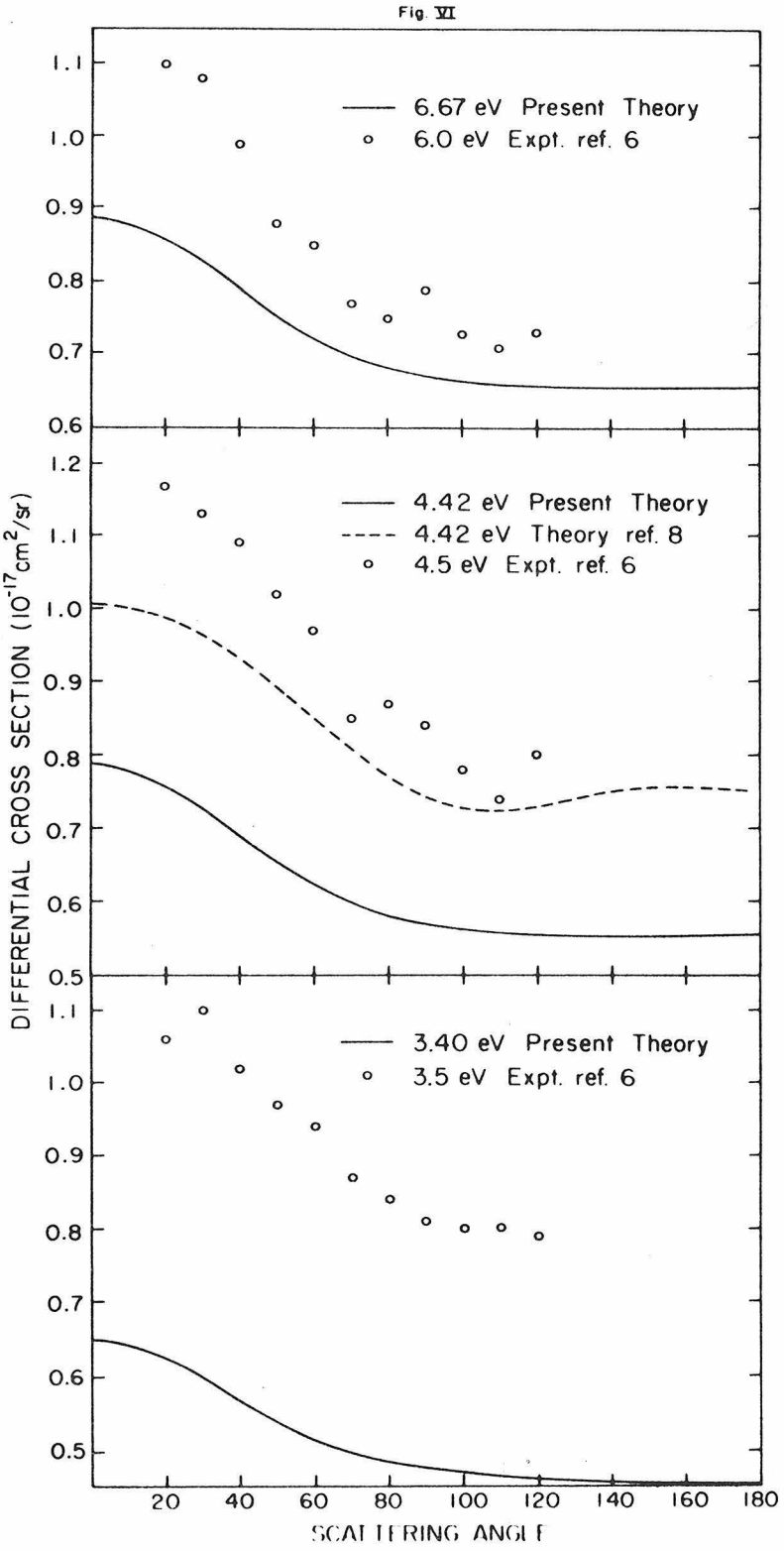
Fig. VI
6.67 eV Present Theory
6.0 eV Expt. ref. 6
4.42 eV Present Theory
4.42 eV Theory ref. 8
4.5 eV Expt. ref. 6
3.40 eV Present Theory
3.5 eV Expt. ref. 6
DIFFERENTIAL CROSS SECTION (10^{-17}cm^2/sr)
SCATTERING ANGLE
20
40
60
80
100
120
140
160
180

Figure 6

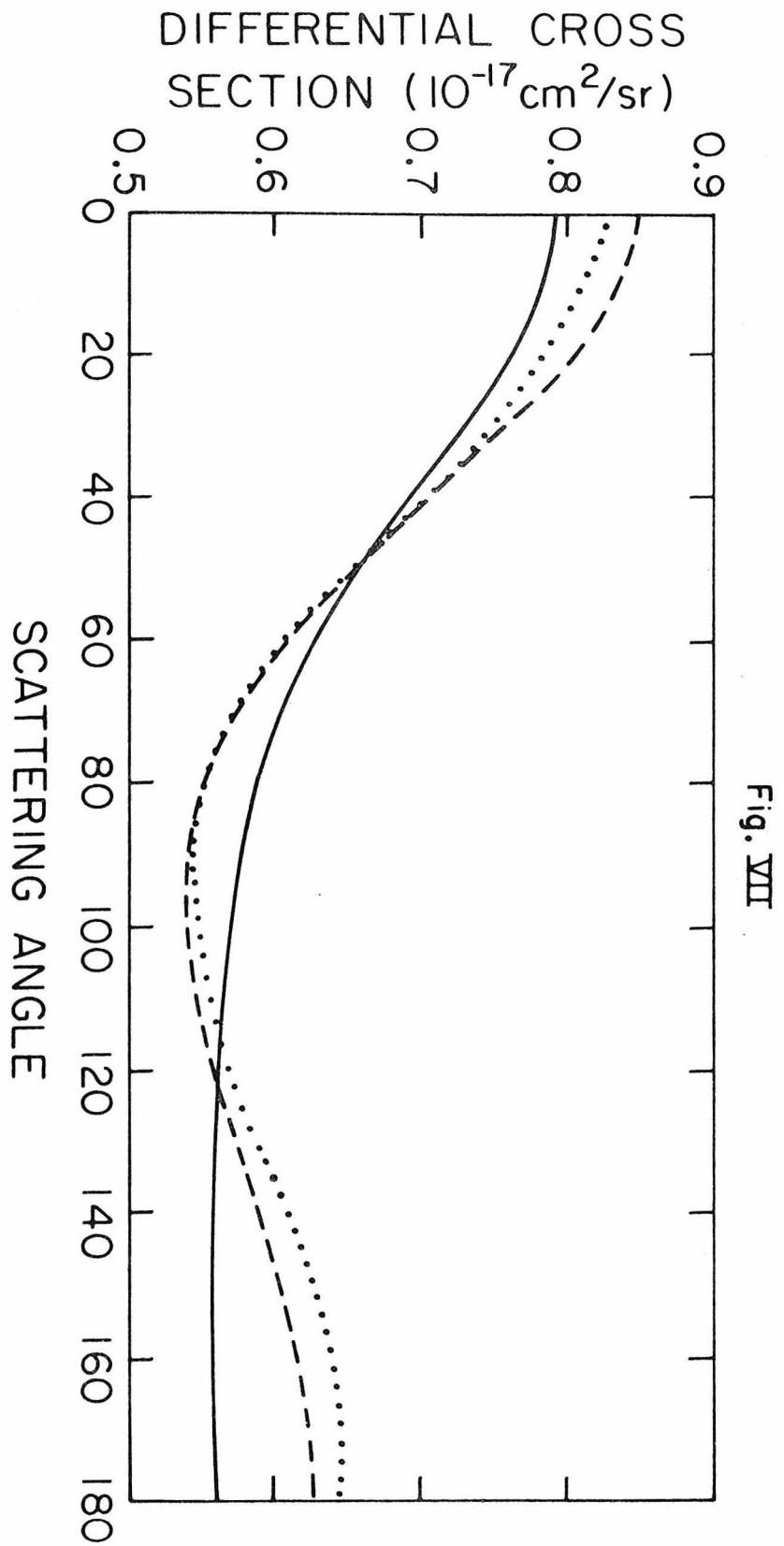
DIFFERENTIAL CROSS SECTION (10^{-17} cm^2/sr)
0.5
0.6
0.7
0.8
0.9
0
20
40
60
80
100
120
140
160
180
SCATTERING ANGLE
Fig. VII

Figure 7

SECTION B

Low Energy Vibrational and Vibrational-Rotational Excitation Cross Sections for N_2 by Electron Impact

I. INTRODUCTION

The 2.4 eV resonance in N_2 has been extensively studied both experimentally[1] and theoretically. The structure in the elastic cross section as well as the degree of vibrational excitation indicate the presence of a compound state with a lifetime of the order of a vibrational period. Studies by Gilmore[2] and Krauss and Mies[3] show that the compound state is formed by the addition of an electron in a π_g orbital to the ground electronic state of N_2. The adiabatic-nuclei approximation[4] which gives the transition amplitude between states, $v\Gamma \rightarrow v'\Gamma'$, as

$$f_{v',\Gamma';\, v,\Gamma}(\hat{\underset{\sim}{r}}) = \langle \psi_{v',\Gamma'}(\underset{\sim}{R}) \left| f(\hat{\underset{\sim}{r}}, \hat{\underset{\sim}{R}}) \right| \psi_{v,\Gamma}(R) \rangle + \epsilon \qquad (1)$$

where $f(\hat{\underset{\sim}{r}}, \hat{\underset{\sim}{R}})$ is a fixed-nuclei amplitude, cannot be used for resonance scattering since the error term in Eq. (1) is not small. This error term, ϵ, is negligible only if the lifetime of the compound state is small compared to the vibrational period of the parent molecule.[5] For the nonresonant scattering in N_2 the adiabatic-nuclei approximation is valid and can be used analogously as in H_2.[6] Chandra and Temkin[5] have developed a hybrid theory for studying these resonant vibrational excitation cross sections. Their theory is close-coupling with respect to the vibrational degrees of freedom but adiabatic-nuclei with respect to rotation. The application of this theory to e-N_2 scattering has the importance of being the first essentially ab initio calculation to reveal the substructure in the resonant

cross sections.

While ab initio methods are clearly very desirable the importance of phenomenological theories should not be overlooked. Birtwistle and Herzenberg[7] have developed a "boomerang" model and applied it to e-N_2 scattering. The "boomerang" model is a compound-state model which reduces the scattering problem to vibrational motion in a complex adiabatic potential. In this application[7] the necessary parameters were extracted from available experimental data. More recently Domcke and Cederbaum[8] have derived explicit algebraic expressions for resonant vibrational excitation cross sections. Although their theory is closely related to that of Birtwistle and Herzenberg[7] in that a compound-state picture is adopted, it does not require the numerical solution of the nuclear wave equation.

In this paper we have used the compound-state model of Domcke and Cederbaum[8] to study the e-N_2 vibrational excitation in the static-exchange approximation. All parameters are extracted from the solution of the Lippmann-Schwinger equation for the T-matrix as a function of internuclear spacing. Absolute peak heights, resonance position,and widths at each internuclear spacing are determined simultaneously from the full scattering calculation. Moreover, our approach yields absolute vibrational excitation cross sections. The results indicate that the static-exchange approximation to the scattering potential can account for many features of the vibrational excitation cross section substructure. We present cross sections for the vibrationally elastic and inelastic processes that are in good qualitative agreement with experimental results. We stress that the occurrence

of the resonance at an energy higher than the experimental value is not nearly as important as accounting for the structure of the resonance. This structure already occurs in the static-exchange model and polarization effects will further modify it. By comparing the cross sections in the static-exchange approximation with the measured cross sections we can reliably assess the correct role of polarization effects on the excitation cross section.

II. THEORY

A. The basic model

In this section we will only briefly review some important features of compound-state theories of vibrational excitation and discuss the extraction of parameters which define these theories from the solution of T-matrix equations. We will also show how the model of Domcke and Cederbaum[8] can be extended to give absolute rotational-vibrational cross sections.

Compound state theories have the advantage of working directly with the resonant electronic state of the (N+1) electron system.[9] The correct vibrational wave function associated with this electronic state incorporates the nuclear motion in a finite-lived compound state. Birtwistle and Herzenberg[7] have shown that the vibrational wave function in the resonant region is a solution of a second order complex inhomogeneous differential equation

$$\left(-\frac{\hbar^2}{2M}\frac{d^2}{dR^2} + E^-(R) - \frac{i}{2}\Gamma(R) - \epsilon_p\right)\xi(R,\epsilon_p) = \zeta'(R)\,\chi_0(R) \qquad (2)$$

where $E^-(R)$ is the potential energy curve for N_2^- ; $\Gamma(R)$ is the lifetime of the complex; ϵ_p is the incident electron energy; M, the reduced mass of the nuclei; χ_0 the initial vibrational wave function of N_2; and, $\zeta'(R)$ is an entry amplitude for the incident electron. Once $\xi(R,\epsilon_p)$ is known the vibrational excitation cross section can be calculated. Equation (2) has the disadvantage that it requires us to know $E^-(R)$ and $\Gamma(R)$ for large values of R where for many systems the Hartree-Fock approximation breaks down. This introduces additional complicating features in constructing the scattering potential in the static-exchange approximation. In this respect we have found the model Hamiltonian approach of Domcke and Cederbaum[8] to be more convenient.

Instead of starting from the full scattering wave function Domcke and Cederbaum[8] derive a Hamiltonian which represents the coupling of the electronic level of positive energy to the continuum of scattering states and to the molecular vibrations. For a simple isolated resonance orbital i of energy ϵ_i^0 and a single vibrational coordinate the Hamiltonian has the form

$$H = H_0 + H_1 \qquad (3a)$$

$$H_0 = \epsilon_i^0(0)\, a_i^+ a_i + \sum_k \epsilon_k a_k^+ a_k + \omega(b^+ b + \tfrac{1}{2}) +$$

$$\kappa_i^0 (a_i^+ a_i - n_i)(b + b^+) \tag{3b}$$

$$H_1 = \sum_k (V_{ik} a_i^+ a_k + V_{ki} a_k^+ a_i) + \sum_{k,k'} V_{kk'} a_k^+ a_{k'} \tag{3c}$$

where we have dropped the quadratic coupling constant describing the interaction between the electronic and vibrational motion. In Eq. (3) the a_i and a_k are the annihilation operators for an electron in a discrete one-particle state φ_i and the continuum one-particle wavefunction φ_k, respectively. The b and b^+ are annihilation and creation operators for vibrational quanta; ω is the ground state vibrational frequency; and, n_i is the occupation number of the i^{th} orbital. H_0 contains electronic, vibrational and electronic-vibrational interactions respectively, $\epsilon_i(0)$ is the energy of the one-particle level φ_i at R_e of the molecule and

$$\kappa_i^0 \equiv \frac{1}{\sqrt{2}} \left(\frac{\partial \epsilon_i^0}{\partial Q} \right)_0 , \text{ linear coupling constant} \tag{4a}$$

$$Q = \sqrt{\mu\omega}\,(R - R_e) , \quad \mu \text{ is the reduced mass.} \tag{4b}$$

The subscript $_0$ indicates that the derivatives should be evaluated at the equilibrium position of the ground state. The first term in H_1 causes an electron to go between the bound state $|\varphi_i\rangle$ and a continuum state $|\varphi_k\rangle$ and converts φ_i into a resonance. In their

notation[8] the explicit form of V_{ik} is

$$V_{ik}(\underset{\sim}{R}) = \int d^3\underset{\sim}{r}\, \varphi_i^*(\underset{\sim}{r}, \underset{\sim}{R})\, H^{e\ell}(\underset{\sim}{r}, \underset{\sim}{R})\, \varphi_k(\underset{\sim}{r}, \underset{\sim}{R}) \quad . \tag{5}$$

The second term in Eq. (3c) represents direct scattering which is usually weak compared to the resonant scattering. By neglecting this term in H_i the perturbation series for the S-matrix may be summed exactly. The differential vibrational cross section, except for kinematic factors, is given by

$$\frac{d\sigma}{d\Omega}(m \rightarrow n) \sim \frac{|p'|}{|p|} \left| \langle n | V_{p'i} (\epsilon_p - \mathcal{H})^{-1} V_{ip} | m \rangle \right|^2 \tag{6}$$

where m and n are the initial and final vibrational states, of the diatomic molecule; ϵ_p is the energy of the incident electron; p' and p are the magnitudes of the final and incident electron momenta; and, $\mathcal{H}$ is a non-Hermitian Hamiltonian that describes the dynamics of the vibrational motion in the resonance state.

For the simple case of one vibrational coordinate Eq. (6) can be evaluated to give the $n \rightarrow m$ vibrational excitation cross section as:

$$\sigma(n, m, \epsilon_p) = \frac{C(n,m)}{\epsilon_{p'}} \frac{|p'|}{|p|} \left| \sum_{\ell} \frac{A_{n\ell}\, B_{m\ell}}{\epsilon_p - \epsilon + \kappa^2/\omega - \ell\omega} \right|^2 \tag{7}$$

where

$$A_{n\ell} = \begin{cases} e^{-a/2} \sqrt{\frac{n!}{\ell!}} \left(\frac{\kappa}{\omega}\right)^{\ell-n} L_n^{\ell-n}(a) , & \ell \geq n \\ e^{-a/2} \sqrt{\frac{\ell!}{n!}} \left(\frac{-\kappa}{\omega}\right)^{n-\ell} L_\ell^{n-\ell}(a) , & \ell \leq n \end{cases} \tag{8a}$$

$$B_{\ell m} = \begin{cases} e^{-a/2} \sqrt{\frac{\ell!}{m!}} \left(\frac{-\kappa}{\omega}\right)^{m-\ell} L_\ell^{m-\ell}(a) , & \ell \leq m \\ e^{-a/2} \sqrt{\frac{m!}{\ell!}} \left(\frac{\kappa}{\omega}\right)^{\ell-m} L_m^{\ell-m}(a) , & \ell \geq m \end{cases} \tag{8b}$$

$$a \equiv (\kappa/\omega)^2 \tag{8c}$$

$$\epsilon = \epsilon^r(0) - \frac{i\Gamma(0)}{2} \tag{8d}$$

$$\kappa = \frac{1}{\sqrt{2}} \left(\frac{\partial \epsilon^R}{\partial Q}\right)_0 - \frac{i}{2\sqrt{2}} \left(\frac{\partial \Gamma}{\partial Q}\right)_0 \tag{8e}$$

and $\epsilon^r(R) = E^-(R)$, $\Gamma(0) = \Gamma(R_e)$, and $C(n,m)$ is a proportionality constant. $L_n^m(a)$ denotes the generalized Laguerre polynomials of complex argument. This expression, Eq. (7), is not explicitly given in Ref. 8 but can be derived from their general relationships.

The formulation of Birtwistle and Herzenberg[7] requires a numerical solution of the differential equation, Eq. (12), and hence a knowledge of the potential energy curves and widths over a wide range of R. However, Eq. (7) only requires the local behavior of these quantitites about the equilibrium geometry of the molecule. This can be an important advantage in the application of these formalisms in the static-exchange approximation since the Hartree-Fock wavefunction can often behave poorly at larger internuclear separations. Moreover, neglecting the energy dependence of Γ all factors can be absorbed in the energy-independent constant C(N, m). With these approximations we can obtain absolute cross sections in the resonance region if we know the absolute cross sections for resonance scattering at any energy.

B. Absolute vibrational cross sections

The structure of the vibrational excitation cross section in the scattering of electrons in the resonance region by N_2 is due to partially overlapping resonances. These resonances correspond to poles in the S-matrix occurring at the complex energies of the vibrational states of the ion. For example, in H_2 we have $\hbar\omega \ll \Gamma$ so that the resonances are broad and overlap to give one broad peak in the cross section.[11] In O_2, $\hbar\omega \gg \Gamma$ which gives a series of peaks in the cross section indicating noninteracting resonances.[11] N_2 is somewhere intermediate between these two cases because $\hbar\omega \approx \Gamma$. At scattering energies much further from the resonance than the distance between peaks in the cross section, the resonant

vibrational excitation scattering amplitude, $f_\ell^{Res}(k)$, should behave effectively as though there were a single pole in the S-matrix. The resonant scattering amplitude may then be written as:[12]

$$f_\ell^{Res}(k) = \frac{\sqrt{a(\epsilon^r)}}{2k} \frac{\Gamma_\ell(R)}{(\epsilon_p - \epsilon_\ell^r(R)) + i\frac{\Gamma_\ell(R)}{2}} \tag{9}$$

where we assume that it is dominated by a single partial wave ℓ and $a(\epsilon^r)$ is the cross section peak height at the resonance energy. Again we emphasize that we consider here resonance scattering contributions only. The total cross section in this energy region is dominated by direct scattering processes which does not have a Breit-Wigner form. Equivalently, we are looking only at the resonance contribution to the tail of the cross section. For these reasons we can write the vibrational excitation cross section at these energies, apart from some kinematic factors, as:

$$\sigma_{vv'}^{Res} = |\langle v' | f_\ell^{Res}(k) | v \rangle|^2 \tag{10a}$$

$$= \left| \int \frac{\chi_{v'}^*(R)/2\sqrt{a(\epsilon^r(R))}\,\Gamma(R)\,\chi_v(R)\,dR}{(\epsilon_p - \epsilon^r(R)) + i\,\Gamma(R)/2} \right|^2 \tag{10b}$$

Neglecting the R dependence in $\Gamma(R)$ in the numerator of Eq. (10b), as is assumed in deriving Eq. (7) in reference 8, we obtain

$$\sigma^{\text{Res}}_{vv'} = \frac{a(\epsilon^r(0))\Gamma^2(0)}{4} \cdot \left\{ \left[\int \frac{\chi^*_{v'}(R)(\epsilon_p - \epsilon^r(R))\,\chi_v(R)\,dR}{D(\epsilon_p, R)} \right]^2 \right.$$

$$\left. + \left[\int \frac{\chi^*_{v'}(R)\,\Gamma(R)\,\chi_v(R)\,dR}{2D(\epsilon_p, R)} \right]^2 \right\} \qquad (10c)$$

where

$$D(\epsilon_p, R) = (\epsilon_p - \epsilon^r(R))^2 + \frac{\Gamma^2(R)}{4} \quad . \qquad (10d)$$

Equation (10c) can be further simplified by expanding $\epsilon^r(R)$ and $\Gamma(R)$ in a Taylor series and retaining only the first order term, (which is again consistent with the approximations used in deriving Eq. (7) of reference 8), to give

$$\sigma_{vv'} = \frac{a(\epsilon^r(0))\Gamma^2(0)}{4} \left\{ \left[\int \frac{\chi^*_{v'}(\rho)(\epsilon_p - E_1 - E_2\rho)\,\chi_v(\rho)\,d\rho}{D(\epsilon_p, \rho)} \right]^2 \right.$$

$$\left. + \frac{1}{4} \left[\int \chi^*_{v'}(\rho)(\Gamma_1 + \Gamma_2\rho)\,\chi_v(\rho)\,d\rho \right]^2 \right\} \qquad (11a)$$

where

$$\Gamma_1 = \Gamma(0) \tag{11b}$$

$$\Gamma_2 = \left(\frac{\partial \Gamma}{\partial \rho}\right)_0 \tag{11c}$$

$$E_1 = \epsilon^r(0) \tag{11d}$$

$$E_2 = \left(\frac{\partial \epsilon^r}{\partial \rho}\right)_0 \tag{11e}$$

$$D(\epsilon_p, \rho) = \epsilon_p^2 \left[1 - \left\{\frac{2(E_1 + E_2\rho)}{\epsilon_p} - \frac{(E_1 + E_2\rho)^2}{\epsilon_p^2} - \frac{(\Gamma(0) + \Gamma_2\rho)^2}{4\epsilon_p^2}\right\}\right] \tag{11f}$$

The values of $a(\epsilon^r)$, $\epsilon^r(R)$, and $\Gamma(R)$ that are obtained from a scattering calculation can be used in Eq. (11a) to give an absolute cross section for resonance scattering in this energy region. In Appendix A, Eqs. (7) and (11a) are shown to have the same energy dependence for incident electron energies much larger than $\epsilon^r(0)$. For resonant vibrational scattering the cross section at high energies has the form $\frac{1}{\epsilon_p^3}$, $\frac{1}{\epsilon_p^5}$, $\frac{1}{\epsilon_p^7}$ for $0 \rightarrow 0$, $0 \rightarrow 1$, $0 \rightarrow 2$ vibrational excitations, respectively. Since Eqs. (7) and (11a) are equivalent forms of the vibrational excitation cross section, they can be equated in the high energy

tail of the resonance to give the energy independent constant C(n, m).

We wish to emphasize that Eq. (11a) is different from the vibrational excitation cross section that is given in the adiabatic-nuclei approximation,[6] namely:

$$\sigma_{vv'}^{AD} = \sum_{\ell\ell' m} \frac{\left| a_{\ell\ell' m}(v, v') \right|^2}{2\ell' + 1} \quad , \tag{12}$$

where $a_{\ell\ell' m}(v, v')$ is given explicitly in Ref. 6, because the dynamical scattering coefficients $a_{\ell\ell' m}(v, v')$ contain both direct and resonance scattering information. We use Eq. (12) to calculate vibrational cross sections in the nonresonant channels at the positive energy eigenvalues corresponding to the diagonalization of

$$H^t \chi_k = \frac{k^2}{2} \chi_k \tag{13a}$$

where

$$H^t = -\frac{1}{2} \nabla^2 + V^t \tag{13b}$$

Consistent with earlier approximations[6] we limit the R dependence of each $a_{\ell\ell' m}$ as

$$a_{\ell\ell' m}(R) \cong a_{\ell\ell' m}(R_e) + \left| \frac{\partial a}{\partial R} \ell\ell' m \right|_{R_e} (R - R_e) \tag{13c}$$

Apart from a factor of $1/\epsilon_p$, we have shown that Eq. (9) may be used to calculate absolute total vibrational excitation cross sections. To calculate total and differential vibrational-rotational excitation cross sections, we need an expression for the resonant dynamical scattering coefficient. We denote this quantity as $a^{vv'}_{\ell\ell' m}$ as in Eq. (12):

$$\sigma^{Res}_{vv'} = \sum_{\ell\ell' m} \frac{|a^{vv'}_{\ell\ell' m}|^2}{2\ell'+1} \tag{14}$$

Since there is primarily d wave scattering from the $^2\Pi g$ resonance in N_2 we obtain

$$|a^{vv'}_{\ell\ell' m}|^2 = \begin{cases} 5\sigma^{Res}_{vv'} & , \ \ell, \ell' = a, m = 1 \\ 0 & \text{otherwise} \end{cases} . \tag{15}$$

In Appendix B we derive a general expression for $a^{vv'}_{\ell\ell' m}$ by using a partial wave expansion of the V_{ip} term in Eq. (6). This allows us to treat the case of a resonance that is characterized by more than one partial wave within the context of the compound state model theory.

C. Extraction of resonance parameters

Finally we discuss the extraction of parameters which characterize both the resonant and nonresonant contribution to the scattering

process. The following relationships strictly refer to the eigenphase sums rather than the eigenphases; however, in N_2 the d wave character is so strong that in practice the two are essentially equivalent. The behavior of an eigenphase $\delta_{\ell m}$ in the vicinity of a resonance is given as:[12]

$$\delta_{\ell m} = f(k^2) + \tan^{-1}\left(\frac{\Gamma_\ell/2}{k_r^2 - k^2}\right) \tag{16a}$$

where $f(k^2)$ is the smoothly varying "background" phase shift of the form

$$f(k^2) = a_0 + a_2 k^2 + a_4 k^4 + \ldots . \tag{16b}$$

and k_r^2 is the position of the resonance in units of Rydbergs. Earlier scattering calculations by Burke and Sinfailam[13] and Buckley and Burke[14] report resonance widths and positions at $R = 2.068$ a. u. obtained by using an effective range expansion for the phase shift

$$k^{2\ell+1} \cot \delta_{\ell m}(k) = -\frac{1}{a} + \frac{r_{o\ell}}{2} k^2 \tag{17}$$

where nonlinear terms of the order k^4 and greater are neglected. We will use a nonlinear least-squares fitting procedure for determining all the parameters in the expansion of Eqs. (16a) and (16b). We have found that it is important to include the higher order k-dependence in the background phase shifts. At smaller internuclear separations

where the resonance becomes broad the neglect of background terms of order k^4 can introduce errors in the extraction procedure.

III. CALCULATIONS AND RESULTS

A. Extraction of resonance parameters

In a recent paper[5] we applied the discrete basis set method of Rescigno, McCurdy, and McKoy[15] to vibrational excitation for low energy e-H_2 scattering. The method involves projecting the scattering potential onto a subspace of discrete basis functions:

$$U^t(\underset{\sim}{r}, \underset{\sim}{r}') = 2 \sum_{\alpha\beta}^{N} | \alpha \rangle \langle \alpha | V | \beta \rangle \langle \beta | \tag{18}$$

Inserting Eq. (18) into the Lippmann-Schwinger equation we obtain an $N \times N$ matrix form for the transition operator:

$$T^t = [1 - U^t G_0^+]^{-1} U^t \tag{19}$$

where G_0^+ is the free-particle Green's function for the outgoing-wave boundary condition.

The truncated static-exchange potential U^t is calculated in two steps as described in greater detail in Ref. 16. In the first step we obtain the occupied target orbitals from an SCF calculation. These orbitals are calculated with respect to a standard basis set of contracted Cartesian Gaussian functions referred to as the target basis.

The second step involves calculating the matrix elements of the static-exchange potential over the scattering basis. In addition to the primitive (uncontracted) Gaussians used in the target SCF calculation, the scattering basis set includes diffuse functions at the center or on the nuclei. These additional diffuse basis functions span the asymptotic region of the scattering space while the repeated target functions facilitate orthogonality between the target orbitals and the scattering wave function.

For the SCF calculation of the occupied target orbitals we use a $[4s\ 3p_x\ 3p_y\ 3p_z\ 2d_{xz}\ 2d_{yz}\ 2d_{zz}]$ contracted basis set on each nucleus plus two diffuse p_z functions on the center. The [4s 3p] basis is constructed from a (9s 5p) set of primitives with the contraction coefficients given by Dunning.[17] Since the scattering potential is block diagonal in the symmetries $^2\Sigma_g$, $^2\Sigma_u$, $^2\Pi_u$, $^2\Pi_g$, ..., the Lippmann-Schwinger equation can be solved separately in each case. The scattering basis sets for each symmetry are identical to those given in Table I of Ref. 16.

To obtain the scattering parameters for vibrational excitation we need to calculate V(R) and $E_{HF}^{N_2}(R)$, the N_2 ground state potential curve. The Hartree-Fock approximation to the ground state of N_2 is particularly suitable around the equilibrium internuclear separation. We repeat the SCF calculation of the occupied target orbitals for R = 1.968, 2.068, 2.168, and 2.268 a.u. to obtain the potential energy curve for the ground electronic state of N_2 given in Fig. 1. From a

cubic spline fit to the five energy points given above we obtain a vibrational frequency of 0.01238 a.u. and an R_e of 2.0206 a.u. Nesbet[18] obtained values of 0.0124 a.u. and 2.026 a.u. respectively from Hartree-Fock calculations with extended basis sets. These values can be compared with the experimental values of ω_e = 0.01075 a.u. and R_e = 2.068 a.u. To be consistent with the static-exchange model we use the values of ω_e and R_e derived from our Hartree-Fock calculations.

We calculate widths and positions by repeated use of Eqs. (16a) and (16b) at the internuclear spacings of 1.868, 1.968, 2.068, and 2.168 a.u. Table I. A gives the trial phase shifts obtained by solving Eq. (19) and the appropriate equations of Ref. 16. For a broad resonance such as the Π_g resonance in the static-exchange approximation in N_2 it becomes increasingly difficult to separate the resonance and background contributions to the phase shifts. To obtain a converged solution to a nonlinear least squares form given in Eqs. (16a) and (16b) we need a reliable set of phase shifts with a minimum amount of scatter. The difference between the full and truncated scattering potential, $U - U^t$, contributes to this "noise" in the trial phase shifts. With the variational correction[19,20] to the trial phase shifts we obtain phase shifts which can be well fit to Eqs. (16a) and (16b). The various fits with the variationally corrected phase shifts are given in Table I. B. Varying the number of parameters in the background phase shift generally affects the value of the width and position only slightly. Table I. C. gives a summary of our final widths and positions

used in computing the necessary parameters for the compound state model. The variational correction to the phase shift is only applied in the Π_g channel for this calculation. Details of the computational method are presented elsewhere.[20]

In Table II we compare our result of $\Gamma(2.068) = 1.19$ eV and $\epsilon_R(2.068) = 3.829$ eV with various other theoretical calculations. The variation of $\Gamma(R)$ is shown in Fig. 2, along with the results of Krauss and Mies,[3] the semi-empirical "boomerang" model of Birtwistle and Herzenberg,[7] and the static-exchange calculation of Hazi.[21] We estimate the accuracy of our widths to be ± 3%; i. e., the largest difference in values obtained from a nonlinear least squares fit at $R = 1.868$ a. u. A recent calculation by Robb[22] gives $\Gamma(1.868) = 2.117$ eV and $\epsilon_R(1.868) = 4.993$ eV, in agreement with our static-exchange result at that internuclear spacing. It is interesting to compare our results with those of Hazi[21] as our calculations are similar in many respects. Also a discrete basis set method, his procedure[23] involves using the Stieltjes-moment-theory technique to extract a width $\Gamma(E_R)$ from a discrete representation of the background continuum. Some difficulties in his procedure for the calculation of the shift in the resonance energy, ϵ_R, may account for our differences at smaller internuclear spacings.[21] While this will cause some differences in the parameters used in calculating the vibrational cross section the final static-exchange cross sections are very similar.

From the relationship between the position of the resonance and the potential energy curve for the ion,

$$\epsilon_{HF}^{N_2^-}(R) = \epsilon_{HF}^{N_2}(R) + \frac{k^2(R)}{2} \qquad (20)$$

we derive the real part of the N_2^- potential energy curve, $\epsilon_{HF}^{N_2^-}(R)$. This is shown in Fig. 1. A spline fit about the R_e of the neutral gives for N_2^- $\omega_e = 0.01344$ a. u. and $R_e^- = 2.146$ a. u. The ab initio calculation of Krauss and Mies[3] gives an $\omega_e^- = 0.0089$ a. u. at $R_e^- = 2.16$ a. u. In view of the differences in our calculations from those of Krauss and Mies[3] this agreement is good.

Table III gives the five parameters needed in the calculation of the vibrational cross section [Eq. (7)]. To obtain these parameters at $R_e = 2.0206$ a. u. we fit a cubic spline through our calculated results at the four internuclear separations mentioned above. It is instructive to compare our results with those extracted by Herzenberg and Birtwistle from experimental data.[7] Our larger value for ϵ^r is consistent with our earlier results for elastic e-N_2 scattering in that the static-exchange approximation puts the resonance at a higher energy than is experimentally observed. The difference in the width at R_e and its dependence on R about R_e is also due to the static-exchange model. Inclusion of polarization will lower the position of the resonance. The last row of Table III contains the ratio of Γ/ω. This ratio demonstrates why the parameters of the static-exchange model can qualitatively predict the correct vibrational substructure despite the differences in the four other parameters. Birtwistle and Herzenberg[7] have discussed how the cross sections depend on this ratio. If Γ is of the order of ω, the S-matrix will have the correct pole structure to reproduce the structure

of the vibrational cross section.

In Fig. 3a we present pure vibrational excitation cross sections from $v = 0$ to $v' = 0$ through 7 in arbitrary units. Figure 3b shows the relative cross sections of Domcke and Cederbaum.[8] The static-exchange cross sections show the expected oscillatory behavior and peak shapes and separations similar to those of Domcke and Cederbaum.[8] Domcke and Cederbaum[8] used the parametrization of Birtwistle and Herzenberg[7] which should be close to the true values of these parameters. The qualitative changes in substructure going from lower to higher v' excitations are in fair agreement with those of Ref. 8 and our cross sections also exhibit the observed shifting of the peaks to higher energy. There are obviously several differences in these results. The amplitudes of the oscillations drop off too fast with electron energy and the cross sections reveal fewer peaks with a more rapid drop off in peak height. This is due to our larger ratio of Γ/ω obtained in the static-exchange model.

B. Absolute cross sections

To obtain absolute cross sections we use the procedure outlined in Section II. B. A spline fit through the values of $(a(\epsilon^{r}(R))^{1/2}\,\Gamma(R)$ at these R-values in Table I. C. gives a value of 0. 1305 a. u. at $R_e = 2.0206$. Comparison of the cross section given by Eqs. (11a) and (7) at energies on the high side of the resonance gives values of 0. 626, 0. 626, 0. 644, and 0. 655 for C(0, 0), C(0, 1), C(0, 2) and C(1, 2), respectively. From these values we obtain the absolute cross sections corresponding to our

maximum peak height for the four vibrational transitions $0 \rightarrow 0$, $0 \rightarrow 1$, $0 \rightarrow 2$, $1 \rightarrow 2$. Using Eqs. (41) and (43) of Ref. 16 and the approximation given in Eq. (15) the differential cross section for vibrational excitation is

$$\frac{d\sigma}{d(\cos\theta)}(v, v') = \frac{5}{4}\sigma_{vv'}^{Res}\left(\frac{2}{5} + \frac{2}{7}P_2(\cos\theta) + \frac{16}{35}P_4(\cos\theta)\right) \quad (21)$$

which reduces to a multiplicative factor relating the total and differential cross sections. With the use of Eq. (21) we compare our maximum peak height of the differential cross section at 90° for different vibrational excitations with the experimental results of Wong and Dube[24] in Table IV. Our results are in good agreement with their experimental absolute differential cross sections. This procedure assumes that the background contribution to the cross sections is small relative to the resonance contribution. Assuming that our phase shifts exhibit pure resonance behavior we can use the pure Breit-Wigner form[13] of Eq. (17) to obtain a width at R = 2.068 a.u. equal to 1.41 eV. This analysis suggests that the absolute cross sections for vibrational excitation may be 15% too high.

To calculate vibrational excitation contributions from the nonresonant channels we use the adiabatic-nuclei theory given in Eq. (12). We solve the Lippmann-Schwinger equation at R = 1.7444, 2.068, and 2.3916 a.u. at the eigenvalues of the static-exchange Hamiltonian in the scattering basis. These eigenenergies of Eq. (13a) remain quite constant for the range of R-values of interest. With Eq. (13c) we

estimate the total $\Sigma_g + \Sigma_u + \Pi_u$ contribution to the $0 \rightarrow 0$ and $0 \rightarrow 1$ vibrational excitation cross section to be constant in the resonance region and equal to 16. 2$\mathring{A}^2$ and 0. 08$\mathring{A}^2$, respectively. We hence ignore the nonresonant contributions to the vibrational process for $v \neq v'$.

Figure IV shows our absolute vibrationally elastic cross section, $\sigma(v \rightarrow v' = 0 \rightarrow 0)$. The total cross section with contributions from the inelastic and elastic processes, i. e., $\sum_{v'=0}^{2} \sigma_{0v'}$ and the previous results of our fixed nuclei calculation are given in Fig. 5. The effect of the inelastic contributions is to fill in the structure of the $0 \rightarrow 0$ transition. The maximum value of this cross section is about equal to that of the measured values of Golden[1] (insert to Fig. 5). It is interesting to compare our previous fixed-nuclei calculation[16] with the present one. The inclusion of vibrational excitation shifts our total cross section to lower energy by 10% or approximately 0. 4 eV. This difference should be recognized in the determination of the parameters of semi-empirical polarization potentials by comparing fixed-nuclei cross sections with observed cross sections directly.

In Figs. 6, 7, and 8, we show our absolute values for the $\sigma(0 \rightarrow 1)$, $\sigma(0 \rightarrow 2)$ and $\sigma(1 \rightarrow 2)$ vibrational excitation cross sections. In Fig. 9 we present our simultaneous rotational-vibrational differential cross section for $v \rightarrow v' = 0 \rightarrow 1$, and $\Delta j = 4$. The results of Chandra and Burke[25] suggest that the rotational cross sections for $\Delta j = 4$ at T = 300° K is given as $1/3 \frac{d\sigma}{d(\cos\theta)} (j \rightarrow j' = 0 \rightarrow 4) +$

$1/2 \frac{d\sigma}{d(\cos\theta)}$ $(j \rightarrow j' = 1 \rightarrow 5)$. Hence the cross section is given as

$$\frac{d\sigma}{d(\cos\theta)}(v \rightarrow v' = 0 \rightarrow 1; \Delta j = 4) = \frac{\sigma^{vv'}}{2\pi} \cdot \frac{44}{63}$$

$$\times \left[\frac{1}{5} + \frac{4}{49} P_2(\cos\theta)\right.$$

$$\left. + \frac{1}{245} P_4(\cos\theta)\right] \quad . \tag{22}$$

At $\theta = 60°$ we obtain a maximum peak height of 0.86×10^{-17} cm^2/sr which again compares well with the experimental result[24] of 0.68×10^{-17} cm^2/sr.

IV. CONCLUSIONS

These results for the e-N_2 system represent the first ab initio application of the compound state approach to the calculation of resonant vibrational excitation cross sections. All the necessary parameters have been extracted from the results of a full scattering calculation in the static-exchange approximation. The cross sections were obtained from the discrete basis set approach to the solution of the Lippmann-Schwinger equation for the T-matrix.[16] To be certain the structure of the vibrational excitation cross sections will change upon inclusion of the polarization effects. However, our cross sections do show that many features of the resonant vibrational excitation cross sections are already present in the static-exchange approximation. These results are a necessary first step in systematic quanitative studies of these cross sections.

We have also suggested a procedure for making these cross sections absolute. The resulting absolute cross sections agree reasonably well with the measurements of Wong[24] in their magnitude suggesting that the procedure is quantitatively useful and reliable. Their shapes do not agree as well but these differences are probably due to polarization effects. Both this procedure and the compound state formulation are being extended to include polarization effects in a physically motivated model. The formulation of Domcke and Cederbaum[8] is well suited for these extensions. Finally, we have also shown that by using a variational correction to the basis set representation of the scattering potential we can reliably determine the width and position of a resonance broader than 2 eV. The

ability to characterize such broad resonances in other related electron-molecule continuum problems will be useful in future problems.

ACKNOWLEDGMENT

We would like to thank Dr. Arne Fliflet for many helpful discussions and for the use of his computer codes for carrying out the variational corrections. This research was supported by grant No. CHE76-05157 from the National Science Foundation and by an Institutional Grant from the U. S. Department of Energy, No. EY-76-G-03-1305.

APPENDIX A

High energy limit form of Eqs. (7) and (11a) of text

In this appendix we derive the high energy limits of the resonant scattering cross section for a $0 \rightarrow 1$ vibrational transition. The procedure is valid for any excitation.

Using Eqs. (10a) and (10b) we can write an explicit form for $\sigma(0, 1, \epsilon_p)$ of Eq. (9) as

$$\sigma(0,1,\epsilon_p) \alpha \left| e^{-a/2} \left\{ \frac{-a^{1/2}}{\epsilon_p - \epsilon + \kappa^2/\omega} + \right. \right.$$

$$\left. \left. + \sum_{m=1}^{\infty} \frac{a^{(2m-1)/2}(m-a)}{(\epsilon_p - \epsilon + \kappa^2/\omega - m\omega)\, n!} \right\} \right|^2 \qquad \text{(A1)}$$

The demoninator in Eq. (A1) may be approximated for very high Σp as

$$\frac{1}{\epsilon_p - \epsilon + \kappa^2/\omega - m\omega} \approx \frac{1}{\epsilon_p} \left\{ 1 + \frac{1}{\epsilon_p}(\epsilon - \kappa^2/\omega + m\omega) \right\} \qquad \text{(A2)}$$

where terms of higher order in $(1/\epsilon_p)$ may be retained for greater numerical accuracy. Substitution of Eq. (A2) into Eq. (A1) gives

$$\sigma(0,1,\epsilon_p) \alpha \left| \frac{e^{-a/2}}{\epsilon_p} \left\{ - a^{1/2} \left(1 + \frac{1}{\epsilon_p} \cdot (\epsilon - \kappa^2/\omega) \right) + \right. \right.$$

$$+ a^{-1/2} \left(1 + \frac{(\epsilon - \kappa^2/\omega)}{\epsilon_p} \right) \sum_{m=1}^{\infty} a^m \frac{(m-a)}{m!} +$$

$$\left. \left. + \frac{\omega a^{-1/2}}{\epsilon_p} \sum_{m=1}^{\infty} a^m \frac{(m-a)\, m}{m!} \right\} \right|^2 \qquad \text{(A3)}$$

Using the identity $e^a = \sum_{m=0}^{\infty} \frac{a^m}{m!}$ and its related expressions Eq. (A3) reduces to

$$\sigma(0,1,\epsilon_\rho) \alpha \frac{\omega^2}{\epsilon_p^4} \left| a^{1/2} e^{a/2} \right|^2 \qquad \text{(A4)}$$

We apply a similar procedure as above to both terms in Eq. (4a) by expanding the demoninator

$$\left| D(\epsilon_p, \rho) \right|^{-1} \cong \frac{1}{\epsilon_p^2} \left(1 + \left\{ \frac{2(E_1 + E_2\rho)}{\epsilon_p} - \frac{(E_1 + E_2\rho)^2}{\epsilon_p^2} \right. \right.$$

$$\left. \left. + \frac{(\Gamma(0) + \Gamma_2\rho)^2}{4\epsilon_p^2} \right\} \right| \qquad \text{(A5)}$$

Substituting Eq. (A5) into Eq.(11a) gives us an expression for $\sigma_{vv'}$ which is completely analytical. For a $0 \rightarrow 1$ excitation only integrals of the form $H_{01} \equiv \int_{-\infty}^{\infty} \chi_1^{\infty}(\rho)\, \rho\, \chi_0(\rho)\, d\rho$ are nonzero hence the high energy limit of Eq. (11a) is given as

$$\sigma_{01} = \frac{a(\epsilon^R(0))\,\Gamma^2(0)\,H_{01}^2}{4} \; E_2^2 \cdot \frac{1}{\epsilon_p^4} \tag{A6}$$

APPENDIX B

Expression for the resonance dynamic scattering coefficients

We start with the general transition operator

$$\langle F, p' \,|\, T \,|\, I, p \rangle = V_{p',i}\, V_{ip}\, T_{vv'}(p) \tag{B1}$$

where $|\, I, p \rangle$ and $|\, F, p \rangle$ are the initial and final vibrational-electronic states and

$$T_{vv'}(p) \equiv \frac{|p'|}{|p|} \langle v \,|\, (\epsilon_p - \mathcal{H})^{-1} \,|\, v' \rangle \; . \tag{B2}$$

Using a plane wave expansion

$$\varphi_k (\underset{\sim}{r}, \underset{\sim}{R}) = 4\pi \sum_{\ell m} j_\ell (p'r)\, Y_{\ell m} (\hat{r})\, Y^*_{\ell m} (\hat{k}) \tag{B3}$$

for the continuum state $\varphi_k (\underset{\sim}{r}, \underset{\sim}{R})$ in Eq. (7) we obtain

$$\langle F, p' \mid T \mid I, p \rangle = (4\pi)^2\, T_{vv'} (p) \sum_{\ell\ell' m} L_{\ell\ell' m}\, Y_{\ell m} (\hat{p}')$$

$$\times\ Y^*_{\ell' m} (\hat{p}) \tag{B4}$$

where

$$L_{\ell\ell' m} (p, p') \equiv \langle j_\ell (p' r)\, Y^*_{\ell m} (\hat{r}) \mid H^{e\ell} (\underset{\sim}{r}, \underset{\sim}{R}) \mid \varphi_i (\underset{\sim}{r}, \underset{\sim}{R}) \rangle$$

$$\times\ \langle \varphi_i (\underset{\sim}{r}, \underset{\sim}{R}) \mid H^{e\ell} (\underset{\sim}{r}, \underset{\sim}{R}) \mid j_{\ell'} (p'r)\, Y_{\ell' m} (\hat{r}) \rangle \tag{B5}$$

The general transition operator may also be written in a single center form as

$$\langle F, p' \mid T \mid I, p \rangle = \frac{1}{p} \sum_{\ell\ell' m} i^{\ell' - \ell}\, T^{vv'}_{\ell\ell' m} (p)\, Y_{\ell m} (\hat{p}')\, Y^*_{\ell' m} (\hat{p}) \tag{B6}$$

where

$$T^{vv'}_{\ell\ell' m} = i^{-\ell' + \ell + 1}\, \frac{2p}{(2\ell' + 1)^{1/2}}\, a^{vv'}_{\ell\ell' m} \tag{B7}$$

Equating the right hand side of Eq. (B6) with Eq. (B4) we obtain the vibrationally closed copuled scattering coefficients

$$a^{vv'}_{\ell\ell' m}(p) = \frac{(4\pi)^2 (2\ell' + 1)^{1/2}}{2i} T_{vv'}(p) L_{\ell\ell' m} \qquad \text{(B8)}$$

The last term in Eq. (B8), $L_{\ell\ell' m}$, is strictly a function of energy; however, to first order we can neglect this nonadiabatic effect as we did in Eq. (7). $L_{\ell\ell' m}$ can then be viewed as the partial wave analogue of $C(n, m)$ and can be computed by a similar matching procedure. Equation (B8) can be used to compute the resonance contribution to absolute rotational-vibrational, differential and total cross sections. It is particularly useful to work with the partial wave formalism of Eq. (B8) when one has a resonance which couples different ℓ values.

References

[1] D. E. Golden, H. W. Bandel, and J. A. Salerno, Phys. Rev. 146, 40 (1966).

[2] F. R. Gilmore, J. Quant. Spectrosc. Radiat. Transfer 5, 369 (1965).

[3] M. Krauss and F. H. Mies, Phys. Rev. A 1, 1592 (1970).

[4] D. M. Chase, Phys. Rev. 104, 838 (1956).

[5] N. Chandra and A. Temkin, Phys. Rev. A 13, 188 (1976).

[6] D. A. Levin, A. W. Fliflet, and V. McKoy, "Low Energy Rotational and Vibrational-Rotational Excitation Cross Sections for H_2 by Electron Impact," Phys. Rev. A - accepted for publication.

[7] D. T. Birtwistle and A. Herzenberg, J. Phys. B 4, 53 (1971).

[8] W. Domcke and L. S. Cederbaum, Phys. Rev. A 16, 1465 (1977).

[9] B. I. Schneider, Phys. Rev. A 14, 1923 (1976).

[10] A. Herzenberg and F. Mandl, Proc. R. Soc. A 270, 48 (1962).

[11] A. Herzenberg, Methods and Problems of Theoretical Physics, ed. by J. E. Bowcook (North-Holland, Amsterdam, 1970), p. 131.

[12] J. R. Taylor, Scattering Theory, (Wiley, New York, 1972), Chap. 13.

[13] P. G. Burke and A. L. Sinfailam, J. Phys. B 3, 641 (1970).

[14] B. D. Buckley and P. G. Burke, J. Phys. B 10, 725 (1977).

[15] T. N. Rescigno, C. W. McCurdy, Jr., and V. McKoy, Phys. Rev. A 11, 825 (1975).

[16] A. W. Fliflet, D. A. Levin, M. Ma, and V. McKoy, Phys. Rev. A 17, 160 (1978).

[17] T. H. Dunning, J. Chem. Phys. 13, 2823 (1970).

[18] R. K. Nesbet, J. Chem. Phys. 40, 3619 (1964).

[19] A. W. Fliflet and V. McKoy, "Discrete Basis Set Method for Electron-Molecule Continuum Wavefunctions," Phys. Rev. A - accepted for publication.

[20] A. W. Fliflet, D. A. Levin, V. McKoy, and T. N. Rescigno, "Variationally Corrected Discrete Basis Set Calculations for e^- - N_2 Scattering in the Static-Exchange Approximation," in preparation.

[21] A. U. Hazi, private communication.

[22] D. Robb, private communication.

[23] A. U. Hazi, J. Phys. B 11, 1259 (1978).

[24] S. F. Wong and L. Dubé, "Rotational Excitation of N_2 by Electron Impact: 1-4 eV," Phys. Rev. - submitted for publication.

[25] N. Chandra and P. G. Burke, J. Phys. B 6, 2355 (1973).

TABLE I. A. Trial and variationally corrected d_π phase shifts at different internuclear spacings.

R = 1.868 a.u.			R = 1.968 a.u.		
k	δ_{21}^{t*}	δ_{21}^{s**}	k	δ_{21}^{t}	δ_{21}^{s}
0.45	0.1426	0.0643	0.40	0.0697	0.05509
0.55	0.4209	0.3291	0.50	0.2973	0.3013
0.60	0.8802	0.6877	0.55	0.8225	0.6806
0.65	1.3949	1.3817	0.60	1.5225	1.5257
0.70	1.9229	1.8799	0.65	2.0561	2.1109
0.80	2.341	2.2245	0.70	2.2824	2.304
0.90	2.426	2.3307	0.80	2.5243	2.379
R = 2.068 a.u.			R = 2.168 a.u.		
k	δ_{21}^{t}	δ_{21}^{s}	k	δ_{21}^{t}	δ_{21}^{s}
0.30	0.02914	0.0053	0.30	0.0345	0.0123
0.40	0.10049	0.0867	0.40	0.1621	0.1433
0.50	0.57188	0.6358	0.45	0.4675	0.4316
0.55	1.7499	1.6778	0.50	1.797	1.6554
0.60	2.1787	2.260	0.55	2.416	2.3241
0.70	2.4817	2.4982	0.60	2.523	2.5138
0.80	2.6406	2.4971	0.70	2.599	2.5899

* Superscript t refers to the trial, or uncorrected, phase shift.

** Superscript s refers to the corrected phase shift. See text for further discussion.

TABLE I. B. Results of various nonlinear least squares fits of the d_π phase shift to the functional form:

$$\delta_{21}(k^2/2) = \tan^{-1}\left(\frac{\Gamma_\ell}{2(\frac{k_r^2}{2} - \frac{k^2}{2})}\right) + a_0 + a_2\frac{k^2}{2} + a_4\frac{k^4}{4} + a_6\frac{k^6}{8} .$$

#of par.[a]	Φ[b]	$\frac{k_r^2}{2}$(eV)	Γ(eV)	a_0	a_2	a_4	a_6
			R = 1.868 a.u.				
4	2.65×10^{-3}	5.480	2.326	-0.226	-0.499		
5	8.17×10^{-4}	5.417	2.334	-0.209	-0.788	0.359	
6	4.78×10^{-4}	5.420	2.269	-0.207	-0.529	-0.603	0.792
			R = 1.968 a.u.				
4	9.107×10^{-4}	4.601	1.644	-0.169	-0.598		
5	4.370×10^{-4}	4.622	1.638	-0.179	-0.428	-0.271	
6	3.722×10^{-4}	4.623	1.658	-0.179	-0.569	0.387	0.682
			R = 2.068 a.u.				
4	2.4×10^{-5}	3.8325	1.1928	-0.342	-1.10		
5	2.39×10^{-5}	3.8325	1.1928	-0.342	-1.09	-0.009	
6	9.89×10^{-6}	3.8298	1.1958	-0.317	-1.447	-1.134	-1.011
			R = 2.168 a.u.				
4	2.599×10^{-3}	3.2369	0.8507	-0.143	-0.630		
5	1.153×10^{-3}	3.2212	0.8546	-0.125	-0.976	0.717	
6	1.2846×10^{-4}	3.2241	0.8344	-0.128	-0.585	-1.531	3.0017

[a] The number of parameters used in the fit equals the width, position and number of background terms.

[b] Φ is the sum of the squares of the deviation of each given phase shift from the nonlinear least squares predicted phase shift. The set of data points used for a given R is given in Table I. A. All fits are for corrected phase shifts only.

TABLE I. C. Final resonance parameters used in computing vibrational excitation cross sections.

R(a. u.)	$\frac{k_r^2}{2}$ (eV)	Γ (eV)
1. 868	5. 4201	2. 2694
1. 968	4. 6228	1. 6578
2. 068	3. 8298	1. 1958
2. 168	3. 2241	0. 8344

TABLE II. Comparison of the $^2\Pi_g$ resonance widths and positions determined from various calculations. [a]

Authors	Γ(eV)	ϵ^r(eV)	Effects Included
Krauss and Mies [b]	0.8 ± 0.3	3.07	local potential
Birtwistle and Herzenberg [c]	0.57 ± 0.02	1.925 ± 0.015	phenomenological
Buckley and Burke [d]	0.64 ± 0.02	2.39	S, E, P [f]
Chandra and Temkin [e]	0.4	1.197	S, E, P
Present	1.19	3.829	S, E

[a] All widths are given at an internuclear separation R_e = 2.068 a.u. except for that of Krauss and Mies which is given at R_e = 2.0 a.u.

[b] Ref. 3

[c] Ref. 7

[d] Ref. 14

[e] Ref. 5

[f] S - Static, E - exchange, P - polarization.

TABLE III. Comparison of parameters for the vibrational excitation cross section $\sigma(n, m, \epsilon_p)$ given in Eq. (8) of the text.

	Birtwistle and Herzenberg[a] parametrization	T-matrix[b] calculation
$\epsilon^R(eV)$[c]	2.35	4.120
$\epsilon^I(eV)$	-0.285	-0.698
$\epsilon^R(eV)$	-0.382	0.447
$\epsilon^I(eV)$	0.051	0.1276
ω	0.293	0.3369
$\Gamma(R_e)/\omega$	1.95	4.14

[a] Parameters were extracted from Birtwistle and Herzenberg (Ref. 7) and listed in the work of Domcke and Cederbaum (Ref. 8).

[b] These parameters are for $R_e = 2.0206$ a.u.

[c] Superscripts R and I denote the real and imaginary parts of the complex numbers ϵ and κ. See Eqs. (8c) and (8d) of text.

TABLE IV. Comparison of absolute differential cross sections[a] corresponding to maximum peak heights.

$v \rightarrow v'$	T-matrix $\frac{d\sigma}{d\Omega}(v \rightarrow v', \theta = 90°)$	Experimental[b] $\frac{d\sigma}{d\Omega}(v \rightarrow v', \theta = 90°)$
$0 \rightarrow 0$	1.51	1.1
$0 \rightarrow 1$	0.33	0.48
$0 \rightarrow 2$	0.16	0.36
$1 \rightarrow 2$	0.57	0.51

[a] Units are $Å^2/sr$.

[b] Experimental results of Wong and Dubé.[24]

Figure Captions

Fig. 1: Potential energy curves of $X\ ^1\Sigma_g^+$ state of N_2 and the real part of the complex energy of the metastable N_2^- state.

Fig. 2: Comparison of the R dependence of $\Gamma(R)$ for the T-matrix (solid curve); Stieltjes-moment-theory technique of Hazi (circles in dashed curve); Stabilization calculation of Krauss and Mies (crosses); and boomerang model of Birtwistle and Herzenberg (dashed line).

Fig. 3a: T-matrix relative cross sections for resonant vibrational scattering as a function of incident electron energy.

Fig. 3b: Relative cross sections for resonant vibrational scattering from the parametrization of experimental results by Domcke and Cederbaum. n is the final vibrational state. The initial vibrational state is v = 0.

Fig. 4: T-matrix absolute $0 \rightarrow 0$ cross section for resonant and nonresonant vibrational scattering.

Fig. 5: T-matrix absolute total cross section (solid curve); and fixed nuclei T-matrix calculation of Ref. 15 (crosses). The insert is the experimental results of Golden (Ref. 3).

Fig. 6: Absolute T-matrix vibrational cross section for $v \rightarrow v' = 0 \rightarrow 1$.

Fig. 7: Absolute T-matrix vibrational cross section for $v \rightarrow v' = 0 \rightarrow 2$.

Fig. 8: Absolute T-matrix vibrational cross section for $v \rightarrow v' = 1 \rightarrow 2$.

Fig. 9: Absolute differential-rotational-vibrational cross section for $\Delta j = 4$, $v \rightarrow v' = 0 \rightarrow 1$, $\theta = 60°$ for T-matrix calculation.

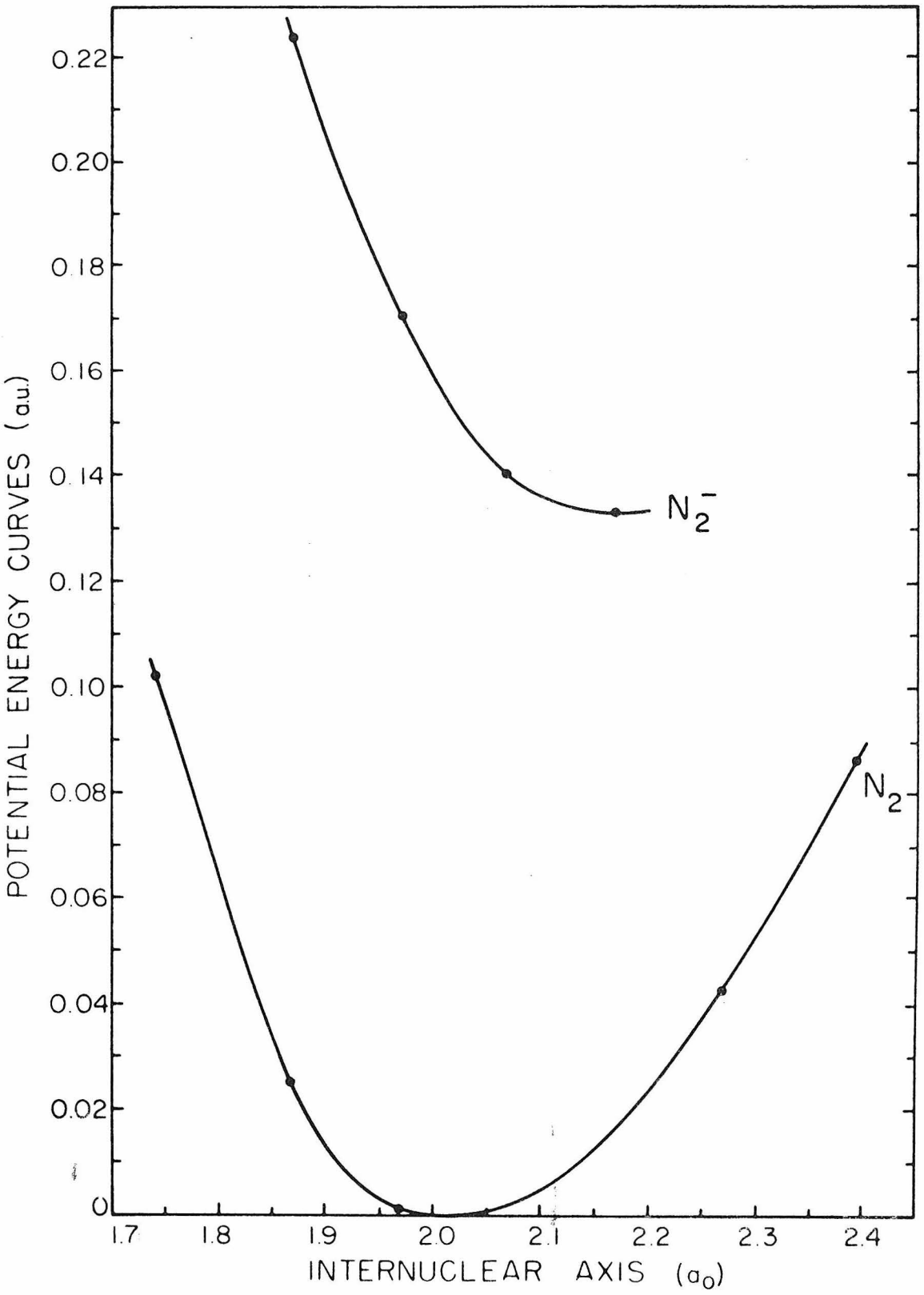
POTENTIAL ENERGY CURVES (a.u.)
0.22
0.20
0.18
0.16
0.14
0.12
0.10
0.08
0.06
0.04
0.02
0
1.7
1.8
1.9
2.0
2.1
2.2
2.3
2.4
INTERNUCLEAR AXIS (a0)
N2−
N2

Figure 1

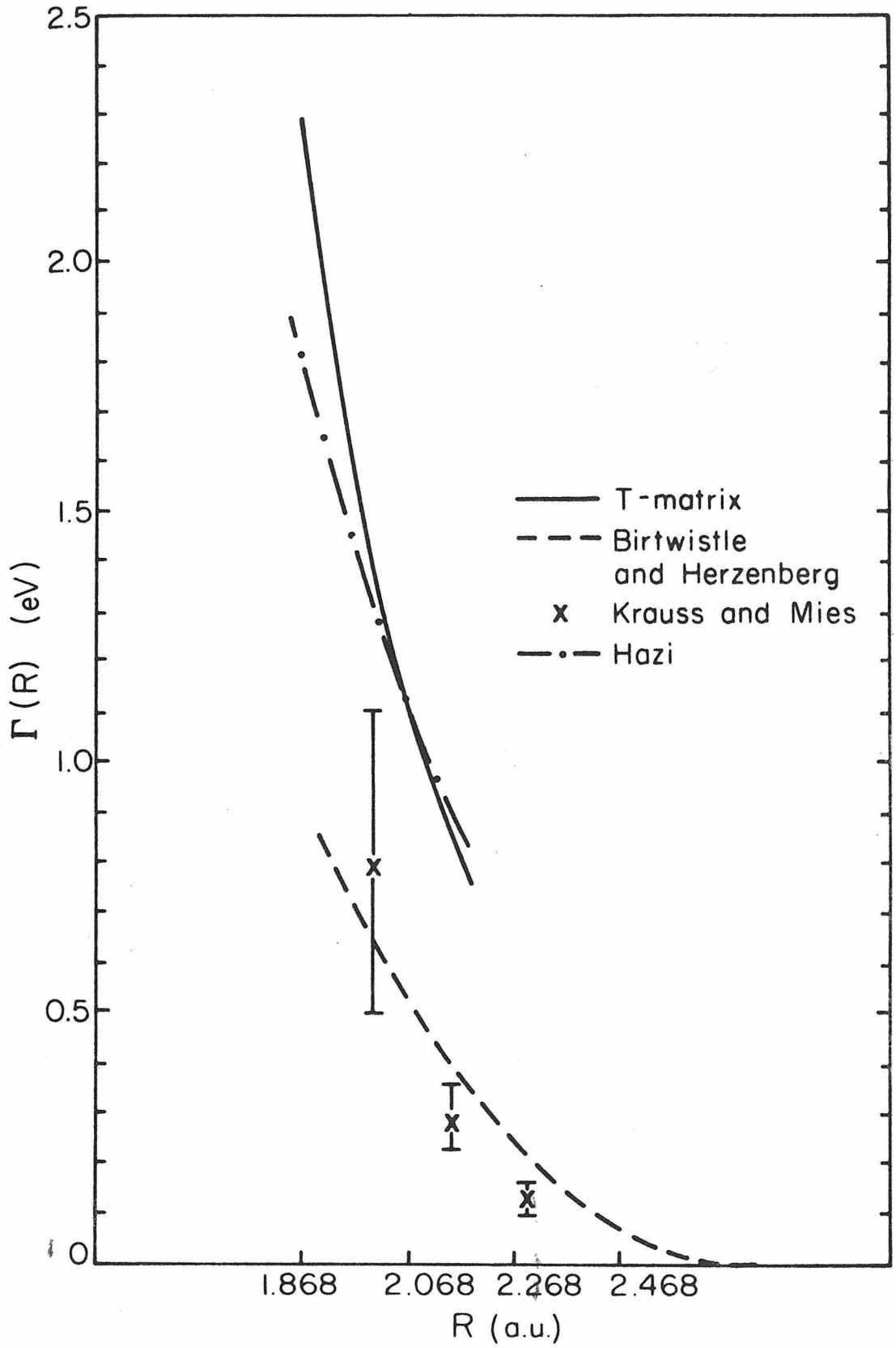
2.5
2.0
1.5
1.0
0.5
0
Γ(R) (eV)
1.868
2.068
2.268
2.468
R (a.u.)
T-matrix
Birtwistle and Herzenberg
Krauss and Mies
Hazi

Figure 2

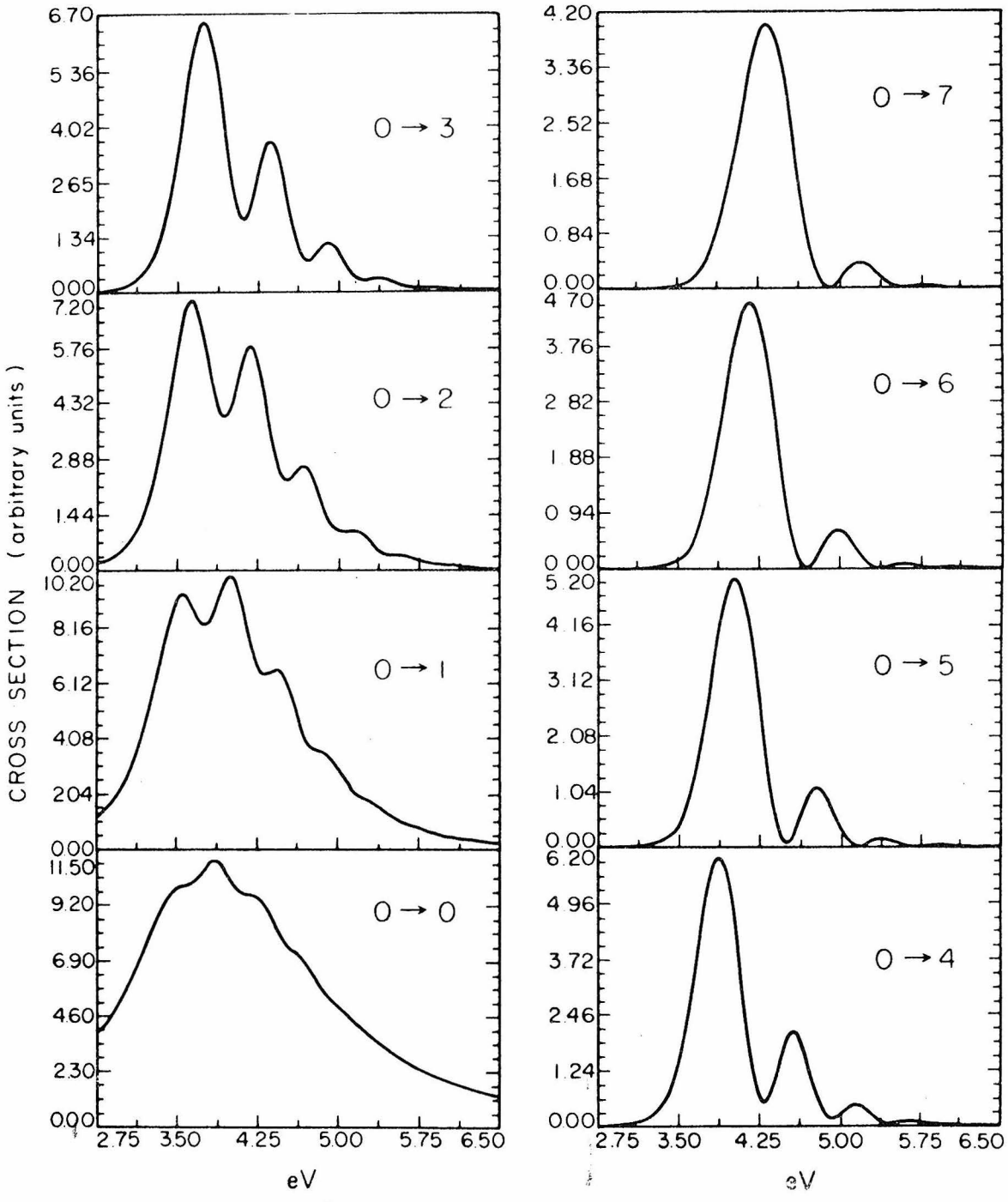
CROSS SECTION (arbitrary units)
0 → 3
0 → 2
0 → 1
0 → 0
0 → 7
0 → 6
0 → 5
0 → 4
6.70
5.36
4.02
2.65
1.34
0.00
7.20
5.76
4.32
2.88
1.44
0.00
10.20
8.16
6.12
4.08
2.04
0.00
11.50
9.20
6.90
4.60
2.30
0.00
4.20
3.36
2.52
1.68
0.84
0.00
4.70
3.76
2.82
1.88
0.94
0.00
5.20
4.16
3.12
2.08
1.04
0.00
6.20
4.96
3.72
2.46
1.24
0.00
2.75 3.50 4.25 5.00 5.75 6.50
eV

Figure 3a

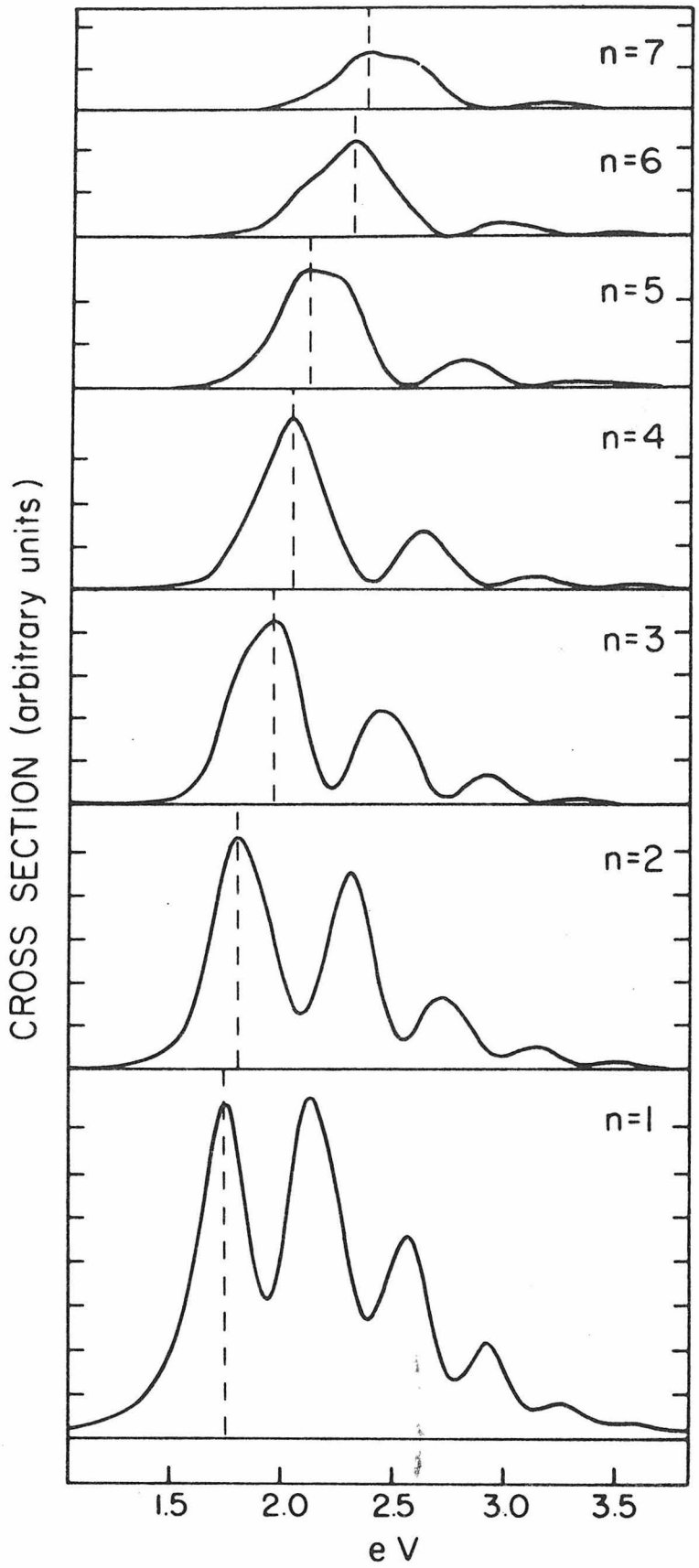
n=7
n=6
n=5
n=4
n=3
n=2
n=1
CROSS SECTION (arbitrary units)
1.5
2.0
2.5
3.0
3.5
eV

Figure 3b

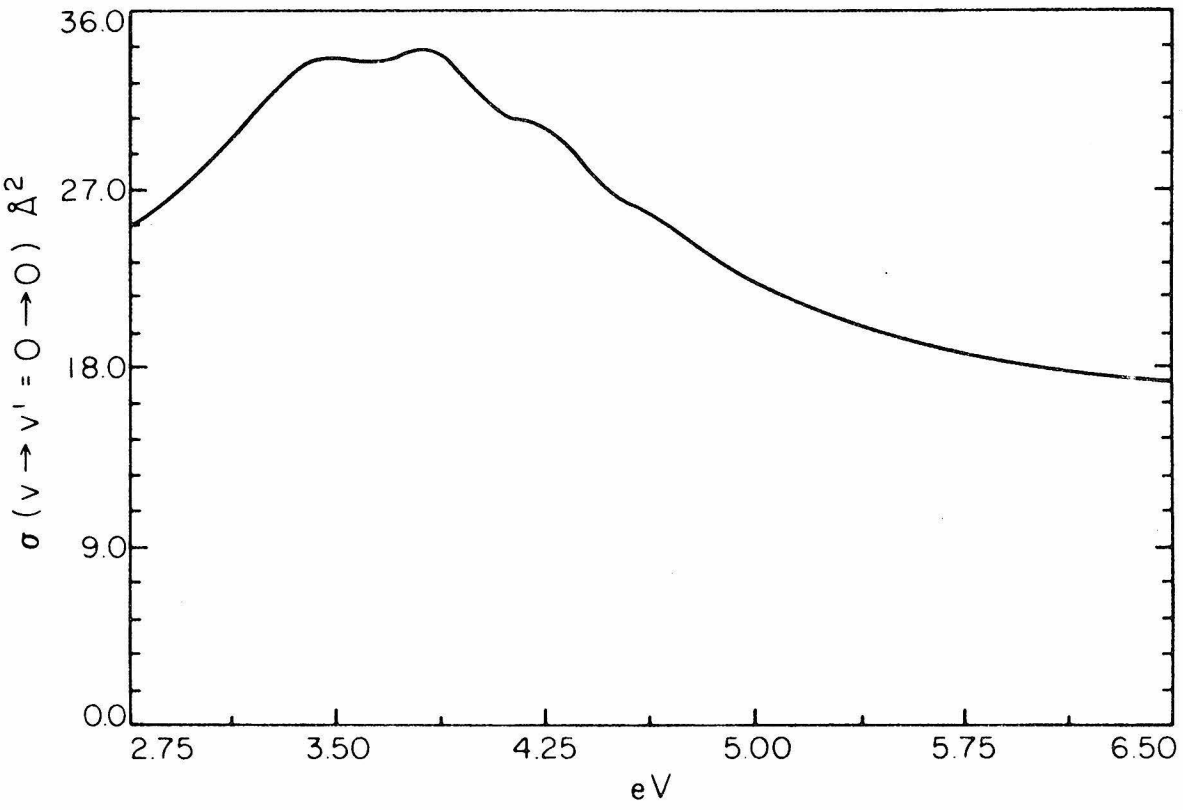

Figure 4

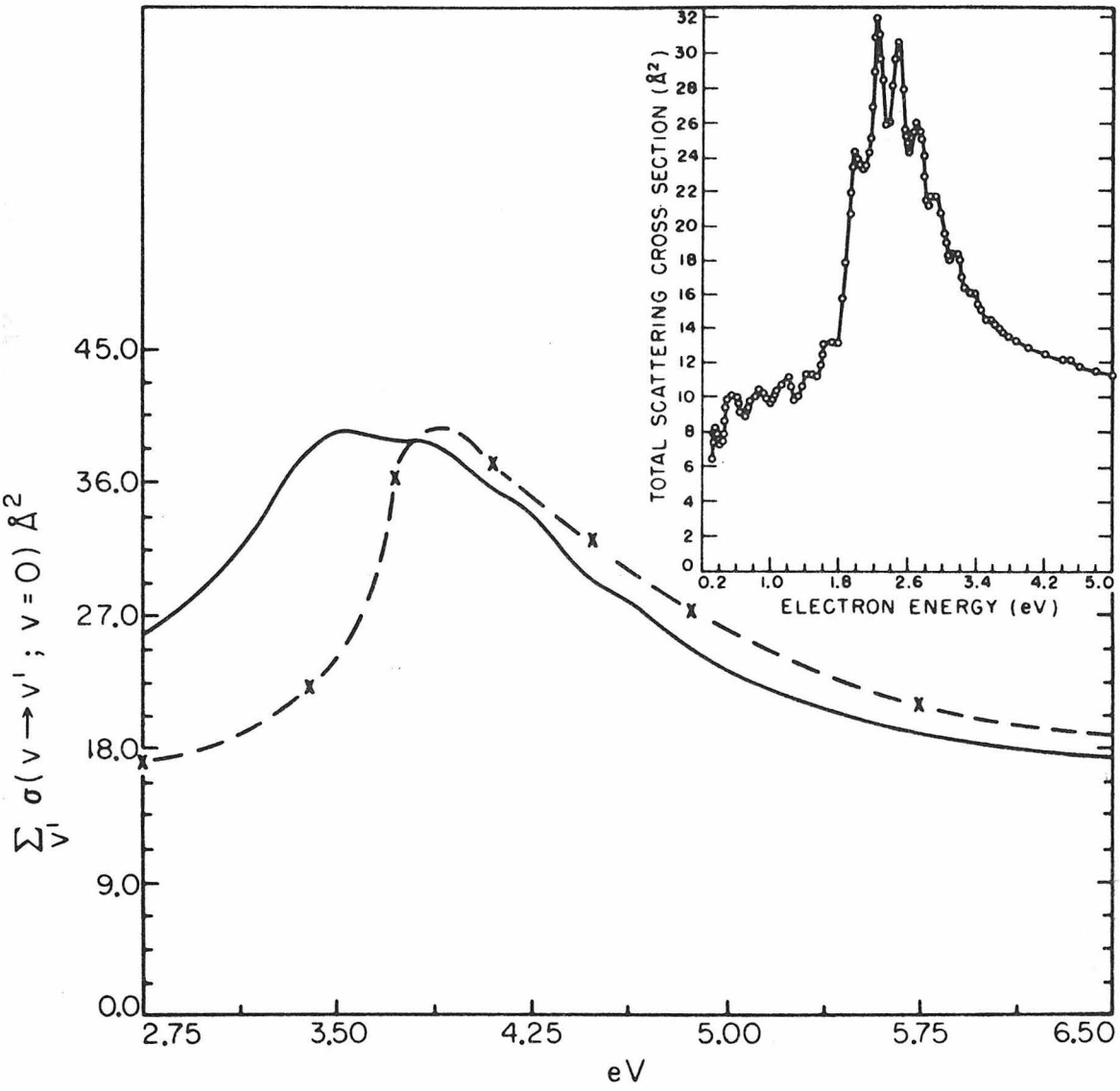
TOTAL SCATTERING CROSS SECTION (Å²)
ELECTRON ENERGY (eV)
0.2
1.0
1.8
2.6
3.4
4.2
5.0
0
2
4
6
8
10
12
14
16
18
20
22
24
26
28
30
32
$\sum_{v'} \sigma(v \rightarrow v'; v=0)$ Å²
45.0
36.0
27.0
18.0
9.0
0.0
2.75
3.50
4.25
5.00
5.75
6.50
eV

Figure 5

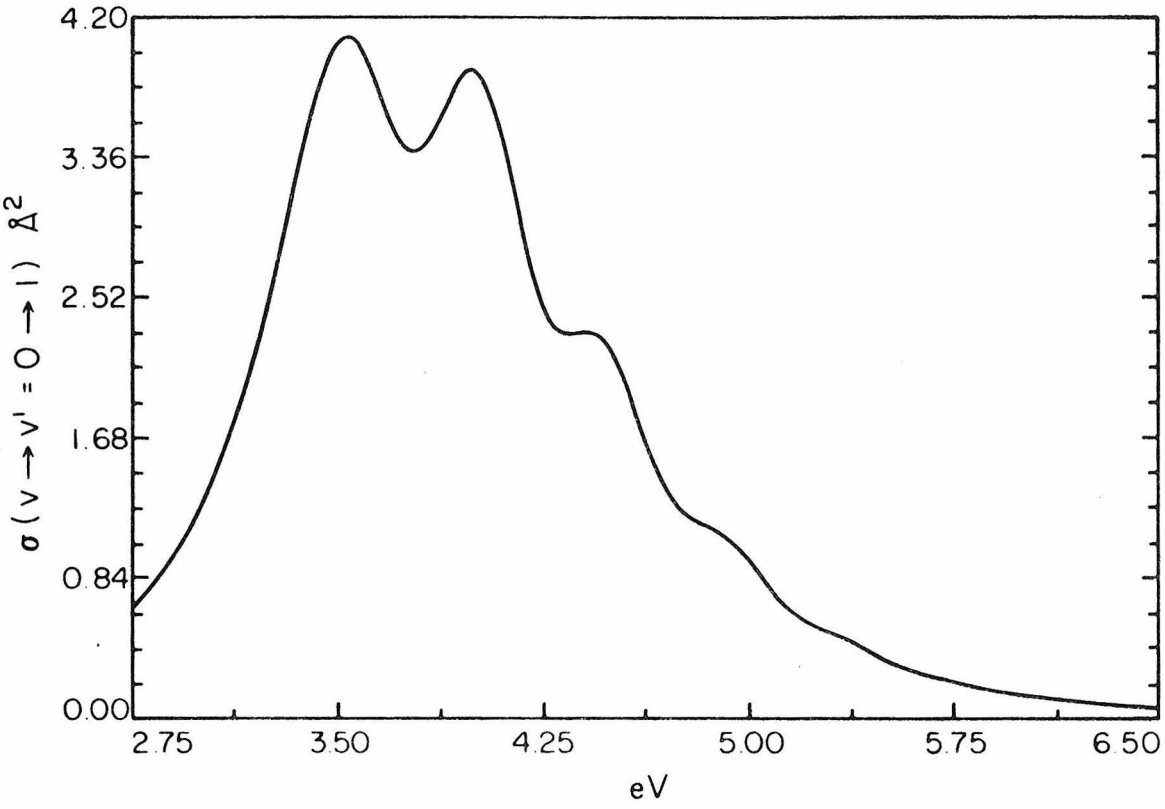

Figure 6

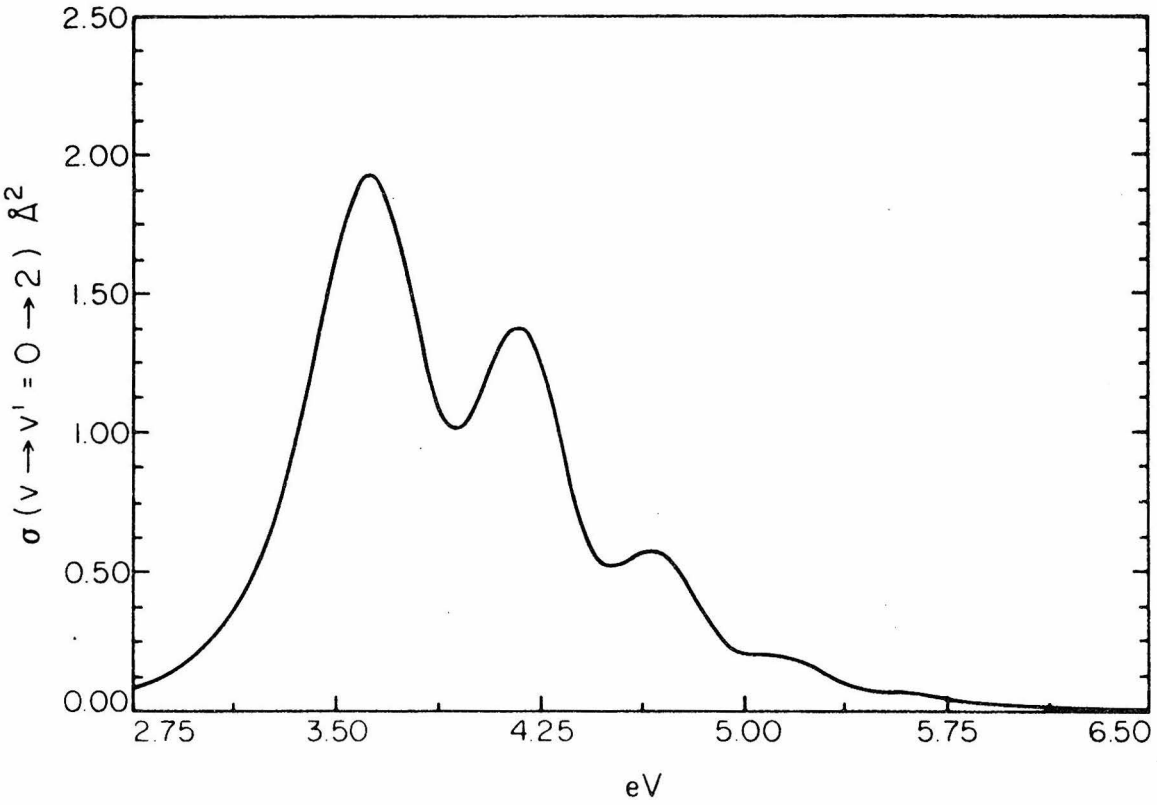

Figure 7

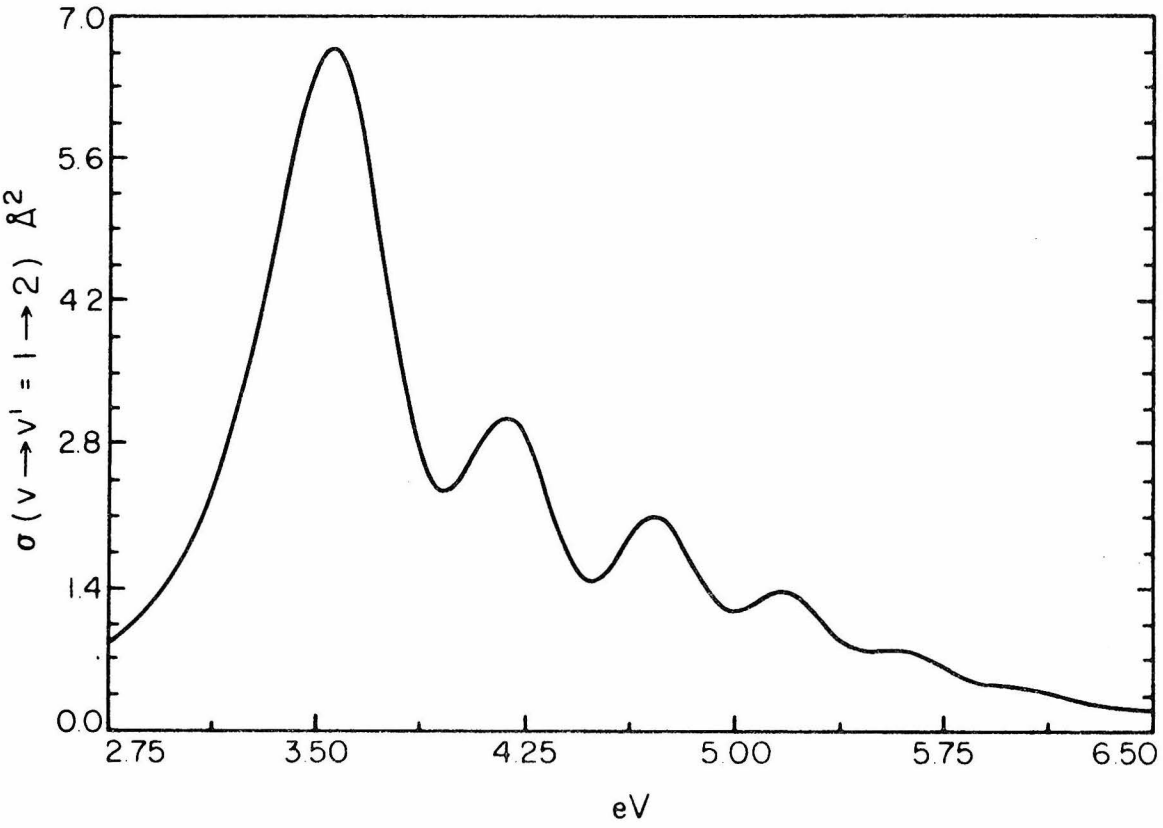

Figure 8

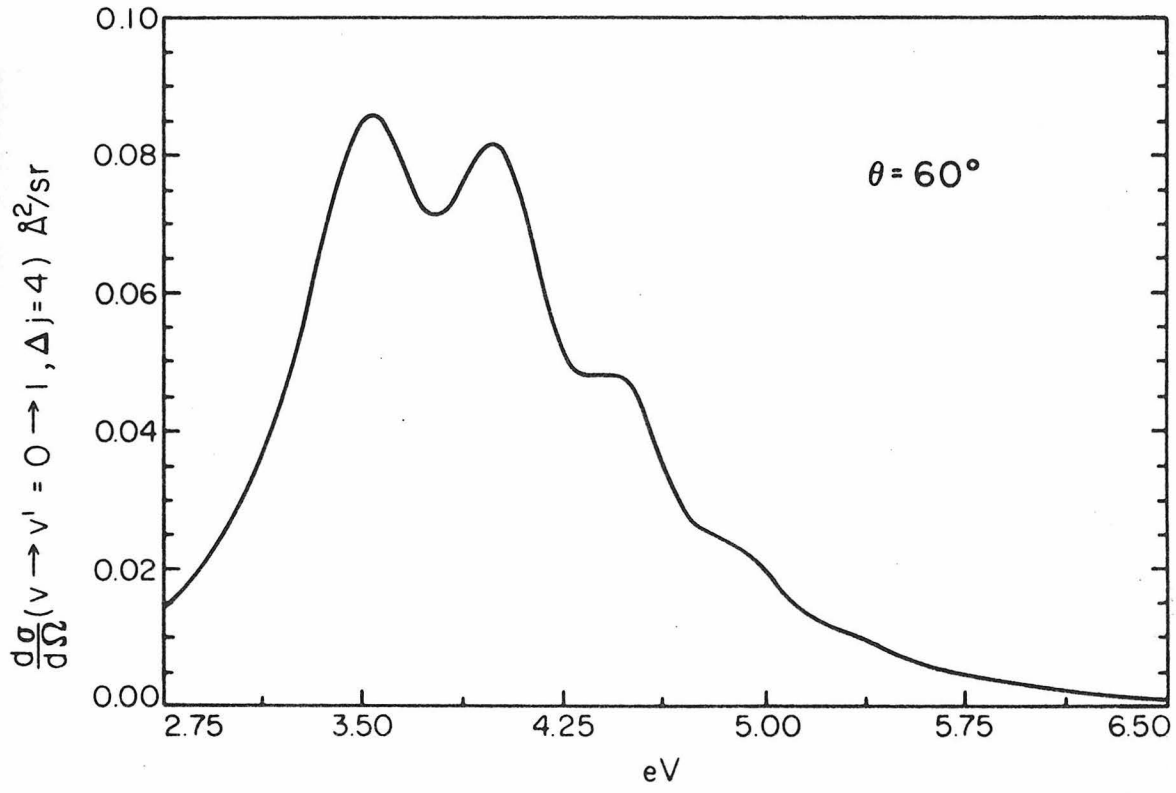
0.10
0.08
0.06
0.04
0.02
0.00
$\frac{d\sigma}{d\Omega}(v \rightarrow v' = 0 \rightarrow 1, \Delta j = 4)$ Å^2/sr
$\theta = 60°$
2.75
3.50
4.25
5.00
5.75
6.50
eV

Figure 9

SECTION C

A Simple Model for the Inclusion of Polarization Effects in Shape Resonances

I. INTRODUCTION

Charge polarization effects can be important for the low-energy scattering of electrons by atoms and molecules. In particular, polarization effects play a major role in resonant scattering where the electron spends much more time in the neighborhood of the molecule than is characteristic of the normal transit time.[1] For example, in shape resonance the increased interaction time leads to a greater distortion of the molecule and hence an enhancement in vibrational excitation. The nature of vibrational excitation via resonance processes is strongly influenced by the lifetime of the resonance. In fact, compound state models of vibrational excitation cross sections[2,3] require a knowledge of the position and width of the temporary negative ion as well as the dependence of these parameters on internuclear separation.

The complexities of methods for electron-molecule scattering make it difficult to include the effects of polarization in non-empirical studies. Although polarization effects have been included recently for the e - H_2 system in a rigorous way in both the T-matrix[4] and R-matrix[5] methods, it has been popular to use some semi-empirical functional form to represent the polarization potential for electron scattering by molecules. A common choice for linear molecules has been[6,7]

$$V_{pol}^{R}(\vec{r},\vec{R}) = \left\{ -\frac{\alpha_0(R)}{2r^4} - \frac{\alpha_2(R)}{2r^4} P_2(\hat{r}\cdot\hat{R}) \right\} \cdot C(r) \qquad (1)$$

where α_0 and α_2 are the isotropic and anisotropic components of the static electric dipole polarizability and $C(r)$ is a cut-off function, e. g. ,

$$C(r) = [\, 1 - \exp\,(-\frac{r}{r_c})^6\,] \quad . \tag{2}$$

This cut-off function ensures that $V_{pol}(r)$ tends to zero as r goes to zero and r_c is a parameter whose value is determined semi-empirically. The value for r_c is usually chosen so that a shape resonance peak in the cross section occurs at the correct energy.

Our concern in this paper is whether a polarization potential of the form of Eq. (1) is in fact suitable for describing the charge polarization effects occurring at the resonance energies. The main justification for this choice of the polarization potential is that it is known that the asymptotic behavior of the exact optical potential at energies below the first electronic excitation threshold is

$$V_{pol}(\vec{r}, \vec{R}) \underset{r \to \infty}{\sim} - \frac{\alpha_0(R)}{r^4} - \frac{\alpha_2(R)}{r^4}\, P_2(\hat{r} \cdot \hat{R}) \tag{3}$$

For nonresonant scattering this is a physically reasonable choice for the functional form of the polarization potential. However, for resonances the physical nature of the negative ion state strongly suggests that the small r behavior of the polarization must be important and hence there is no justification for neglecting other terms in the expansion of the polarization potential, i. e. ,

$$V_{pol}(\vec{r}, \vec{R}) = \sum_{\ell=0}^{\infty} V_\ell(r, R)\, P_\ell(\hat{r} \cdot \hat{R}) \qquad (4)$$

at small r, although these other terms do decrease more rapidly than r^{-4} at large r. If this is true an appropriate procedure for including such effects in resonant scattering would be to carry out a stabilization calculation on the negative ion state and to use the potential field of these core orbitals in the scattering calculation. Such a potential must include the dominant polarization effects in the resonant state where the electron penetrates into a well of the size of the molecule. This potential would not be adequate outside of the resonance region, i. e., for nonresonant scattering. We have used this model to study the $^2\Pi_g$ shape resonance in N_2 and obtained encouraging results for the position and width of this resonance.

Studies of the $^2\Pi_g$ resonance by Krauss and Mies[8] were motivated by the same observation. They calculated the resonance state of N_2 in an orbital approximation and used this to develop a local potential for electron scattering. There are similar implications in the recent work of Schneider and Hay[9] in which they also used the static-exchange field of the F_2^- core orbitals in their studies of the elastic scattering of electrons by F_2.

In the following sections we briefly outline the procedure for obtaining these "compound state" core orbitals and for carrying out the scattering calculation in this potential. We also calculate the width and position of the $^2\Pi_g$ resonance in the $e - N_2$ system using two

different basis sets to show that the results are quite independent of such choices. Finally, we discuss the implications of these results for future studies of the positions and widths of shape resonances in other diatomic and polyatomic molecules. The results of these calculations also suggest a critical reexamination of the current procedure of tuning the parameters of the polarization potential of Eq. (1) so as to fit resonance peaks in the observed cross sections.

II. THEORY

In this model the scattering potential for the resonance region is taken to be the static-exchange field of the core orbitals of the temporary negative ion, e. g. , the N_2 core of the $(1\sigma_g^2\ 1\sigma_u^2\ 2\sigma_g^2\ 2\sigma_u^2\ 1\pi_u^4\ 3\sigma_g^2\ 1\pi_g)\ ^2\Pi_g$ state of N_2^-. To obtain these core orbitals we approximate the resonance state function by the SCF wave function of N_2^- and carry out a stabilization-type calculation on this state.[10] The molecular orbitals are expanded in a basis of Gaussian functions positioned at the atomic centers and at the center of the molecule. In these calculations the basis functions for the expansion of the π_g orbital are chosen to be valence-like and hence describe the large inner portion of the resonance function well. This is the important region in determining the polarization distortions of the core in the resonance. The SCF wave function for N_2^- is then determined in this basis set. The calculation is repeated with different basis sets and the procedure converges to essentially the solution for the N_2^-

orbitals. The core orbitals of this SCF wave function for N_2^- now define the static-exchange potential which describes the elastic scattering of electrons by N_2 in the resonance region.

To obtain the eigenphases for the scattering of low-energy electrons by this potential we use the discrete basis set approach to solve the Lippmann-Schwinger equation for the on-shell partial wave K-matrix. The details of this method have been discussed in an earlier publication[11] and the present application is straightforward. The relationship between the eigenphase sum, $\delta(k)$, and the resonance parameters is given by

$$\delta(k) = \tan^{-1}\left(\frac{\Gamma/2}{k_{r/2}^2 - k^2/2}\right) + a_0 + a_2\frac{k^2}{2} + a_4\frac{k^4}{4} + \ldots \qquad (5)$$

where Γ is the width of the resonance and the polynomial in k^2 represents the smoothly varying background phase shift. The resonance energy E^R is related to $k_{r/2}^2$ by

$$E^R = E_{HF} + \frac{k_r^2}{2} \qquad (6)$$

where E_{HF} is the ground state SCF energy of N_2.

III. RESULTS

We carried out SCF calculations on the $^2\Pi_g$ resonance state of N_2^- with two different basis sets to determine how stable the results were with respect to changes in the basis set. These two SCF basis sets are given in Table I. Basis set A is made up of Dunning's [4s3p] contracted basis[12] augmented with d functions on the atomic centers and p_z functions at the midpoint of the molecule. In addition to basis set A, set B contains d_{xz} and d_{yz} functions at the center of the molecule. These additional d functions should enhance the description of the inner-region of the resonance π_g orbital. The SCF orbitals resulting from these two calculations are very similar and the SCF energies are -108.84146 a.u. and -108.84177 a.u. for basis sets A and B respectively. These results indicate that the static-exchange fields of the core orbitals of N_2^- for these two calculations should be very similar.

In the solution of the Lippmann-Schwinger equation for the K-matrix, and hence the Π_g eigenphase sum, for these two core potentials, we used a set of Gaussian basis functions given in Table I of reference 11. To obtain the width and position of the resonance we use a nonlinear least squares fit of the eigenphase sum to Eq. (1). In Table II we give the widths and positions of the $^2\Pi_g$ resonance in $e-N_2$ scattering for these two calculations. The estimates of the possible errors in these results are based on the spread of the results obtained in the various nonlinear least squares fit of the eigenphase

sums.

In Table III we compare our results for the position and width of this resonance with those of the calculations of Krauss and Mies[8] and the results of the parametrization of Birtwistle and Herzenberg.[3] For convenience our result is just the average of the results shown in Table II. The agreement between our results and those of Birtwistle and Herzenberg[3] is very encouraging. The value of Γ Krauss and Mies[8] is for an internuclear separation of 2.0 a.u. and this accounts for some of the difference between our value of Γ which corresponds to a separation of 2.068 a.u. Moreover, Krauss and Mies[8] included a semi-empirical estimate of the correlation energies.

IV. CONCLUSIONS

From these results we conclude that the static-exchange field of the core of the temporary negative ion adequately represents both the exchange and electrostatic polarization effects in the $e - N_2$ system at the resonance energy. This model emphasizes the small r behavior of the polarization potential. From the physical characteristics of the negative ion state it is not surprising that the small r behavior of the polarization potential would be important in a resonance.

Our procedure for obtaining the appropriate core potential and the eigenphases for the scattering by this ptoential is simple. The necessary stabilization-type calculations on the negative ion

state can be done with available SCF computer codes. For the scattering problem we used the discrete basis set approach to the solution of the T-matrix equation.[11] Of course, there are other methods which can be used to solve for the electron scattering cross sections.[9]

To illustrate our procedure we did the calculations at the equilibrium geometry of N_2. The method can obviously be used to obtain the dependence of these resonance parameters on internuclear distance. This dependence of $\Gamma(R)$ and $E^R(R)$ is required in compound state theories of resonance vibrational excitation cross sections. Use of these theories[3] with semi-empirical choices of the resonance parameters does give results in good agreement with measured cross sections. Our method for obtaining the resonance parameters will be useful in these applications.

These results also seriously question the current use of semi-empirical polarization potentials with the asymptotic form of Eq. (3) in the resonance region. This form is known to represent the large r behavior of the polarization potential and our model shows that the small r behavior is very important in the resonance region. The choice of Eq. (3) neglects the other terms in the expansion of the polarization potential in Eq. (4) which can be important at small r.

References

[1] G. J. Schulz, in Principles of Laser Plasmas, edited by G. Bekefi (John Wiley and Sons, New York, 1976), p. 33.

[2] W. Domcke and L. S. Cederbaum, Phys. Rev. A 16, 1465 (1977).

[3] D. T. Birtwistle and A. Herzenberg, J. Phys. B 4, 53 (1971).

[4] A. Klonover and U. Kaldor, J. Phys. B 11, 1623 (1978).

[5] B. Schneider, Chem. Phys. Lett. 51, 578 (1977).

[6] P. G. Burke and N. Chandra, J. Phys. B 3, 641 (1972).

[7] N. Chandra and A. Temkin, Phys. Rev. A 13, 188 (1976).

[8] M. Krauss and F. H. Mies, Phys. Rev. A 1, 1592 (1970).

[9] B. I. Schneider and P. J. Hay, Phys. Rev. A 13, 2049 (1976).

[10] See, for example, A. U. Hazi and H. S. Taylor, Phys. Rev. A 1, 1109 (1970).

[11] A. W. Fliflet, D. A. Levin, M. Ma, and V. McKoy, Phys. Rev. A 17, 160 (1978).

[12] T. H. Dunning, J. Chem. Phys. 53, 2823 (1970).

TABLE I. Two target basis sets. [a]

A. (ℓ, m, n)	α_i	C_i
	$\vec{A} = (0., 0., \pm 1.034)$	
0 0 0	5909.44	0.0020040
"	887.451	0.0153100
"	204.749	0.0742930
"	59.8376	0.2533640
"	19.9981	0.6005760
"	2.68600	0.2451110
"	7.1927	1.0
"	0.7	"
"	0.2133	"
1 0 0	26.7860	0.0382440
"	5.95640	0.2438460
"	1.70740	0.8171930
"	0.53140	1.0
"	0.16540	"
0 1 0	same α_i's and C_i's as (1, 0, 0)	
0 0 1	same α_i's and C_i's as (1, 0, 0)	
0 0 2	1.225	1.0
"	0.3628	"
1 0 1	1.940	"
"	0.576	"
0 1 1	same α_i's and C_i's as (1, 0, 1)	
	$\vec{A} = (0., 0., 0.)$	
0 0 1	0.05	1.0
"	0.01	"

B. (ℓ, m, n)	α_i	C_i
	$A = (0., 0., \pm 1.034)$	
	Same exponents and contraction coefficients as Basis A.	
	$\vec{A} = (0., 0., 0.)$	
1 0 1	1.0	1.0
1 0 1	0.5	"
0 1 1	same α_i's and C_i's as (1 0 1)	

[a] The Cartesian Gaussian function is of the form $\mu_{\ell mn}^{\alpha_i \vec{A}} \equiv N_{\ell mn}(x - A_x)^{\ell}(y - A_y)^{m}(z - A_z)^{n} e^{-\alpha_i |\vec{r} - \vec{A}|^2}$ where $N_{\ell mn}$ is a normalization factor. C_i denotes the contraction coefficient of the ith basis function.

TABLE II. Comparison of resonance parameters.

	Basis Set A	Basis Set B
$\Gamma(R_e)$	0.49 ± 0.04 eV	0.47 ± 0.03 eV
$E^R(R_e)$	2.18 ± 0.02 eV	2.23 ± 0.02 eV

TABLE III. Comparison of resonance parameters.[a, b]

	E^R	Γ
Present	2. 20	0. 50
Birtwistle and Herzenberg	2. 35	0. 57
Krauss and Mies	3. 07	0. 8 ± 0. 3

[a] Units are eV.

[b] All values are given at R = 2. 068 a. u. except for those of Krauss and Mies which are for R = 2. 0 a. u.

CHAPTER III

Analytic Evaluation of Gaussian Matrix Elements of the Free-Particle Green's Functions for Polyatomic Systems

SECTION A

Gaussian Matrix Elements of the Free-Particle Green's Function

1. Introduction

Recently we proposed a method for calculating electron-molecule scattering cross sections which requires the evaluation of matrix elements of the free-particle Green's function over Cartesian Gaussian basis function [1]. This arises when the scattering potential, V, is approximated by a sum of separable terms of the form

$$V(\vec{r}, \vec{r}') \simeq V^t = \sum_{\alpha, \beta=1}^{N} \varphi_\alpha(\vec{r})\, V_{\alpha\beta}\, \varphi_\beta^*(\vec{r}') \tag{1}$$

where

$$V_{\alpha\beta} = \int \varphi_\alpha^*(\vec{r})\, V(\vec{r})\, \varphi_\beta(\vec{r})\, d^3r \tag{2}$$

and the basis functions $\varphi_\alpha(\vec{r})$ are Cartesian Gaussian functions. Inserting the truncated potential, Eq. (1), the Lippmann-Schwinger equation for the transition operator

$$T^t = U^t + U^t G_0^+ T^t \tag{3}$$

becomes a matrix equation with elements

$$T^t_{\alpha\beta} = U^t_{\alpha\beta} + \sum_{\gamma, \delta} U^t_{\alpha\gamma} (G_0^+)_{\gamma\delta} T^t_{\delta\beta} \tag{4}$$

where $U = 2V$ and G_0^+ is the free-particle Green's function. Equation (3) is then solved by a simple matrix inversion. This procedure requires the evaluation of the matrix elements of G_0^+ over the basis functions $\varphi_\alpha(\vec{r})$. For molecular systems a convenient choice of functions for the expansion of the potential, Eq. (1), is Cartesian Gaussian basis functions. A large number of such Gaussian functions can be required to adequately represent a scattering potential and hence it is important to have an efficient procedure for the evaluation of the matrix elements $(G_0^+)_{\alpha\beta}$

In this paper we present a method for generating analytic formulas for Gaussian matrix elements of the free particle Green's function. The method is based on Ostlund's technique for evaluating scattering integrals involving Gaussian and plane wave functions [2] but derives its simplicity from some recursive properties of the spherical Bessel functions.

In Section 2 we present our technique for deriving formulas for Gaussian matrix elements of G_0^+. Our results are tabulated in Section 3 for matrix elements involving Cartesian Gaussian functions of up to f-type symmetry. The formulas given are valid for polyatomic systems but only those combinations of Gaussian functions which contribute to the Σ, Π, and Δ symmetries of a linear molecule are listed.

2. Theory

The free-particle Green's function satisfies the equation

$$(\nabla^2 + k^2)\, G_0(k;\vec{r},\vec{r}') = \delta(\vec{r} - \vec{r}') \tag{5}$$

The solution for the outgoing wave boundary condition is

$$G_0^+(k;\vec{r},\vec{r}') = -\frac{1}{4\pi}\,\frac{e^{ik|\vec{r}-\vec{r}'|}}{|\vec{r}-\vec{r}'|} \tag{6a}$$

and the solution for the standing wave boundary condition is the principal-value Green's function

$$G^P(k;\vec{r},\vec{r}') = \frac{\cos(k|\underset{\sim}{r}-\underset{\sim}{r}'|)}{|\vec{r}-\vec{r}'|}\quad . \tag{6b}$$

We are interested in matrix elements of the form $\langle \mu_{\ell mn}^{\alpha,\vec{A}} | G_0^+ | \mu_{\ell' m' n'}^{\beta,\vec{B}} \rangle$ where $\mu_{\ell mn}^{\alpha,\vec{A}}$ is a normalized Cartesian Gaussian function with center at $\vec{A}$

$$\mu_{\ell mn}^{\alpha,\vec{A}} = N_{\ell mn}(x-A_x)^{\ell}(y-A_y)^{m}(z-A_z)^{n}\, e^{-\alpha|\vec{r}-\vec{A}|^2} \tag{7}$$

where $N_{\ell mn}$ is a normalization factor

$$N_{\ell mn}^{-2} = \frac{\sqrt{(2\ell-1)!!(2m-1)!!(2n-1)!!}}{(2\sqrt{\alpha})^{\ell+m+n}}\left(\frac{\pi}{2\alpha}\right)^{3/4} \tag{8}$$

and

$$n!! = n(n-2)(n-4)\ldots 1 \tag{9}$$

Taking Fourier transforms we obtain the integral representation

$$\langle \mu^{\alpha,\vec{A}}_{\ell mn} | G_0^+(E) | \mu^{\beta,\vec{B}}_{\ell' m' n'} \rangle = \lim_{\epsilon \to 0^+} \frac{1}{(2\pi)^3} \int d^3\vec{k} \; \langle \mu^{\alpha,\vec{A}}_{\ell mn} | \vec{k} \rangle \cdot$$

$$\langle \vec{k} | \mu^{\beta,\vec{B}}_{\ell' m' n'} \rangle \Big/ (k_0^2 - k^2 + i\epsilon) \qquad (10)$$

where $E = k_0^2 / 2$. The Fourier transform of a Gaussian function may be evaluated by elementary methods and is given by

$$\langle \mu^{\alpha,\vec{A}}_{\ell mn} | \vec{k} \rangle = \left(\frac{2\pi}{\alpha}\right)^{3/4} \frac{i^{\ell+m+n}}{[(2\ell-1)!!(2m-1)!!(2n-1)!!]^{1/2}} \cdot$$

$$e^{i\vec{k}\cdot\vec{A} - \frac{k^2}{4\alpha}} H_\ell\left(\frac{k_x}{2\sqrt{\alpha}}\right) H_m\left(\frac{k_y}{2\sqrt{\alpha}}\right) H_n\left(\frac{k_z}{2\sqrt{\alpha}}\right) \qquad (11)$$

where H_ℓ is the Hermite polynomial of order ℓ. Introducing the Cauchy principal value, Eq. (10) may be written in the form,

$$\langle \mu^{\alpha,\vec{A}}_{\ell mn} | G_0^+ | \mu^{\beta,\vec{B}}_{\ell' m' n'} \rangle = \frac{1}{(2\pi)^3} \left[P \int d^3k \; \frac{\langle \mu^{\alpha,\vec{A}}_{\ell mn} | \vec{k} \rangle \langle \vec{k} | \mu^{\beta,\vec{B}}_{\ell' m' n'} \rangle}{k_0^2 - k^2} \right.$$

$$\left. - i\pi \langle \mu^{\alpha,\vec{A}}_{\ell mn} | \vec{k}_0 \rangle \langle \vec{k}_0 | \mu^{\beta,\vec{B}}_{\ell' m' n'} \rangle \right] \qquad (12a)$$

where P denotes the Cauchy principal value integral and the second term is the residue. The corresponding matrix element for the principal-value Green's function is

$$\langle \mu^{\alpha,\vec{A}}_{\ell mn} | G_0^P | \mu^{\beta,\vec{B}}_{\ell' m' n'} \rangle = \frac{4\pi}{(2\pi)^3} P \int d^3k \; \frac{\langle \mu^{\alpha,\vec{A}}_{\ell mn} | \vec{k} \rangle \langle \vec{k} | \mu^{\beta,\vec{B}}_{\ell' m' n'} \rangle}{k_0^2 - k^2} \qquad (12b)$$

Evaluation of the residue term on the RHS of Eq. (12a) is straightforward. Evaluation of the first term, which is just the matrix element of G_q^P, is the subject of this paper. Substituting Eq. (11) into Eq. (12b) and using the expansion of the plane wave

$$e^{i\vec{k}\cdot\vec{R}} = 4\pi \sum_{LM} i^L j_L(kR)\, Y_{LM}(\hat{R})\, Y^*_{LM}(\hat{k}) \tag{13}$$

where

$$\vec{R} = \vec{A} - \vec{B} \tag{14}$$

leads to the expansion

$$\langle \mu^{\alpha,\vec{A}}_{\ell mn} | G_0^{(P)} | \mu^{\beta,\vec{B}}_{\ell' m' n'} \rangle = \sum_{LM} i^L\, C(\ell mn, \ell' m' n')\, f_{LM}(k_0, \alpha, \beta ; \ell mn, \ell' m' n')\, Y_{LM}(\hat{R}) \tag{15}$$

where

$$C(\ell mn; \ell' m' n') = \frac{\sqrt{2}}{\sqrt{\pi}} \frac{1}{(\alpha\beta)^{3/4}} [(2\ell-1)!!\,(2m-1)!!\,(2n-1)!!\,(2\ell'-1)!!\,(2m'-1)!!\,(2n'-1)!!]^{1/2} \cdot i^{\ell-\ell'+m-m'+n-n'} \tag{16}$$

and

$$f_{LM}(k_0, \alpha, \beta\ ;\ \ell mn, \ell' m' n') = P \int_0^\infty dk\ \frac{k^2\, e^{-ak^2} j_L(kR)}{k^2 - k_0^2} \cdot$$

$$\int d\hat{k}\ Y^*_{LM}(\hat{k})\, H_\ell\left(\frac{k_x}{2\sqrt{\alpha}}\right) H_m\left(\frac{k_y}{2\sqrt{\alpha}}\right) H_n\left(\frac{k_z}{2\sqrt{\alpha}}\right) H_{\ell'}\left(\frac{k_x}{2\sqrt{\beta}}\right) \cdot$$

$$H_{m'}\left(\frac{k_y}{2\sqrt{\beta}}\right) H_{n'}\left(\frac{k_z}{2\sqrt{\beta}}\right) \tag{17}$$

Evaluation of the coefficients, f_{LM}, leads to integrals of the form

$$I_L^p = P \int_0^\infty dk\ \frac{k^p\, e^{-ak^2} j_L(kR)}{k_0^2 - k^2} \tag{18}$$

where

$$a = \frac{\alpha + \beta}{4\alpha\beta}\ , \tag{19a}$$

and

$$p \geq L + 2\ . \tag{19b}$$

The evaluation of matrix elements of G_0^P for all combinations of Cartesian Gaussian functions of up to f-type symmetry requires the integrals I_L^p for $0 \leq L \leq 6$, $2 \leq p \leq 8$. The straightforward way to obtain all these I_L^p is to differentiate the lower order ones, i.e., in L and p, successively with respect to a and R. However, by using the recursive properties of the spherical Bessel functions, i.e.,

$$\frac{(2L+1)}{kR}\, j_L(kR) = j_{L-1}(kR) + j_{L+1}(kR) \tag{20}$$

we can establish the relation

$$I_L^p = \frac{R}{2L+1}\left[I_{L-1}^{p+1} + I_{L+1}^{p+1} \right] \tag{21}$$

With the result, Eq. (21), we need only obtain I_0^p, $p = 4, 6, 8$ and I_1^p, $p = 5, 7$ by successive differentiations. To see this we start from the relation, pointed out by Ostlund [2], of I_0^2 to the error function of complex argument

$$I_0^2 = \frac{\pi}{2R}\, e^{-aq^2}\, \mathrm{Re}\left[e^{iqR}\, \mathrm{erf}\left(\frac{R}{2\sqrt{a}} + i\sqrt{a}\, q \right) \right] \; ; \; q = k_0 \tag{22}$$

The formula for I_1^3 is obtained by differentiating Eq. (22) with respect to R:

$$I_1^3 = \frac{\pi}{2}\, e^{-aq^2}\, \mathrm{Re}\left[\left(\frac{1}{R^2} - i\,\frac{q}{R} \right) e^{iqR}\, \mathrm{erf}\left(\frac{R}{2\sqrt{a}} + i\sqrt{a}\, q \right) \right]$$

$$- \frac{\sqrt{\pi}}{2}\, \frac{e^{-R^2/4a}}{R\sqrt{a}} \tag{23}$$

Formulas for I_0^p, p = 4, 6, 8 and I_1^p, p = 5, 7 are generated from Eqs. (22) and (23), respectively, by differentiating these expressions with respect to a. Formulas for I_L^p, $L \geq 2$ are then obtained using the recurrence relations, Eq. (21). Our experience has shown that this procedure for evaluating the integrals I_L^p is much less tedious than successive differentiation.

Our results for I_L^p, $0 \leq L \leq 6$, $2 \leq p \leq 8$ are given in the Appendix. For Gaussian basis functions on the same center only the integrals I_0^p are non-vanishing.

Matrix elements of the Green's function G_0^+ are obtained by adding the residue term on the right hand side of Eq. (12a) to the matrix element of G_0^p. Substituting Eq. (11) into the second term on the RHS of Eq. (12a) we find for the s-type Gaussians:

$$i\pi \, \mathrm{Res}\{ \langle \mu_{000}^{\alpha, \vec{A}} | G_0^+ | \mu_{000}^{\beta, \vec{B}} \rangle \} = i \frac{\pi}{2} \sin \frac{(qR)}{R} \, e^{-aq^2} . \qquad (24)$$

Differentiating Eq. (24) with respect to R gives

$$i\pi \, \mathrm{Res} \{ \langle \mu_{000}^{\alpha, \vec{A}} | G_0^+ | \mu_{001}^{\beta, \vec{B}} \rangle \} = i \frac{\pi}{2} e^{-aq^2} \left(\frac{\sin(qR)}{R^2} \right) - q \frac{\cos(qR)}{R} \qquad (25)$$

Eqs. (24) and (25) correspond to the imaginary parts of I_0^2 and I_1^3, respectively. For L = 0, p = 4, 6, 8 the residues are calculated by differentiating Eq. (24) with respect to a. We obtain the residue values for L = 1, p = 5, 7 in a similar way by differentiation of Eq. (25) with respect to a.

3. Results

We have used this approach to obtain explicit expressions for the matrix elements of the Green's function with Cartesian Gaussian functions of s, p, d, and f-type. For convenience we list the matrix elements appropriate for axially symmetric molecules, i.e., Σ, Π, and Δ cases. The matrix elements for the Σ, Π, and Δ symmetries are shown in Tables I, II, and III respectively.

In Table IV we also give actual numerical values for matrix elements of the Green's function for several choices of Gaussian basis functions. In these calculations we used a program based on Gautschi's algorithm for evaluating the complex error function [3].

4. Conclusions

We have described an efficient method for generating analytic formulas for Gaussian matrix elements of the free-particle Green's function. The method is based on Ostlund's technique for evaluating integrals involving Gaussian and plane wave functions but derives its simplifying features from some recursive properties of spherical Bessel functions. The procedure is straightforward and avoids a great deal of the successive differentiations previously involved in generating these matrix elements. The method is applicable to general polyatomic systems.

Acknowledgment

We would like to thank Professor Ostlund for communicating his results for the matrix elements of G_0^+ for p-type Gaussian functions to us prior to publication.

Appendix: The Basic Integrals I_L^p, Eq. (18), for $0 \leq L \leq 6$, $2 \leq p \leq 8$

The basic integrals I_L^p which define the matrix elements of the principal value of the Green's function through Eq. (17) are listed for the cases $0 \leq L \leq 6$, $2 \leq p \leq 8$. The I_L^p for $2 \leq L \leq 6$, $4 \leq p \leq 8$ are related to the first seven I_L^p below through Eq. (21).

$$I_0^2 = \frac{\pi}{2R} e^{-aq^2} \operatorname{Re}\left[e^{iqR} \operatorname{erf}\left(\frac{R}{2\sqrt{a}} + i\sqrt{a}\, q\right)\right]$$

$$I_0^4 = q^2 I_0^2 + \frac{\sqrt{\pi}}{4} a^{-3/2} e^{-R^2/4a}$$

$$I_0^6 = q^2 I_0^4 - \frac{\sqrt{\pi}}{4} e^{-k^2/4a}\left[\frac{R^2 a^{-7/2}}{4} - \frac{3}{2} a^{-5/2}\right]$$

$$I_0^8 = q^2 I_0^6 - \frac{\sqrt{\pi}}{4} e^{-R^2/4a}\left[-\frac{R^4}{16} a^{-11/2} + \frac{5}{4} R^2 a^{-9/2} - \frac{15}{4} a^{-7/2}\right]$$

$$I_1^3 = \frac{\pi}{2} e^{-aq^2} \operatorname{Re}\left[\left(\frac{1}{R^2} - \frac{iq}{R}\right) e^{iqR} \operatorname{erf}\left(\frac{R}{2\sqrt{a}} + i\sqrt{a}\, q\right)\right]$$

$$- \frac{\sqrt{\pi}}{2} e^{-R^2/4a} \frac{a^{-1/2}}{R}$$

$$I_1^5 = q^2 I_1^3 + \frac{\sqrt{\pi}}{8} e^{-R^2/4a} R a^{-5/2}$$

$$I_1^7 = q^2 I_1^5 + \frac{\sqrt{\pi}}{8} e^{-R^2/4a} \left(\frac{5}{2} Ra^{-7/2} - \frac{R^3}{4} a^{-9/2} \right)$$

$$I_2^4 = \frac{3}{R} I_1^3 - I_0^4$$

$$I_2^6 = \frac{3}{R} I_1^5 - I_0^6$$

$$I_2^8 = \frac{3}{R} I_1^7 - I_0^8$$

$$I_3^5 = - I_1^5 + \frac{15}{R^2} I_1^3 - \frac{5}{R} I_0^4$$

$$I_3^7 = - I_1^7 + \frac{15}{R^2} I_1^5 - \frac{5}{R} I_0^6$$

$$I_4^6 = - \frac{10}{R} I_1^5 + \frac{105}{R^3} I_1^3 + I_0^6 - \frac{35}{R^2} I_0^4$$

$$I_4^8 = - \frac{10}{R} I_1^7 + \frac{105}{R^3} I_1^5 + I_0^8 - 35 I_0^6/R^2$$

$$I_5^7 = I_1^7 - \frac{105}{R^2} I_1^5 + \frac{945}{R^4} I_1^3 + \frac{14}{R} I_0^6 - \frac{315}{R^3} I_0^4$$

$$I_6^8 = \frac{21}{R} I_1^7 - \frac{1260}{R^3} I_1^5 + \frac{10395}{R^5} I_1^3 - I_0^8 + \frac{189}{R^2} I_0^6 - \frac{3465}{R^4} I_0^4$$

References

[1] T. N. Rescigno, C. W. McCurdy, Jr., and V. McKoy, Phys. Rev. A 11 (1975) 825.

[2] N. S. Ostlund, Chem. Phys. Lett. 34 (1975) 419.

[3] W. Gautschi, SIAM J. Num. Anal. 7, (1970) 187.

TABLE I. Matrix elements of the principal value part of the free particle Green's function for Σ cases. [a, b, c]

$$S\overset{A}{\sim} - S\overset{B}{\sim} = A\, I_0^2$$

$$Z\overset{A}{\sim} - S\overset{B}{\sim} = -\frac{A}{\sqrt{\alpha}}\, P_1\, I_1^3$$

$$Z\overset{A}{\sim} - Z\overset{B}{\sim} = \frac{A}{\sqrt{\alpha\beta}}\left\{-\frac{2}{3}\, P_2\, I_2^4 + \frac{1}{3}\, I_0^4\right\}$$

$$ZZ\overset{A}{\sim} - S\overset{B}{\sim} = \frac{A}{\sqrt{3}}\left\{\frac{2}{3\alpha}\, P_2\, I_2^4 - \frac{1}{3\alpha}\, I_0^4 + 2\, I_0^2\right\}$$

$$ZZ\overset{A}{\sim} - Z\overset{B}{\sim} = \frac{A}{\sqrt{3}}\left\{\frac{2}{5\alpha\sqrt{\beta}}\, P_3\, I_3^5 - \frac{3}{5\alpha\sqrt{\beta}}\, P_1\, I_1^5 + \frac{2}{\sqrt{\beta}}\, P_1\, I_1^3\right\}$$

$$ZZ\overset{A}{\sim} - ZZ\overset{B}{\sim} = \frac{A}{3}\left\{\frac{8}{35\alpha\beta}\, P_4\, I_4^6 - \frac{4}{7\alpha\beta}\, P_2\, I_2^6 + \frac{4}{3}\, B\, P_2\, I_2^4 + \frac{1}{5\alpha\beta}\, I_0^6 - \frac{2}{3}\, B\, I_0^4 + 4\, I_0^2\right\}$$

$$ZZZ\overset{A}{\sim} - S\overset{B}{\sim} = \frac{A}{\sqrt{15}}\left\{-\frac{2}{5\alpha^{3/2}}\, P_3\, I_3^5 + \frac{3}{5\alpha^{3/2}}\, P_1\, I_1^5 - \frac{6}{\sqrt{\alpha}}\, P_1\, I_1^3\right\}$$

$$ZZZ\overset{A}{\sim} - Z\overset{B}{\sim} = \frac{A}{\sqrt{15}}\left\{-\frac{8}{35\alpha\sqrt{\alpha\beta}}\, P_4\, I_4^6 + \frac{4}{7\alpha\sqrt{\alpha\beta}}\, P_2\, I_2^6 - \frac{1}{5\alpha\sqrt{\alpha\beta}}\, I_0^6 - \frac{4}{\sqrt{\alpha\beta}}\, P_2\, I_2^4 + \frac{2}{\sqrt{\alpha\beta}}\, I_0^4\right\}$$

Table I. (continuation)

$$ZZZ^{A}_{\sim} - ZZ^{B}_{\sim} = \frac{A}{3\sqrt{5}}\{-\frac{8}{63\alpha^{3/2}\beta} P_5 I_5^7 + \frac{4}{9\alpha^{3/2}\beta} P_3 I_3^7$$

$$- \frac{3}{7\alpha^{3/2}\beta} P_1 I_1^7 - \frac{4B^*}{5\sqrt{\alpha}} P_3 I_3^5 + \frac{6B^*}{5\sqrt{\alpha}} P_1 I_1^5 - \frac{12}{\sqrt{\alpha}} P_1 I_1^3 \}$$

$$ZZZ^{A}_{\sim} - ZZZ^{B}_{\sim} = \frac{A}{15}\{-\frac{16}{231(\alpha\beta)^{3/2}} P_6 I_6^8 + \frac{24}{77(\alpha\beta)^{3/2}} P_4 I_4^8$$

$$- \frac{10}{21(\alpha\beta)^{3/2}} P_2 I_2^8 + \frac{1}{7(\alpha\beta)^{3/2}} I_0^8 - \frac{48}{35}\frac{B}{\sqrt{\alpha\beta}} P_4 I_4^6$$

$$+ \frac{24}{7}\frac{B}{\sqrt{\alpha\beta}} P_2 I_2^6 - \frac{6B}{5\sqrt{\alpha\beta}} I_0^6 - \frac{24}{\sqrt{\alpha\beta}} P_2 I_2^4 + \frac{12}{\sqrt{\alpha\beta}} I_0^4 \}$$

[a] A, B, and B^* are defined as follows

$$A = \sqrt{\frac{2}{\pi}}\frac{1}{(\alpha\beta)^{3/4}}, \quad B = (\frac{1}{\alpha} + \frac{1}{\beta}), \quad B^* = \frac{1}{\alpha} + \frac{3}{\beta}$$

where α and β are the exponents of the Cartesian Gaussian function.

[b] The argument of all P_L is $\hat{R}$.

[c] $S^{A}_{\sim}$, $Z^{A}_{\sim}$, $ZZ^{A}_{\sim}$ are related to $\mu^{\alpha,\vec{A}}_{\ell mn}$ of Eq. (7) as follows: $S^{A}_{\sim} = \mu^{\alpha,\vec{A}}_{000}$, $Z^{A}_{\sim} = \mu^{\alpha,\vec{A}}_{001}$, $ZZ^{A}_{\sim} = \mu^{\alpha,\vec{A}}_{002}$. Higher orders follow analogously. $ZZZ^{A}_{\sim} - ZZZ^{B}_{\sim}$ is a shorthand notation for $\langle \mu^{\alpha,\vec{A}}_{003} \mid G_0^+(p) \mid \mu^{\beta,\vec{B}}_{003} \rangle$ of Eq. (15).

TABLE II. Matrix elements of the principal value part of the free particle Green's function for II cases.[a, b, c]

$$\underset{\sim}{X}^{A} - \underset{\sim}{X}^{B} = \frac{A}{\sqrt{\alpha\beta}}\left\{-\sqrt{\frac{2\pi}{15}}\, Q_{22}\, I_2^4 + \frac{1}{3}\, P_2\, I_2^4 + \frac{1}{3}\, I_0^4\right\}$$

$$\underset{\sim}{XZ}^{A} - \underset{\sim}{XZ}^{B} = \frac{A}{\alpha\beta}\left\{\frac{1}{21}\sqrt{\frac{8\pi}{5}}\, Q_{42}\, I_4^6 - \frac{1}{7}\sqrt{\frac{2\pi}{15}}\, Q_{22}\, I_2^6 - \frac{4}{35}\, P_4\, I_4^6 - \frac{1}{21}\, P_2\, I_2^6 + \frac{1}{15}\, I_0^6\right\}$$

$$\underset{\sim}{XZZ}^{A} - \underset{\sim}{XZZ}^{B} = \frac{A}{(\alpha\beta)^{3/2}}\,\frac{1}{3}\left\{-\frac{8}{3465}\sqrt{\frac{420\pi}{13}}\, Q_{62}\, I_6^8 + \frac{2}{77}\sqrt{\frac{8\pi}{5}}\, Q_{42}\, I_4^8 - \frac{1}{21}\sqrt{\frac{2\pi}{15}}\, Q_{22}\, I_2^8 + \frac{8}{231}\, P_6\, I_6^8 - \frac{16}{385}\, P_4\, I_4^8 - \frac{1}{21}\, P_2\, I_2^8 + \frac{1}{35}\, I_0^8 - \frac{2B\alpha\beta}{21}\sqrt{\frac{8\pi}{5}}\, Q_{42}\, I_4^6 - \frac{2B\alpha\beta}{7}\sqrt{\frac{2\pi}{15}}\, Q_{22}\, I_2^6 + \frac{8B\alpha\beta}{35}\, P_4\, I_4^6 + \frac{2\alpha\beta B}{21}\, P_2\, I_2^6 - \frac{2B\alpha\beta}{15}\, I_0^6 - 4\alpha\beta\sqrt{\frac{2\pi}{15}}\, Q_{22}\, I_2^4 + \frac{4\alpha\beta}{3}\, P_2\, I_2^4 + \frac{4\alpha\beta}{3}\, I_0^4\right\}$$

$$\underset{\sim}{XZ}^{A} - \underset{\sim}{X}^{B} = \frac{A}{\alpha\sqrt{\beta}}\left\{\sqrt{\frac{2\pi}{105}}\, Q_{32}\, I_3^5 - \frac{1}{5}\, P_3\, I_3^5 - \frac{1}{5}\, P_1\, I_1^5\right\}$$

Table II. (continuation)

$$XZZ\overset{A}{\sim} - X\overset{B}{\sim} = \frac{A}{\sqrt{\alpha\beta}\sqrt{3}} \{ -\frac{1}{21\alpha}\sqrt{\frac{8\pi}{5}}\, Q_{42}\, I_4^6 + \frac{1}{7\alpha}\sqrt{\frac{2\pi}{15}}\, Q_{22}\, I_2^6$$

$$+ \frac{4}{35\alpha} P_4 I_4^6 + \frac{1}{21\alpha} P_2 I_2^6 - \frac{1}{15\alpha} I_0^6 - 2\sqrt{\frac{2\pi}{15}}\, Q_{22}\, I_2^4$$

$$+ \frac{2}{3} P_2 I_2^4 + \frac{2}{3} I_0^4 \}$$

$$XZZ\overset{A}{\sim} - XZ\overset{B}{\sim} = \frac{A}{\sqrt{3}} \frac{1}{\beta\sqrt{\alpha}} \{ -\frac{2}{315\alpha}\sqrt{\frac{210\pi}{11}}\, Q_{52}\, I_5^7 + \frac{1}{3\alpha}\sqrt{\frac{2\pi}{105}}\, Q_{32}\, I_3^7$$

$$+ \frac{4}{63\alpha} P_5 I_5^7 - \frac{1}{45\alpha} P_3 I_3^7 - \frac{3}{35\alpha} P_1 I_1^7 - 2\sqrt{\frac{2\pi}{105}}\, Q_{32}\, I_3^5$$

$$+ \frac{2}{5} P_1 I_1^5 + \frac{2}{5} P_3 I_3^5 \}$$

[a] See footnote a of Table I for the definitions of A, B, and B^*.

[b] We define $Q_{LM} = Y_{LM} + Y_{L-M}$.

[c] $X\overset{A}{\sim}$, $XZ\overset{A}{\sim}$, and $XZZ\overset{A}{\sim}$ are related to $\mu_{\ell mn}^{\alpha,\vec{A}}$ of Eq. (7) as follows: $X\overset{A}{\sim} = \mu_{100}^{\alpha,\vec{A}}$, $XZ\overset{A}{\sim} = \mu_{101}^{\alpha,\vec{A}}$, and $XZZ\overset{A}{\sim} = \mu_{102}^{\alpha,\vec{A}}$. Also see footnote of Table I.

TABLE III. Matrix elements of the principal value part of the free particle Green's function for Δ cases.[a]

$$XY\tilde{}^{A} - XY\tilde{}^{B} = \frac{A}{\alpha\beta}\left\{-\frac{1}{6}\sqrt{\frac{8\pi}{35}}\,Q_{44}\,I_4^6 + \frac{1}{35}\,P_4\,I_4^6 + \frac{2}{21}\,P_2\,I_2^6 + \frac{1}{15}\,I_0^6\right\}$$

$$XYZ\tilde{}^{A} - XYZ\tilde{}^{A} = \frac{A}{(\alpha\beta)^{3/2}}\left\{\frac{2}{33}\sqrt{\frac{2\pi}{91}}\,Q_{64}\,I_6^8 - \frac{1}{66}\sqrt{\frac{8\pi}{35}}\,Q_{44}\,I_4^8 - \frac{2}{231}\,P_6\,I_6^8 + \frac{1}{105}\,I_0^8 - \frac{1}{55}\,P_4\,I_4^8\right\}$$

$$XYZ\tilde{}^{A} - XY\tilde{}^{B} = \frac{A}{\alpha^{3/2}\beta}\left\{\frac{2}{3}\sqrt{\frac{\pi}{770}}\,Q_{54}\,I_5^7 - \frac{1}{63}\,P_5\,I_5^7 - \frac{2}{45}\,P_3\,I_3^7 - \frac{1}{35}\,P_1\,I_1^7\right\}$$

[a] See footnotes a, b, and c of Table II.

TABLE IV. Some numerical values for matrix elements of the free-particle Green's function.

A. Σ Symmetry Cases

Basis Functions	Matrix Element[a]	
1 - 1	-0.16922 (-3)	-0.10364 (-6)
1 - 2	-0.35845 (-3)	-0.42964 (-6)
2 - 3	-0.40672 (-2)	-0.306211 (-4)
4 - 4	-0.12444 (-1)	-0.59651 (-8)
4 - 5	-0.98178 (-2)	-0.34388 (-5)
6 - 6	-0.88728	-0.46259 (-1)
6 - 3	-0.10915	-0.49350 (-2)
3 - 7	-0.23692	-0.23196 (-1)
3 - 9	0.334011 (-2)	-0.52021 (-6)
3 - 8	0.182042	-0.19020 (-1)
4 - 8	0.27396 (-2)	-0.143465 (-5)
6 - 8	-0.16438 (1)	-0.17828

The exponents, symmetry type, and coordinates of basis functions 1 to 9 are

Basis Function	Type	Exponent	Coordinates
1	S	5909.44	(0, 0, R)
2	S	887.451	"
3	S	19.9981	"
4	Z	26.786	"
5	Z	0.1654	"
6	ZZ	1.225	"
7	S	0.128	(0, 0, 0)
8	ZZ	0.202	"
9	Z	5.9564	"

Where R = -1.034 a.u. and (a, b, c) are the coordinates of the Cartesian Gaussian function.

Table IV. (continuation)

B. Π Symmetry Cases

Basis Functions	Matrix Element[b]	
1 - 1	-0.166675 (-2)	-0.7385 (-9)
1 - 2	-0.73788 (-3)	-0.96335 (-5)
3 - 3	-0.200066 (-1)	-0.26408 (-9)
2 - 5	0.49331 (-1)	0.14935 (-4)
3 - 4	-0.106265 (-1)	-0.497154 (-7)
1 - 6	-0.255868 (-6)	-0.73535 (-9)
4 - 5	-0.96181 (-1)	-0.27830 (-5)

The exponents, symmetry type, and coordinates of basis functions 1 to 6 are

Basis Function	Type	Exponent	Coordinates
1	X	200.	(0, 0, R)
2	X	0.1	"
3	XZ	10.0	"
4	XZ	0.5	"
5	XZ	1.0	(0, 0, 0)
6	X	200.	(0, 0, -R)

Where R = -1.034 a.u.

[a]For k_0 = 0.03756808. The two columns are the real and imaginary parts of the matrix element and the numbers in parentheses are the powers of ten by which the numbers are to be multiplied.

[b]For k_0 = 0.1. See also footnote a.

CHAPTER IV

Calculation of Scattering Wave Functions at Arbitrary Energies by the Minimum-Variance Method

SECTION A

Discrete-basis-set Approach to the Minimum-Variance Method in Electron Scattering

I. INTRODUCTION

The use of discrete basis sets offers considerable advantages in the calculation of electron scattering processes.[1] For example, these methods require only standard matrix techniques in their applications rather than the more usual approach of numerical integration of the differential equations. Moreover these methods can be extended to the calculation of scattering amplitudes for nonspherical potentials, thus avoiding the need for single-center expansions of the nonspherical potentials or their scattering wave functions. We have recently proposed one such method which is based on the use of Gaussian-type orbitals in the direct solution of the Lippmann-Schwinger equation for the full elastic scattering amplitude.[2] With Gaussian basis functions being the usual choice for the multicenter molecular problem this approach can be implemented with standard bound state integral programs. Schneider has also developed an approach to electron-molecule scattering based on the R-matrix formalism in which discrete basis functions are used to expand the scattering wave functions in the internal region.[3]

Although these two methods rely on the use of discrete basis functions to achieve their critical simplifications they do not avoid the continuum completely. Specifically the free-particle Green's function must be dealt with in the solution of the T-matrix equation and a numerical integration is needed in the outer region in the R-matrix approach. Two methods which use discrete basis functions exclusively have been developed and applied to electron-atom scattering. These

methods are the Fredholm determinant method, its related equivalent quadrature approach of Reinhardt and coworkers[4] and the J-matrix technique of Heller and Yamani.[5] However these methods are restricted to systems with spherical potentials and, at present, do not seem rigorously applicable to scattering by non-spherical potentials, e. g., electron-molecule scattering, without resorting to a single-center expansion.

In this paper we discuss an approach to scattering problems which uses discrete basis functions entirely and which is applicable to both electron atom and electron-molecule scattering. The method is essentially a variational approach to scattering and is based on the minimization of a variance integral, $U[\tilde{\Psi}]$, defined as

$$U[\tilde{\Psi}] = \frac{\int w(r)\,[(H-E)\tilde{\Psi}]^2\,d\tau}{\int \tilde{\Psi}\tilde{\Psi}\,d\tau} \qquad (1)$$

where r represents the coordinates of all particles. The function $w(r)$ is an arbitrary but positive weight-function. This variance integral is non-negative for any trial function $\tilde{\Psi}$ and is zero only for the exact wave function. Minimization of the value of this variance integral obviously provides a criterion for the determination of the parameters appearing in $\tilde{\Psi}$. The method is referred to as the minimum variance or least-square's method and has been applied to the determination of bound states[6] and, more recently, to potential scattering problems.[7] However in this work[7] trial functions $\tilde{\Psi}$ of the Kohn-type explicitly containing continuum functions are used and

hence, in this form, the method would not be practical for applications to electron-molecule scattering.

In our proposed method we will use Eq. (1) to determine scattering wave functions but these functions will be expanded entirely in discrete basis functions. This procedure leads to a sample matrix equation which determines the linear parameters in the expansion of $\tilde{\Psi}$. Scattering information can then be extracted from the approximate scattering wave function which is known to be proportional to the true scattering solution over the region of space spanned by the discrete basis functions.[8,9] Our choice of Gaussian basis functions as the discrete basis set for the expansion of $\tilde{\Psi}$ makes the method particularly applicable to molecular problems. Moreover by using a separable representation of the scattering potential, the evaluation of the variance integral, $U[\tilde{\Psi}]$ of the quadratic variational principle, leads to only one new class of matrix elements in addition to those already required in the direct diagonalization of the Hamiltonian. This is an important consideration since the method can provide approximate scattering wave functions at arbitrary energies whereas the direct diagonalization of the Hamiltonian in a discrete basis yields such wave functions only at the discrete eigenvalues. Thus in contrast to the Harris method,[10] a single choice of an expansion basis can give scattering information over an arbitrary number of energies.

The outline of the paper is as follows: In section II we review the minimum variance method and some previous applications of the method to scattering problems. There we will also derive the simple

matrix eigenvalue equation which results from Eq. (1) if $\tilde{\Psi}$ is expanded exclusively in a discrete basis set. In section III we present the results of the application to some model potentials and to s-wave scattering for helium in the static-exchange approximation. Finally in section IV we discuss future applications of the method.

II. THEORY

The minimization of the variance integral and of the related variance sum has been used to determine the energies and wave functions of bound[6] and autoionizing states and, more recently, has been applied directly to scattering problems.[7] In these applications both Bardsley[7] and Miller[11] employed trial functions, $\tilde{\Psi}$, of the Kohn-type in the variance integral to obtain s-wave phase shifts for an attractive exponential potential and for the hydrogen atom in the static approximation with and without exchange. The trial functions $\tilde{\Psi}$ are hence of the form (for s-wave scattering),

$$\tilde{\Psi}(r) = \sum_{n=1}^{N} c_n \phi_n + S(kr) + \tan\delta\, C(kr) \qquad (2)$$

where ϕ_n are bound-like functions and S and C behave asymptotically like sine and cosine respectively. The minimum variance method obviously leads to integrals which do not arise in the Kohn and Hulthén variational procedures. For these simple one-dimensional problems the additional integrals are tractable. In these cases the method can offer some advantages since the positive definite character of the variance integral eliminates the occurrence of false resonances which appear in the Kohn procedures and the variance integral can be used to derive bounds to the phase shifts.

Our purpose is to exploit certain features of this minimum variance method to develop a purely discrete basis set approach for obtaining scattering wave functions at arbitrary energies. For

applications of the minimum variance method to electron-molecule scattering trial functions of the form of Eq. (1) containing continuum-like functions are clearly not practical since they lead to intractable integrals. However, a number of studies have shown that approximate scattering wave functions can be obtained by diagonalizing the Hamiltonian in a large discrete basis set since the eigenfunctions are proportional to the scattering wave functions over the region spanned by the basis.[1,8] Unfortunately one can obtain such information only at scattering energies equal to the eigenvalues of the Hamiltonian matrix. For many applications this is a severe limitation. We can cite two obvious examples. In a distorted-wave formalism, to obtain the electronically inelastic amplitude in electron-impact excitation we would require the scattering wave functions at specific incident and final energies. Furthermore, a sum over all partial wave amplitudes at one energy is required just to evaluate the total elastic cross section; with the phase shifts obtained only at a discrete number of points, an interpolation would be necessary since it is not in general possible to make the various partial wave eigenvalues coincide. Such an interpolation is particularly difficult in the vicinity of a resonance. Our goal then is to use the quadratic variational principle, i.e., the minimum variance method, to generate scattering wave functions at arbitrary energies in a completely discrete basis set representation at any energy.

The formulation is straightforward. We expand $\tilde{\Psi}$ in a discrete basis set, i.e.

$$\tilde{\Psi} = \sum_{i=1}^{N} c_i \varphi_i \tag{3}$$

and substitute this expansion into Eq. (1) to obtain

$$U[\tilde{\Psi}] = \frac{\sum_{i,j} c_i c_j \int w(r)[(H - E)\varphi_i][(H - E)\varphi_j]\, d\tau}{\sum_{i,j} c_i c_j \int \varphi_i \varphi_j \, dr} \tag{4}$$

Minimization of U with respect to the linear coefficients $\{c_i\}$ leads to a set of equations which can be written in matrix form as

$$\underset{\sim}{Q}\underset{\sim}{C} = U\underset{\sim}{S}\underset{\sim}{C}, \tag{5}$$

where $\underset{\sim}{C}$ is the vector of coefficients $\{c_i\}$ and

$$Q_{ij} \equiv \int w(r)\,[(H - E)\varphi_i\,][(H-E)\varphi_j\,]\,d\tau \tag{6}$$

$$S_{ij} \equiv \int \varphi_i \varphi_j \, d\tau \tag{7}$$

E is the scattering energy. For the exact solution the variance integral is zero. To minimize the variance we simply obtain the solution of the eigenvalue equation, Eq.(5), corresponding to the smallest eigenvalue. Writing $H = T + V$, we obtain for Q_{ij}

$$Q_{ij} = \int W(r)\,[\,T\varphi_i\,T\varphi_j + V\varphi_i V\varphi_j + T\varphi_i V\varphi_j$$

$$+ V\varphi_i T\varphi_j - 2E(\varphi_i T\varphi_j + \varphi_i V\varphi_j) + E^2 S_{ij}\,]\,d\tau \tag{8}$$

The evaluation of the various terms appearing in Q_{ij}, for a many-particle Hamiltonian, will undoubtedly involve very difficult integrations.

Let us assume that H is a single-particle Hamiltonian determined by an effective one-body target potential, e. g., the Hartree-Fock static-exchange or optical potential. Assuming for the moment that a convenient form can be chosen for the weighting function, w(r), the last three terms in the integral, Eq. (8), correspond to elements of the kinetic energy, potential energy, and overlap matrices arising in normal variational calculations. The remaining integrals are greatly simplified if we assume a non-local, separable form for the potential V, i.e.,

$$V(r, r') = \sum_{\alpha, \beta=1}^{N} V_{\alpha\beta} \varphi_\alpha(r) \varphi_\beta(r') \tag{9}$$

and

$$V\Psi = \sum_{\alpha,\beta=1}^{N} V_{\alpha\beta} \varphi_\alpha(r) \int \varphi_\beta(r') \Psi(r') \, d^3r' \tag{10}$$

The scattering potential is thus represented by an $N \times N$ matrix with elements $V_{\alpha\beta}$. With this form of V we have

$$\int V\varphi_i V\varphi_j \, d\tau = \sum_\alpha V_{\alpha j} V_{\alpha i} \tag{11}$$

$$\int T\varphi_i V\varphi_j \, d\tau = \sum_\alpha V_{\alpha j} T_{\alpha i} \tag{12}$$

These quantities again require just the potential energy and kinetic energy matrices. We emphasize that the assumption of a separable interaction has only been made with respect to the scattering potential and not the kinetic energy. However the integral containing $T\varphi_i T\varphi_j$ is a new integral not appearing in ordinary variational calculations. In the next section we will see that with φ_i and φ_j chosen as Gaussian functions this integral is very simple and can be done analytically.

Once the vector of coefficients, $\underset{\sim}{C}$, corresponding to the minimum eigenvalue of Eq. (5) is obtained the scattering wave function $\tilde{\Psi}$ is known. The phase shift can be extracted by examining the quantity

$$\tan \delta_\ell(r) = \frac{W[R_\ell, j_\ell]}{W[R_\ell, n_\ell]} \tag{13}$$

as a function of r until it acquires a nearly constant value. This value is obviously the phase shift. In Eq. (13) R_ℓ is the radial function derived from $\tilde{\Psi}$, $j_\ell(kr)$ and $n_\ell(kr)$ the Bessel and Neuman functions respectively and W the Wronksian. This procedure has been discussed in recent applications to the scattering of electrons by H_2, N_2,[8] and F_2.[12] One may also use the approach recently suggested by Dalgarno for obtaining phase shifts from these approximate scattering wave functions.[13] In using Eq. (13), we have assumed that the analytic

radial functions, R_ℓ, are accurate in the potential-free region and can therefore be matched to Bessel and Neuman functions. Although we have not done so, one could clearly modify this procedure to match R_ℓ to any numerically generated zeroth-order distorted wave, e. g., those generated by a quadrupole field. If there is significant off-diagonal long-range coupling a more general matching procedure such as that involving the solution of coupled equations in the external region would have to be employed.

III. RESULTS

We have used this discrete basis set approach to the minimum variance method to study the scattering of electrons by several model potentials and by helium in the static-exchange approximation. These potentials include the attractive exponential potentials, $-e^{-r}$ and $-e^{-r^2}$, and the screened Coulomb potentials of the form $\frac{e^{-r^2}}{r}$. Although we present results for s-wave scattering only the approach is clearly applicable to the higher partial waves. Our primary purpose is to test an approach which may have specific advantages in future applications to electron-molecule scattering.

All the results except those for the exponential, $V(r) = -e^{-r}$, were obtained using a basis set of Gaussian functions. We choose Gaussian basis functions since this choice is the most convenient for future applications. The integral containing $(-\frac{1}{2}\nabla^2\varphi_i)(-\frac{1}{2}\nabla^2\varphi_j)$, which is the only new integral appearing in this method if we assume the separable form for the potential, has a simple form. For basis functions of the form

$$\varphi_{jk\ell}^{\vec{A},\alpha} = (x - A_x)^j (y - A_y)^k (z - A_z)^\ell \, e^{-\alpha(\vec{r} - \vec{A})^2} \tag{14}$$

where $\vec{A}$ is the vector locating center A and j, k, ℓ determine the order of the Gaussian, i.e., s, p, d..., we have

$$\int \left(-\tfrac{1}{2}\nabla^2 \varphi_{000}^{\vec{B},\beta}\right)\left(-\tfrac{1}{2}\nabla^2 \varphi_{000}^{\vec{A},\alpha}\right) d\tau = \frac{\alpha^2\beta^2\pi^{3/2}}{(\alpha+\beta)^{7/2}} e^{-\eta D} \times$$

$$\left[\frac{4\alpha^2\beta^2 D^2}{(\alpha+\beta)^2} - 20\frac{D\alpha\beta}{(\alpha+\beta)} + 15\right] \qquad (15)$$

with $D = (\vec{A}-\vec{B})^2$ and $\eta = \frac{\alpha\beta}{\alpha+\beta}$. Integrals involving other Gaussian functions can be determined by taking the appropriate derivative of Eq. (15) with respect to the coordinates of a particular center.[14]

For several applications, particularly those of scattering by potentials with a Coulomb behavior at short distances, the use of an appropriate weighting function, w(r), proved very helpful. Our choice of weighting function was fixed by requiring that the resulting variance integral still be evaluated by standard bound-state molecular integral programs for Gaussian basis sets. This is a reasonable choice to keep the method applicable to realistic problems. This suggests the weighting function

$$w(r) = 1 - \alpha e^{-\tau r^2} \quad ; \quad 1 \geq \alpha \geq 0 \qquad \tau > 0 \qquad (16)$$

which does lead to a variance integral, Eq. (4), that can be evaluated with multicenter Gaussian integral programs. This function increases from a value of $1-\alpha$ as $r \rightarrow 0$ to unity as r becomes large. Hence

$w(r)$ weights the outer region more than the inner. This choice of weighting function yielded approximate scattering solutions which show significant amplitude in the physically significant inner regions and hence are simpler to analyze for scattering information. In this way we avoid the apparent tendency of the least-squares method to yield solutions with small amplitudes in those regions where the scattering potential is large. Since it is precisely in this inner region where one desires a solution with large amplitude, we choose a weighting function which forces a small amplitude at large r. By varying the parameters α and τ we can change the relative weights of the outer and inner regions so as to obtain a lower value for the variance integral.

Tables I and II show results for several model potentials. The phase shifts in Table I are for the attractive exponential potential $V(r) = -e^{-r}$. We used a basis set of nine Slater orbitals and did not use a weighting function, i.e., $w(r) = 1$. Comparison of the calculated phase shifts with the exact phase shifts at increasing values of k shows the obvious trend that solutions with small variances yield more accurate phase shifts. This basis set obviously cannot represent the scattering functions at larger incident momentum as well as those at lower k. For this potential we also solved the minimum variance equations without assuming a separable form for the potential. These calculated phase shifts agreed well with those derived by assuming a separable form for V indicating that this representation of the potential is adequate.

Table II gives the s-wave phase shifts for several potentials and the effect of the weighting function on the value of the variance integral and the phase shifts. Comparison of the phase shift at

$k = 0.5$ demonstrates the advantage of using an adequate weighting function. In this case a basis set of 17 Gaussian functions along with a weighting function gives the same value of the phase shift and variance integral as a basis of 28 Gaussian functions used without a weighting function.

Table III lists the phase shifts for the scattering of electrons by the static-exchange potential of helium from $k = 0.1$ to $k = 0.8$ These phase shifts were calculated with a basis of 17 Gaussian functions and agree well with the results of Schneider.[15] In these calculations most of the matrix manipulations are independent of the impact energy so scattering solutions can be obtained at very many energies quite economically. While the matrix Eq. (5) must be solved for each energy, it is only the lowest eigenvalue and corresponding eigenvector that are required. For large matrices, this can represent a substantial savings. Finally Table IV illustrates the effect of the weighting function on the phase shift and variance integral for the e^--helium scattering. By increasing the weighting of the outer region over the inner region the variance integral can be decreased leading subsequently to an improved value of the phase shift. We also noted that, at the same energy, the scattering wave function obtained by the minimum variance method is generally a smoother function than that given by the direct diagonalization of the Hamiltonian. It is worth noting that although the Lippmann-Schwinger equations are exactly soluble with the approximation of Eq. (9), the present approach does not require the free-particle Green's function nor the construction of any matrix inverse.

IV. CONCLUSIONS

We have shown that minimization of the variance integral provides a method for the determination of scattering wave functions which uses discrete basis functions exclusively and completely avoids the continuum. The applications of this method to scattering by several model potentials and by the static-exchange potential of helium show that the method can provide reliable scattering wave functions economically.

The choice of Gaussian basis functions for the expansion of the scattering wave function should make the method particularly applicable to electron-molecule scattering. Moreover by using a separable representation of the scattering potential only one new class of matrix element appears in the evaluation of the variance integral which is not already required in the diagonalization of the Hamiltonian. The analysis presented here, which is appropriate for treating single-channel potential problems, would have to be modified to handle problems in which the reactance matrix is not diagonal. In such cases, no simple formula for the reactance matrix can be given which is independent of the normalization of the wave function because at any energy there may be more than one linearly independent solution. One possible method for dealing with this problem in an L^2 basis has been discussed by Hazi.[16] If N-linearly independent solutions are needed at a particular energy, we can simply repeat the calculations for several choices of

expansion bases and use the appropriate multi-channel extension of Eq. (13). A simpler, but approximate, approach would be to use a decoupling scheme (low ℓ-spoiling) as has been done by several authors.[17]

There are several features of our approach to the minimum variance method which should lead to significant advantages in solving certain problems. For example, we found that the approximate scattering wave function obtained from the minimum variance method is usually a smoother function than the eigenfunction obtained by diagonalization of the Hamiltonian in the same discrete basis set. This feature can be important if one wants to use these scattering wave functions to obtain information other than the phase shifts. Such an application would be the use of these wave functions to evaluate an electronically inelastic scattering amplitude in the distorted wave approximation. For this application one may also use a weighting function so as to obtain wave functions with desirable features in the important regions of space.

ACKNOWLEDGMENTS

We want to thank Mr. Larry Yaffe and Dr. C. William McCurdy, Jr., for helpful discussions in the early stages of this work. We also thank Dr. Andrew Hazi for extensive clarification of the contents of Reference 16.

References

*Supported by a grant from the National Science Foundation.

†Present address: Lawrence Livermore Laboratory, University of California, Livermore, California 94550.

[1]See, for example, A. U. Hazi and H. S. Taylor, Phys. Rev. A 2, 1109 (1970) and W. P. Reinhardt, D. W. Oxtoby, and T. N. Rescigno, Phys. Rev. Letts. 28, 401 (1971).

[2]T. N. Rescigno, C. W. McCurdy, Jr., and V. McKoy, Phys. Rev. A 10, 2240 (1974).

[3]B. Schneider, Chem. Phys. Letts. 31, 237 (1975).

[4]W. P. Reinhardt, Computer Phys. Comm. 6, 303 (1973).

[5]E. J. Heller and H. A. Yamani, Phys. Rev. A 9, 1201 (1974).

[6]See, for example, M. H. Lloyd and L. M. Delves, Intern. J. Quantum Chem. 3, 169 (1969).

[7]J. N. Bardsley, E. Gerjuoy, and C. V. Sukumar, Phys. Rev. A 6, 1813 (1972); F. H. Read and J. R. Soto-Montiel, J. Phys. B 6, L15 (1973).

[8]C. W. McCurdy, Jr., T. N. Rescigno, and V. McKoy, J. Phys. B 9, 691 (1976).

[9]A. U. Hazi and M. Fels, Chem. Phys. Lett. 8, 582 (1971).

[10]F. E. Harris and H. H. Michels, Phys. Rev. Letts. 22, 1036 (1969).

[11]K. J. Miller, Phys. Rev. A 3, 607 (1971).

[12] T. N. Rescigno, C. F. Bender, C. W. McCurdy, and V. McKoy, J. Phys. B 9, 2141 (1976).

[13] M. Oppenheimer, H. Doyle, and A. Dalgarno, Chem. Phys. Letts. 32, 6 (1975).

[14] I. Shavitt, Methods of Computational Physics, Vol. II, p. 30, (Academic Press, New York, 1963).

[15] B. Schneider, Chem. Phys. Letts. 25, 140 (1974).

[16] A. U. Hazi, Chem. Phys. Lett. 20, 251 (1973), and private communications.

[17] T. Winter and N. F. Lane, Chem. Phys. Lett. 30, 363 (1975); M. A. Morrison and N. F. Lane, Phys. Rev. A 12, 2361 (1975).

TABLE I. Phase-shift values for the potential $V(r) = -e^{-r}$

k (au)	U [a]	δ [b]	δ_{ex} [c]
0.3	6.6×10^{-4}	1.56	1.57
0.4	1.8×10^{-3}	1.31	1.36
0.5	2.4×10^{-3}	1.14	1.20
0.6	5.1×10^{-3}	0.99	1.08
0.7	6.7×10^{-3}	0.91	0.98

[a] Value of the variance integral defined in Eq. (4).

[b] Phase shifts calculated by the minimum variance method with a basis set of nine Slater functions of the form $r^n e^{-\alpha r}$ with $\alpha = 1$.

[c] Exact phase shift obtained by Calogero's method. See text.

TABLE II. Phase-shifts for various model potentials.

k(au)	V(r)	U[b]	w(r)[c]	δ[d]	δ_{ex}
0.287	$-e^{-r^2}$	1.45×10^{-4}	$1-0.79e^{-0.28r^2}$	0.62	0.65
0.287	$-e^{-r^2}$	1.03×10^{-4}	1	0.64	0.65
0.287	$-e^{-r^2}/r$	1.42×10^{-4}	$1-0.99e^{-0.28r^2}$	0.42	0.41
0.287	e^{-r^2}/r	1.51×10^{-4}	$1-0.79e^{-0.28r^2}$	-0.14	-0.14
0.500[a]	$-2\frac{e^{-r^2}}{r}$	2.21×10^{-3}	1	2.64	2.65
0.500	$-2\frac{e^{-r^2}}{r}$	2.45×10^{-3}	$1-0.88e^{-0.28r^2}$	2.63	2.65

[a] A set of 28 Gaussian basis functions was used in this calculation. All the other calculations were done with a set of 17 Gaussian functions.

[b] Value of the variance integral.

[c] w(r) is the weighting function used in minimizing the variance integral.

[d] The phase shift extracted from the approximate scattering wave function. See text.

TABLE III. Phase shifts for e - He scattering in the static - exchange approximation.

k(au)	U	δ^a	δ^b
0.1	4.5×10^{-6}	2.98	3.00
0.2	2.3×10^{-5}	2.84	2.88
0.3	1.1×10^{-4}	2.69	2.72
0.4	6.0×10^{-4}	2.58	2.59
0.5	2.4×10^{-3}	2.40	2.45
0.6	5.9×10^{-3}	2.33	2.33
0.7	8.7×10^{-3}	2.17	2.19
0.8	1.9×10^{-2}	2.08	2.10

[a] Calculated from the minimum variance method with a basis of Gaussian basis functions and a weighting function of the form of Eq. (16) with $\tau = 0.28$ and $.79 \leq \alpha \leq .99$.

[b] Accurate phase shifts from Ref. 15. These values are those of Ref. 15 rounded off to three significant digits.

TABLE IV. Effect of the weighting function on the phase shift.

α[a]	U	δ
0.7986	1.35×10^{-3}	2.593
0.8865	1.13×10^{-3}	2.587
0.9899	5.98×10^{-4}	2.580

[a] The weighting function is of the form $w(r) = 1 - \alpha e^{-\tau r^2}$ with $\tau = 0.28$. The phase shift is for $k = 0.4$ where the accurate value is 2.58. The relative weighting of the outer region ($r = 4$ au) to the inner region ($r = 1$ au) varies from 2.5 to 3.9 for these choices of α.